| | KUNGL TEKNISKA HÖGSKOLAN | Report Dept. of Energy Technology Div. of Nuclear Power Safety Prof: Seghal, Bal Raj | |
|---|---|---|---|

| **Title:** Study of Film Boiling Over Sphere In Subcooled Pool of Nanofluid Using Quenching Experiment | | **Keywords:** Subcooled, Vapor film, nanofluid, nanoparticles, quenching | |
|---|---|---|---|
| **Author:** Dereje Shiferaw | | **Report nr: 1** | |
| **Project title:** Master Thesis | **Pages: 103** | **Drawings:** | |
| **Supervisor at KTH:** Dr.Hyun Sun Park | **Date: 2003-12-15** | **Appendices:** | |
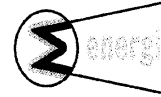
**Overall responsible at KTH:** Prof. Bal Raj Sehgal

| **Approved at KTH by:** Prof. Bal Raj Sehgal | **Signature:** |
|---|---|

**Overall responsible at industry:**

**Industrial partners:**

| **Approved by industrial partners:** | **Signature:** |
|---|---|
| **Approved for distribution: Restricted, to distribution list** | |
| **Open: X** | |

## Abstract

The prediction of the heat transfer during quenching a metal surface, that are at temperatures higher than the saturation temperature of the liquid is an important aspects of boiling systems, metallurgical processing, steam generators and many other applications. Knowledge of the film boiling heat transfer and the minimum temperature to sustain film boiling is essential to determine core coolability after a hypothetical loss of coolant accident.

Though the film boiling study has counted several years, experimental works that illustrate nearly the real phenomena are quite few. Most of the studies are theoretical model development of film boiling over common geometries (horizontal plate, cylinders, sphere, etc) under common fluids (water, Refrigerants, Cryogenic fluids, etc). Consequently there aren't enough data to prove theoretical models.

Researches have been investigating ways to enhance the heat transfer performance in every aspect One of the options was replacing the type of fluid. Recently new fluid named "nanofluid" (suspending low volume percent of nano-particles in water) is under investigation the fluid has shown up to 40% rise of thermal conductivity compared with the base fluid.

The paper attempts to investigate experimentally the change in the film boiling heat transfer in using the new fluid instead of water.
Transient quenching experiment of highly heated, SKF bearing balls RB-10/G20W and RB-20/G20W with diameters 10 and 20 mm respectively was conducted in a pool of different subcooled liquids: distilled water and (5, 10 and 20) Volume percent of 30nm in diameter $Al_2O_3$ nano-particles suspended in distilled water with ultrasonic vibration.

The heat transfer coefficient in the film boiling regime is observed to be lower than the base fluid (water). On the other hand consecutive quenching wit out cleaning the sphere in between the tests caused premature collapse of the vapour film producing a relatively higher quenching rate.

| Distribution list | | | | | | |
|---|---|---|---|---|---|---|
| | | | | | | |

# TABLE OF CONTENTS

# INDEX OF TABLES

# INDEX OF FIGURES

# ACKNOWLEDGMENT

This gives me opportunity to express my deep thankfulness and appreciation to those with out which the realization of the thesis will not be possible.

First of all, I would like to thank Prof. Bal Raj Sehgal for allowing this great opportunity to do my thesis in the division of nuclear power safety and providing me a stipendium for my finance need. His supervision and encouragement were indispensable for the completion of the thesis.

I am grateful to Dr. Hyun Sun Park, for his continual daily supervision and encouragement in all aspects. His kind and energetic pushes were valuable.

I am also indebted to Prof. Mamoun Muhammed at the division of material chemistry for his welcoming response to use his laboratory facility in preparing the nanosolutions and providing the nanophase powder. I appreciate his vision in nanotechnology

Dr. Do Kyung Kim at the division of material chemistry (now at MIT, USA) for his unlimited cooperation and valuable inputs in preparing the solution and sharing important ideas

Mr. Gunnar and Jose for their technical assistance through all the process

Friends and colleagues, who shared their views and socially making me, feel comfortable were important parts of the work.

My immense appreciation and gratitude goes to the SIDA scholarship center for sponsoring my studies and allowing me to join KTH.

Above all, I can't pass with out mentioning the name of God, Who gave me all the strength and devotions. He filled my heart with joy in times of loneliness and deserves all the credit and glory.

Last but not least, I am thankful to my parents who relentlessly encouraged me and have been a backing-up through my entire academic career.

# NOMENCLATURE

| | |
|---|---|
| $Ar$ | Archimedes number, $g(\rho_l - \rho_v)d^3 / (\rho_v \upsilon_v^2)$ |
| $Cp$ | Specific heat, $[J / (Kg\ ^\circ C)]$ |
| $d, D$ | diameter of sphere or cylinder, [m] |
| $d'$ | dimensionless diameter, $d / [\sigma / g \ / (\rho_l - \rho_v)]^{1/2}$ |
| $Fr$ | Froude number, $U(2 / (gd)$ |
| $g$ | gravitional constant, [Kg m/sec2] |
| $Gr$ | Grashof number, $g(((T_{sat} - T()d3)/((2$ |
| $h$ | heat transfer coefficient, $q / \Delta T$ |
| $h_{fg}$ | latent heat of vapourization, $[J / Kg]$ |
| $h_{fg}'$ | latent heat plus sensible heat, $h_{fg} + 0.5 C_{pv}$ (Tsup |
| $K$ | density ratio, $\rho_l / \rho_v$ |
| $k$ | thermal conductivity, $[W / (m^\circ C)]$ |
| $Nu$ | average Nusselt number, $hd / k$ |
| $Pr$ | Prandtl number |
| $q$ | average surface heat flux, $[W / m^2]$ |
| $R$ | radius |
| $Re_l$ | Reynolds number of liquid phase, $U_l d / \upsilon_l$ |
| $Sc$ | dimensionless subcooling, $(C_{pl}\Delta T_{sub}) / (h_{fg}Pr_l)$ |
| $Sc'$ | dimensionless subcooling, $(C_{pl}\Delta T_{sub}) / (h'_{fg}Pr_l)$ |
| $Sp$ | dimensionless superheat, $(C_{pv}\Delta T_{sup}) / (h_{fg}Pr_v)$ |
| $Sp'$ | dimensionless superheat $(C_{pv}\Delta T_{sup}) / (h'_{fg}Pr_v)$ |
| $\alpha$ | thermal diffusivity, $k / (\rho Cp)$ |
| $\Delta T_{sup}$ | average superheat of solid wall, $T_w - T_{sat}$ |
| $\Delta T_{sub}$ | Liquid superheat, $T_{sat} - T_l$ |
| $\varepsilon$ | radiation emissivity |
| $\mu$ | viscosity, $[Kg / (m.Sec)]$ |
| $\nu$ | Kinematic viscosity, $[m^2 / sec]$ |
| $\rho$ | density, $[Kg / m^3]$ |
| $\sigma$ | Surface tension of vapor-liquid interface, $[N / m]$ |

# 1. INTRODUCTION

Suspensions of solid particles (with mm or μm size) in liquid have been recognized long times ago to have potential to enhance heat transfer. The idea is to exploit the very high thermal conductivity of solids. However, this technique suffers from stability and rheological problems, such as:

- Quick particle settlement,
- Sever clogging and significant pressure drop
- Abrasion, erosion and fouling

Therefore the fluids with large suspended particles have little practical application in heat transfer enhancement.

Novel approach of suspension of solid particles (<100 nm) in liquids emerges from the development of nanotechnology. The term nanofluid is envisioned to describe a solid liquid mixture which consists of nanoparticles and a base liquid and which is one of the challenges for thermo-science provided by the nanotechnology. Unlike the coarse-grained particle suspensions, nanofluids are:

- Extremely stable
- Easily Fluidized
- Exhibit no significant settling under static conditions (even after a week or month)

The thesis focuses on subcooled pool film boiling over spheres under highly subcooled water and new fluids (fluids with nanoparticle suspensions). Thus it will be worthwhile to briefly describe boiling in general and film boiling in specific.

Boiling is a phenomenon, which we encounter in our daily activities to large industrial applications. It was a great breakthrough when people found out that large heat transfer rate can be achieved for small temperature difference such as boiling, due to phase change (latent heat). Also the buoyancy forces that occur as a result of density difference between the phases enhance fluid motion near the heater. The result is very interesting as it makes heat transfer equipments economical and handy by largely minimizing the size of the components (e.g. in space applications).

Boiling can be categorized in to two main types in terms of the geometric situation: flow boiling and pool boiling. In flow boiling, the boiling occurs when the liquid is passing through a heated channel. This mode of boiling involves convective heat transfer in addition to nucleate and film boiling. Pool boiling is a boiling from a heated surface submerged in a volume of stagnant liquid. The term saturated pool boiling is used when the temperature of the liquid is at a saturation point. However when it is less than the boiling point, it is termed as subcooled pool boiling.

Nukiyama (1934) performed an experiment immersing electrically heated platinum wire in water. He derived the heat flux and the power from the current in the wire and voltage across the ends; and the temperature of the wire obtained from the resistance of the wire. He plotted the result in heat flux versus the superheat temperature (temperature of the wall of the wire minus the saturation temperature of the water). The result was a hysteresis loop, and then he suggested a complete curve connecting the heating and cooling curves on each side. Later, another method to draw the complete curve was illustrated that was controlling the temperature rather than the heat flux. This time there was no hysteresis. Heat transfer rates in pool boiling are usually presented as a graph of surface heat flux against heater wall surface temperature (Tw) or wall super heat (Tw-Ts).

Basically there are two experimental approaches to derive a boiling curve: steady state and transient quenching methods. The great majority of pool boiling studies have been performed under steady state conditions with either direct electrical heating or the use of high temperature secondary fluid. And boiling curve obtained with this method is assumed to be a "true" boiling curve [Bergles and Thompson (1970)]. However, a limitation to the steady state method is when a very high temperature metal needs to be quenched. In such cases the boiling curve will experience the transition and film boiling region, which couldn't be obtained from a steady state experiment especially with water due to dry out problem. In contrast, transient quenching method is believed to be easy and fast. Predicting the transient temperature of a quenched piece is the interest of metallurgists. They control the hardness of the piece by regulating the temperature history of a quenched piece. This has been performed by deriving the surface heat transfer coefficient from the steady state boiling experiment and applying it to calculate the transient temperature of the metal. The study in this thesis utilises the transient quenching method to draw the boiling curve.
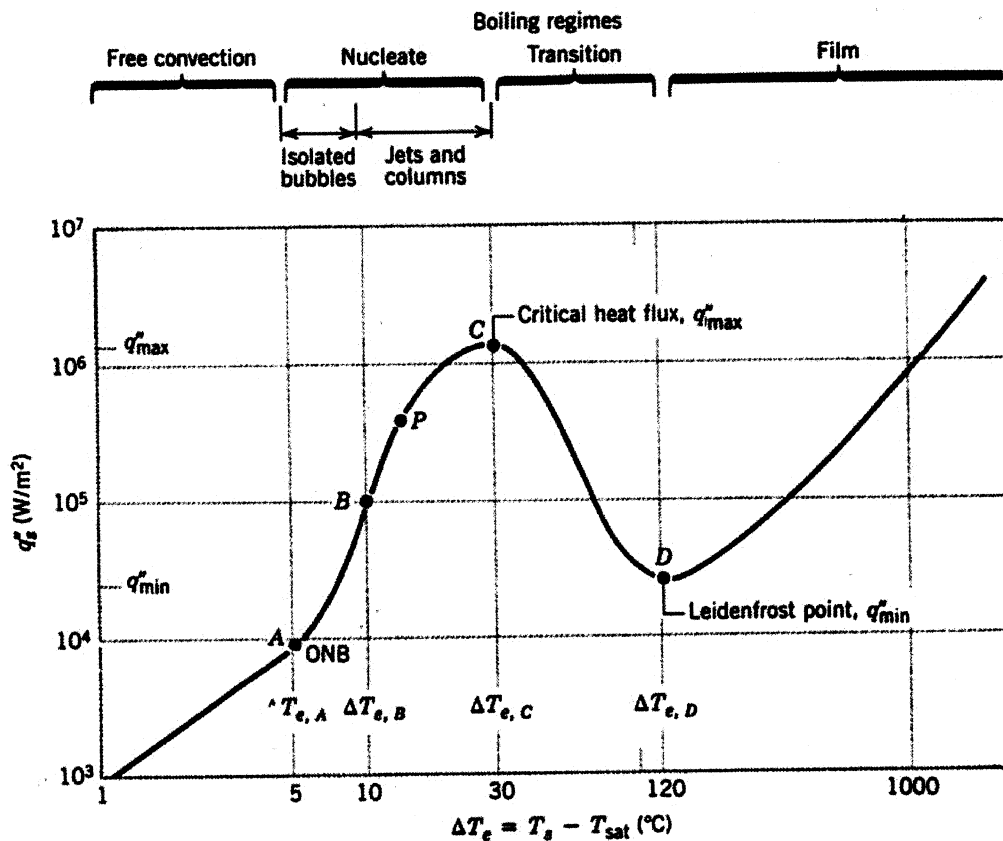
**Figure 1. 1** *Typical boiling curve for water at one atmosphere: surface heat flux $q_s''$ as a function of excess temperature, $\Delta T \equiv T_s\text{-}T_{sat}$. (Incorpera, Fundamentals of Heat Transfer, 1981, book)*

Boiling curve comprises different regions:

- **Natural convection region** – where the temperature gradients are set up in the pool and heat is removed by natural convection to the free surface and thence by evaporation to the vapour space. In this regime since the excess temperature is low, insufficient vapour is in contact with the heated surface for bubble formation

- **Onset of nucleate boiling (ONB)** – where the wall superheat becomes sufficient to cause vapour nucleation at the heating surface.

- **Nucleate boiling region** - where vapour nucleation occurs at the heating surface. At low heat flux and superheat temperature, a few individual nucleation sites produce vapour, which behave independently and departure of isolated bubbles. As heat flux increases, the vapour structure changed and increased bubble formation causes the bubbles to start to merge and to depart from the heated surface by means of jets. These form large bubbles or slugs above the surface. Finally, at high heat flux vapour patches and columns are formed close to the surface. Further rise of temperature, an inflection point is encountered when temperature increase does not result in increase of heat transfer coefficient.

- **Critical heat flux (CHF) point** – where the upper limit of the nucleate boiling reaches the interaction of the liquid and vapour streams cause a limited liquid supply to the heating surface. when the corresponding surface temperature exceeds the melting point of the surface, the surface will melt causing major mechanical failure.
- **Transition boiling region** – when unstable vapour blanket of the heating surface presents. Large patch vapours at more or less regular interval are released. Intermittent wetting of the surface is believed to occur. This region can only be studied under conditions approximately to constant surface temperature. As the minimum film boiling point is approached, larger area of the surface is covered by vapour blanket.
- **Film boiling region** - where a stable vapour film covers the entire heating surface and vapour is released from the film periodically in the form of regulating spaced bubbles.

Film boiling exists when the temperature difference across the interface is sufficiently large enough to sustain it (usually over 100 K – 700 K, depending on subcooling, surface condition and liquid flow velocity). Therefore film boiling is a common phenomenon in quenching of highly heated surface in Iron and Steel Industries, Nuclear Power plants, and others that deal with heating and cooling of specimens.

In general, the transport of heat across the vapour film from the wall to the interface can be accomplished by convection, conduction and radiation. At relatively lower temperature conduction and convection controls the heat transfer through the vapour blanket. As the superheat temperature increases the radiation heat transfer becomes significant. The radiation may depend on the nature of solid surface. When the radiation effect is small, the heat transfer for film boiling is independent of the material properties and finish of the surface.

According to the geometry of the interface, film boiling can be categorized in terms of heat surface geometries, e.g., on plane surface (vertical, horizontal upward, horizontal downward, inclined and curved), on cylinders and on spheres. Actually the film boiling on spheres and cylinders is quite similar to each other, both in vapour film configurations and in the ways that the heat transfer data are correlated.

In accordance with the liquid flow velocity the film boiling can be divided in to two regimes: pool (or natural free convection) film boiling and forced convection film boiling. The criterion to distinguish between the two is using Froude's number ($Fr=U^2/gD$). If $Fr^{1/2} < 1,5$ (which means the liquid velocity does not affect the film boiling heat transfer rate) it is natural free convection film boiling. According to the subcooling of liquid, (which is determined by the liquid temperature and system pressure) film boiling is also classified to: saturated and subcooled film boiling

The thesis is structured in chapters as follows.

Introduction to the general boiling definition and typically film boiling portion is described in chapter one. In chapter two, the background and objective of the thesis is explained. A brief review of the literature survey regarding transient quenching, film boiling and proceedings of the new innovative fluid is incorporated in chapter three. Chapter four deals with theoretical model studies of film boiling heat transfer. The experimental approach and observations are discussed in chapter five. Chapter six holds the data reduction methodologies. A preliminary analysis is made on water experiments to verify the present experimental procedure followed the right approach and to generate a water test data for later comparison with the new fluid. This is presented in chapter seven. The results of the new fluids experimented in this thesis are displayed in chapter 8. Finally a summary and conclusion is made on chapter nine that described the effects of the new fluids tested.

# 2. BACKGROUND AND OBJECTIVE

Improvement of the thermal properties of energy transport fluids may become a trick of augmenting heat transfer. Liquid cooling is preferred compared with air-cooling in almost all the high heat flux application. The cooling liquids usually used are water/chilled water, common refrigerants and liquid nitrogen or similar cryogenic depending on the specific application. While water is a convenient and safer medium, its relatively poor heat transfer characteristic is a major disadvantage. Under the circumstances it makes sense to look at alternatives. Much focus has been given to enhance the heat transfer coefficients in many fields. As a result huge numbers of studies have been conducted to improve heat transfer coefficient consequently minimize size and cost. Among the efforts one was to roughen the surface.

An innovative way of improving the thermal conductivity of fluids is to suspend small solid particles in the fluids. Various types of powders such as metallic, non-metallic and polymeric particles can be added in to fluids to form slurries. The thermal conductivity of fluids with suspended particles is expected to be higher than that of the common fluids. Because of their excellent characteristics, the nanofluids find wide applications in enhancing heat transfer. The key point that makes these fluids interesting is that they give thermal enhancement better than coarse-grained material.

- 5 vol. % CuO nanoparticles showed an increase of 60% in thermal conductivity
- 0.3 vol. % Cu (<10nm) made 40% rise in thermal conductivity.
- Use of $Al_2O_3$ particles, 13nm in diameter at 4.3%, increased thermal conductivity of water by 30%
- Use of some larger particles (40nm) in diameter only led to an increase of less than 10 %.

The interest in subcooled film boiling has revived because of certain hypothetical accident situations in nuclear reactors. It is especially very important in that safety analysis of nuclear power plant where water is used to cool high temperature fuel rods. For example, knowledge of the film boiling heat transfer and the minimum temperature to sustain film boiling is essential to determine core coolabilty after a hypothetical loss-of–coolant accident (LOCA) in light water reactor, also to assess the potential for fuel-coolant interaction after a core disruptive accident in a light water or fast breeder reactor. Awareness of the minimum film boiling temperature under subcooled conditions is also importance to assess the possibility of a fuel-coolant interaction. Although not much consensus exists on the cause and classification of these interactions, it is generally accepted that if the solidification temperature of the molten material were higher than the minimum temperature needed to support a vapour film under natural conditions, the interaction would be benign. [Dhir (1988)]

Film boiling is stable at higher temperature. As the temperature decreases it reaches to the minimum film boiling point where the vapour is collapsed

7

making a pop sound. If the destabilization occurs at relatively higher temperature, such event may lead to other phenomenon called vapour explosion that pose a threat to plant equipment and personnel, particularly in Nuclear and Metallurgy industries. The manner in which a stable vapour film is destabilized at the onset of transition determines the occurrence of vapour explosion. The term vapour explosion is used to describe those non-chemical explosions that can result when molten material, usually a metal is quenched in a liquid. The energy release in vapour explosion is caused by the rapid vaporization of the quenching liquid resulting in pressure wave. It is probable that the triggering mechanism for molten metal particle fragmentation (a massive break up yielding many small particles) and ultimately the vapour explosion may be dependent on the behaviour of the vapour film at the onset of transition. Thus the study has been under taken to enhance the knowledge of film – to - transition phenomena, investigating the physical mechanism of the suppression of vapour explosion in different fluids as a supplement for the steam explosion experiment under way in the division

Numerous investigators have studied film boiling heat transfer theoretically and experimentally. Nevertheless, little information seems to have been generated and consequently experimental data is in large scarce. Besides, more of the earlier experiments and studies were limited to common type of fluids such as water, refrigerants and cryogenic liquids.

On the other hand, if we observe it from the point of view of metallurgists, prediction of the temperature history of a very hot solid quenched in a boiling liquid is of importance heat treatment of metals. Effective cooling method is highly applicable in the field of Steel and Iron industries, nuclear power plants, and some microelectronic devices making thermal management process. Especially, understanding of the heat transfer characteristic of film boiling and transition boiling is very important for actual cooling process of strip mills.

The study will also have a great input in finding means to facilitate proper quenching. Thus the addition of low volume percentage of $Al_2O_3$ nanoparticles in distilled water will be investigated as to how this will affect the destabilization of the vapour blanket.

## 2.1 Objective

The objectives of this study are:
- To investigate the film boiling phenomena in various subcooled liquids using a sphere quenching experiment.
- To study the film boiling in water and nanofluids in terms of liquid subcooling, heated sphere temperature, nanoparticle concentration and sphere diameter
- To study minimum film boiling point for the different fluids as supplement for the steam explosion experiment investigating the physical mechanism of the suppression of vapour explosion in different fluids.
- To examine the sphere diameter effect in the film boiling

- To understand the film boiling and transition boiling to facilitate proper quenching

The complete boiling curve can be derived for the nanofluid, if the film boiling regime and the transition boiling are analysed. The paper is also intended to examine the effect of the nanofluid in the film boiling heat transfer and phenomena.

# 3. LITERATURE SURVEY

A vast number of studies have been made on boiling phenomena and boiling curves either from a steady state or quenching experiments. For film boiling heat transfer, the later method is used more commonly. A brief review of the literature that covers some investigation that deals with nanofluid, quenching, and film boiling is presented.

## 3.1 Nanofluids

Particles suspended in a fluid were reported to have enhancing effect in boiling heat transfer. The improvement was due to their thermal conductivity, which is better than the common fluids. However the industrial application of the large dimension (mm or μm size) suspended particles is limited due to their effect in creating abrasion, rapid settlement, clogging and pressure drop. The nano-technology brought a breakthrough; to avoid the major limitations of large sized suspended particles.

Particles less than 100nm in diameter exhibit properties different from those of conventional solids, their specialty is in providing much larger relative surface area and a great potential heat transfer enhancement of fluids. Investigators continued their research with suspension of nanoparticles in a basic fluid. Choi (1995) used the term "nanofluid" to refer fluids with suspended nano particles. Eastman et al (1999) demonstrated that solid nanoparticle colloids (i.e., colloids in which the grain have dimensions of ≈10-40nm) are extremely stable and exhibit no significant settling under static condition for weeks or months. They are easily fluidized; these particles can be approximately considered to behave like a fluid. The nanofluids showed an increase in viscosity with particle concentration but remains Newtonian in nature. Because of their excellent characteristics, they have wide use in enhancing heat transfer even in micro scale heat transfer.

Experiment results of Eastman et al (1997) showed an increase in thermal conductivity of approximately 60% could be obtained by using 5 vol. % CuO nanoparticles in water. The main reason for the enhancement is believed to be due to:
- The suspended nanoparticles increase the surface area and the heat capacity of the fluid.
- The suspended nanoparticles increase the effective (or apparent) thermal conductivity of the metal.
- The interaction and collision among the particles, fluid and the flow passage surface are intensified.
- The mixing fluctuation and turbulence of the fluid are intensified
- The dispersion of nanoparticles flattens the transverse temperature gradient of the fluid.

### 3.1.1 Preparation of Nanofluids

Preparations of nanofluids require: even suspension, stable suspension, durable suspension, low agglomeration of particles, and no chemical change of the fluid. The effective methods that have been employed to prepare suspensions are: to change the pH value of suspensions, to use surface activators and/or dispersants, and to use ultrasonic vibration. These techniques are believed to result in changing surface properties of suspended particles and suppressing formation of particles cluster in order to obtain stable suspensions.

The common activators and dispersants are thiols, oleic acid, and laurite salt. Xuan, et al (2000) mixed Cu nanoparticles with transformer oil by 2 and 5% volume respectively. Oleic acid was used as a dispersant and the suspension was vibrated for 10 hr in ultrasonic vibrator. The experiment result showed, in case of the percentage of oleic acid amounts to 22 % of the particle, the stabilization of the particle obtained to last up to one week in the stationary state and no sediment was found. On the other hand adding laurite salt to water-Cu nano-particle suspension and using ultrasonic vibration, the stable suspension could last more than 30hr in the stationary state.

Das et al (2003) prepared the suspension, quite stable at lower (1% and 2%) volume concentration. At higher concentration (3% and 4%) very nominal amount of sedimentation occurred after 6hrs. When they prepared the suspensions using ultrasonic vibration for 4hrs, they didn't use any stabilizing agent like laurite acid, to avoid the confusion, which the surfactant could bring considerable effect in reducing surface tension.

### 3.1.2 Heat Transfer Enhancement of Nanofluids

Although a number of studies showed the nanofluids to have a great potential for enhancing heat transfer, research work for developing the theoretical concept, of the enhancement mechanism and application of the nanofluids are still at the infant stage. A better understanding of their characteristic and heat transfer performance is important for the practical application to heat transfer enhancement. Choi (1995) quantitatively analysed some potential benefits of nanofluids for augmenting heat transfer and reducing size, weight and cost of thermal apparatus, while incurring little or no penalty in pressure drop.

Investigations have been carried out to see the enhancements in the different regimes of boiling. In the natural convection regime, Eastman, et al (2000) have observed 40 % increase in heat transfer capability with a 2% particle concentration.

Xuan and Roetzel (2000) analysed heat transfer performance of the nanofluids and discussed the different approaches to understand the

mechanism of the enhancement. Besides, they tried to show some fundamental correlations. Little literature is found in correlating the heat transfer coefficient of nanofluids. The heat transfer coefficient (Nusselt number) of nanofluids is expected to be a function of different parameters as:

- Heat capacity and thermal conductivity of the nano particles and the base fluid,
- The viscosity of the nanofluids,
- The flow pattern,
- The dimension and shape of nano particles and
- The volume fraction of suspended particles.

Thus, the general form of Nusselt number is

$$Nu_{nf} = f\left( \text{Re}, \text{Pr}, \frac{k_s}{k_f}, \frac{(\rho c_p)_s}{(\rho c_p)_f}, \phi, \dim ensions\, and\, shape\, of\, particles,\, flow\, structure \right) \dots$$

..................................................................................(3.1)

Two approaches to study the effect of suspensions were mentioned in the literature: two phase and single phase approaches. The first one needs much computation time and computer memory, but helps to understand the functions of both the fluid phase and solid particles in the heat transfer process. The later simplifies the analysis by assuming thermal and dynamic equilibrium and no motion slip between discontinues phase of the dispersed ultra fine particles and continues liquid. In the second way, nanofluids can be treated as common pure fluids, which imply the Navier Stoke's equation is applicable except the thermal and transport properties are those of the nanofluids. All the dimensionless correlations for the heat transfer of the pure fluids also holds for the nanofluid. In general the approach is a way of approximating the heat transfer coefficient of nanofluids through extending the existing heat transfer coefficients for the basic fluid.

After replacing the thermal properties and transport parameters of pure fluids, Xuan and Roetzel (2000) reported the augmentation effect of heat transfer to be approximetly indicated by the ratio,

$$\frac{h_{nf}(nanofluid)}{h_f(base\, fluid)} \approx \left( \frac{k_{nf}}{k_f} \right)^c \qquad \dots\dots\dots\dots\dots\dots\dots\dots\dots\dots\dots\dots\dots(3.2)$$

c is a constant that depends on the flow pattern. They also noted that with such formulas it could be possible to approximately estimate the heat transfer enhancement of nanofluids increasing its thermal conductivity.

A modified single phase model has been employed in the study of Xuan and Roetzel (2000) to simulate heat transfer process of nanofluids flowing through a tube. It is described that the slip velocity between the fluid and the particles may not be zero although the particles are ultra fine. Besides, because of the effects of several factors such as gravity, Brownian force, and friction force between the fluid and ultra fine solid particles; the phenomena of Brownian

diffusion, sedimentation and dispersion may coexist in the main flow of the nanofluid. These resulted thermal dispersion to take place in the flow of the nanofluid and increase the energy exchange rates in the fluid caused by irregular and random movement of the particles. The thermal dispersion will flatten the temperature distribution and make the temperature gradient between the fluid and the wall steeper which augments heat transfer rate between the fluid and the wall. It is summarized that the enhancement mechanism could be due to either the suspended particles increase the thermal conductivity of the two phase mixture and/or the chaotic movement of the ultra fine particles or the thermal dispersion accelerates the energy exchange process in the fluid.

Keblinski et al (2002) explored the possible explanations for the unusual enhancement of heat transport in nanofluids. They examined separately the comprehensive list of factors and discussed the possibilities that the enhancement arose. Brownian motion of the particles and molecular-level layering of the liquid at the liquid/particle interface was analyzed. They also examined the nature of heat transport in nanoparticles and the validity of the key assumption of the macroscopic theory of diffusive propagation of heat in both particles and in the liquid matrix. Lastly, the effects of clustering of nanoparticles both by forming direct solid-solid paths and by possible clustering effects mediated liquid existing with in the limit of a short inter particle distance was also considered. The result of their analysis showed that:

- Thermal diffusion is much faster than Brownian diffusion even with the limits of extremely small particles, which means the movement of nanoparticles due to Brownian motion is too slow to transport significant amounts of heat through a nanofluid. But Brownian motion could have an indirect role in producing particle clustering
- The presence of an interfacial layer may play a role in heat transport but it is unlikely to be solely responsible for the enhancement of thermal conductivity
- The assumption of diffusive heat transport in nanoparticles is invalid; consequently a macroscopic theory such as the Hamilton Crosses (HC) theory does not apply and a theoretical treatment based on the ballistic phonon transport is required. In particular, if the ballistic phonons initiated in one particle can persist in the liquid and reach a nearby particle, a major increase of thermal conductivity is expected.
- Clustering of particles into percolating patterns would have a major effect on the effective thermal conductivity clustering to the extent that solid agglomerates span large distance would most likely settle. Indeed, although the percolation threshold for random dispersions is ≈ 15% volume fraction in three dimensions, the usual enhancement of thermal conductivity is already observed at very low volume fractions of ≈1% or less, however in general clustering may exert a negative effect on heat transfer enhancement particularly at low volume fraction settling small particles out of the liquid and creating large regions "particles free" liquid with high thermal resistance

- A molecular simulation is required to investigate the effects in more detail and results of their molecular-level simulation demonstrated inside the solid particle. Heat moves in a ballistic manner that involves multiple scattering from solid/liquid interface, also particle/liquid interfaces plays a key role in translating fast thermal transport in particles into high overall conductivity of the nanofluid the main characteristic of interface from this perspective is the transmission coefficient i.e., how much heat is able to go through the solid/liquid interface rather than get reflected back in to the particle thereby not contributing to macroscopic heat transport.

- In conclusion, while the role of the Brownian motion appears not to be important, an understanding of the effects of other proposed mechanisms (layering at the solid/liquid interface, ballistic phonon transport and clustering) require further experimental and simulation studies.

Some studies have estimated the three basic parameters for the nanofluids: - heat capacity, viscosity, and thermal conductivity; these are often applied for heat transfer and are presented to be different from those of the basic fluid. The parameter $(\rho Cp)$ of nanofluids is expressed as [Xuan and Roetezl(200)]

$$(\rho Cp)_{Nf} = (1-\phi)(\rho Cp)_f + \phi \, (\rho Cp)_s \qquad \dots\dots\dots\dots\dots(3.3)$$

The viscosity of the nano fluid could be estimated with the existing relations for the two-phase mixture.

$$\mu_{eff} = \mu_f(1 + 2.5\phi)\dots\dots\dots \text{Einstein's equation ( restricted to low volume fraction } \phi<0.05)\dots\dots\dots\dots\dots\dots\dots \qquad (3.4)$$

Xuan and Li (2000) have experimentally measured the effective viscosity of the water-copper nanofluid and transformer oil-copper nanofluid. Their experimental results approved relatively well agreement with Brinkman's theory.

### 3.1.3 Thermal Conductivity

Xuan et al (2000) introduced a theoretical study for predicting the thermal conductivity of nanoparticles. They applied the Hamilton and Crosses (1962) model to a water-alumina nanoparticle suspension. The effective thermal conductivity, $K_{eff}$ versus Volume fraction of nano particles was estimated and plotted.

The plot showed that the thermal conductivity of nanofluid is strongly dependent on nanoparticle volume fraction and increases with volume fraction of solid particles. It was also stated that the effective thermal conductivity of suspension could be increased by decreasing the sphericity of the particles under the condition of the same volume fraction. Thus it can be said that the

volume fraction, dimension and properties of nanoparticles are central for the effect of nano fluids on thermal conductivity.

A difference was noticed between Eastmann (1997) and Xuan (2000) measurement of thermal conductivity and that was attributed to the fact that Eastman's nanofluids use CuO and Cu nanoparticles of 18nm in diameter where as Xuan applied nanoparticles of size up to 100nm. Consequently Eastman's nanofluid exhibit more excellent properties.

Theoretically Hamilton and Crosses model predicts $K_{eff}$ as.

$$\frac{k_{eff}}{k_f} = \frac{k_p + (n-1)k_f - (n-1)\alpha(k_f - k_p)}{k_p + (n-1)k_f + \alpha(k_f - k_p)} \quad \dots\dots\dots\dots\dots\dots\dots\dots\dots(3.5)$$

$k_p$     Thermal conductivity of the discontinuous particle phase

$k_f$     Thermal conductivity of the fluid

$\alpha$     Volume fraction of theparticles

n     Empirical shape factor given as $n = \dfrac{3}{\psi}$

where $\psi$ is the sphericity defined as the ratio of surface area of a sphere with a volume equal to that of the particle to the surface area of the particle.
The volume fraction $\alpha$ of the particles is defined as

$$\alpha = \frac{V_p}{V_f + V_p} \quad \dots\dots\dots\dots\dots\dots\dots\dots\dots\dots\dots\dots\dots\dots\dots\dots\dots\dots(3.6)$$

However, it is almost impossible to precisely predict the thermal conductivity of nanoparticles using theoretical approach. Therefore Xuan and Eastmann (1995) used the transient hot wire method to measure the thermal conductivity of nanofluids.

Xuan et al (2000) reported the ratio of the thermal conductivity of the nanofluid to that of the base liquid varied from 1.24 to 1.78 for a volume fraction increase from 2.5 to 7.5 % for water-Cu nanoparticles suspension.

The use of $Al_2O_3$ particles $\approx$ 13nm in diameter at 4.3% volume fraction increased the thermal conductivity of water under stationary conditions by 30% [Masuda, et al (1993)]. Use of relatively large particles ($\approx$ 40nm in diameter) only led to an increase less than $\approx$ 10% at the same particle volume fraction [Lee, Choi, and Eastman, (1999)]. Recently Eastman, et al (2000) reported greater enhancement of thermal conductivity for Cu nanofluids, where just a 0.3% volume fraction of 10nm Cu nanoparticles gave rise of up to 40%.

So far researches focused on theoretical approaches to analyze the enhancement mechanism heat transfer. The urgency of experimental research to verify the models has been pointed out by many of the

investigators to be the future task. Research in micro scale is necessary to learn the microstructure of nanofluids to help understand the heat transfer process well.

## 3. Experiments on Nanofluids

Das, Putra and Roetzel (2003) experimentally studied pool boiling of in water-$Al_2O_3$ nanofluids to investigate the question of whether nanofluids could be used for two-phase application or not. The result negates the new possibility of using nanofluid in phase change condition revealing the significant influence in boiling characteristic deterioration. They have observed that with increasing particle concentration degradation of boiling performance took place, which increased the heating surface temperature. The sizes of the nanoparticles (20-50nm) used were one to two orders of magnitude smaller than the roughness of the heating surface. It was concluded that the change of surface characteristics during boiling due to trapped particles on the surface was the cause for the shift of the boiling characteristics in negative direction. It should be noted that, a standard boiling apparatus was not used in their experiment.

Very recently, Vassallo, Kumar and D' Amicon (2004) conducted pool boiling heat transfer experiments in pure water, 0.5% of volume silica micro solutions (3μm) and 2-9 % volume of (15 and 50 nm) silica-nano solutions. They used a 0.4mm diameter NiCr wire submerged in each solution. The data heat flux versus superheat showed a marked increase in critical heat flux limit (~60% higher) for nanofluids and micro solutions compared with pure water, but no appreciable difference in heat transfer was observed for powers below the limit of CHF. A difference was observed between nano and large silica particles. The wire always failed prior to entering film boiling region for micro silica solution than nanoparticle solution that implied stable film boiling is achievable with the nanosolution than micro-solution at temperatures close to the wire melting point. Surprisingly the wire never failed with 50nm solution and was able to sustain the high heat flux.

They examined the roughness of the surface; suppose the improvement in the heat transfer may be the effect of surface roughness that would change the nucleation site density. The result shows that increased roughness led to a higher attainable heat flux at a given wire superheats with in the nucleate boiling regime even a higher CHF than the virgin wire. However it doesn't appear that this alone would explain the dramatic heat flux attained with the nanosolutions, nor for that matter, with the 3μm silica solution.

In their conclusion, it was clearly observed that the addition of nanoparticles vs micro sized particles allows a significant increase in heat transfer at high heat flux and leads to stable operation with in the film boiling regimes at a temperature close to the melting point. The 50nm silica solution allows a maximum heat flux about 3 times higher than that of pure water.

In summary, there is no consensus in the real effect of the nanofluids, the results of the experiments reported on boiling are not consistent. Moreover the fundamental mechanism is still vague and theoretical studies not been made in detail so far.

## 3.2 Transient quenching

The quenching method uses transient values of temperature vs time and converts them to q vs ΔT curves. It has never been clear whether one is justified in identifying the unsteady state quenching results with those of steady [Peyayopankul and Westwater (1978)]. However, several boiling studies have been employing the transient quenching technique to generate pool boiling data, when short test times were dictated. [Bergles and Thompson (1970)]

Transient calorimeter approach is widely used in metallurgical quenching and heat transfer studies. Regulating the temperature history of quenched piece is been used to control hardness as used by metallurgists. The transient temperature distribution in a piece can be predicted if the surface coefficient of heat transfer is known. It is regarded that the heat transfer coefficient can be derived from the extensive data, which have been obtained for pool boiling heat transfer.

The boiling curve from a quenching test depends on the dimensions: quenching solid, its material of construction, the dimensions of the enclosing vessel, and some times the location of the thermocouple used to get the transient temperature data. These factors can be standardized so that the resulting data are applicable to commercial equipment. [Westwater, Hwalek and Irving, (1986)]

Different studies have considered whether transient quenching experiments provide data equivalent to those from steady state boiling tests. Bergles and Thompson (1970) studied the quench and steady state data. They did experiments with three different fluids: Freon-113, water and nitrogen. Solid copper with 0,3 in cross-section diameter and 3 in long rod was employed. Freon–113 and Nitrogen are used to have a film boiling at lower temperatures for the steady state experiment. The steady state experiment with water was limited to nucleate boiling due to burnout problem at maximum heat flux. They explained the results of their observation as; they found the specimen fouled with carbon as the film boiling region was traversed in experiments with Freon-113. Nucleate boiling region was observed to shift to a lower ΔT. This was explained to be due to carbon deposit resulted in change of nucleation site distribution. However, the peak nucleate heat flux was relatively unaffected. The film boiling region showed a slightly higher heat transfer coefficient compared with clean specimen. Besides, repeated quench runs with out cleaning the carbon scale was observed to have effect of shifting the curves in favor of decreasing quenching time. After comparison made with steady state runs, they concluded that in case of quenching with Freon the peak heat flux point shifted to a lower heat flux and considerably higher wall

super heat point, while the minimum film boiling point to lower heat flux and lower wall superheat. This could be attributed to a large scale formation in steady state tests due to longer exposure to higher temperatures. In water tests, they encountered uncertainties in their data to interpret the result; it was reasoned to be the effect of large axial temperature gradient. Nevertheless, the effect of quenching was generalized to be elevating the minimum heat flux. When a steady state tests were made with nitrogen on a copper cylinder 12.7 mm in diameter and 76 mm long, the maximum heat flux was at a higher $\Delta T$ than observed when quenching tests were made on a copper torus of 12.7cm solid diameter x 140 mm ring diameter, but the peak heat flux values were similar. The film boiling minimum heat flux was much bigger for the steady tests compared to the quench tests. However, as the geometries were not the same it was difficult to recognise the observed differences for steady vs. quenching boiling curves.

In the same way, without taking in to account the effect of comparing non-identical geometries, Tachibana and Enya (1973) found that the maximum heat flux during quenching of a copper disc (50 mm in diameter and 2mm thick) with one face in contact with ethanol was slightly lower than the steady state value for ethanol boiling on one end of a 18 mm diameter cylinder. For the minimum film boiling heat flux the difference was even higher.

Veres and Florshuetz (1971) avoided the confusion of non- identical geometry by using a 23.8 mm dia. copper sphere for both steady state and quench tests in Freon-113. For film boiling good consistency between steady state and transient results was obtained, however the results were different in nucleate boiling regime.

Pyayopanakul and Westwater (1978) studied the limits of unsteady quenching method in determining the boiling curve. In their principle study, they did a series of quenching tests with horizontal circular end of a 50.8 mm diameter cylinder copper block in liquid nitrogen at atmospheric pressure. The boiling curves from the quenched data was analysed and the variations in all boiling regimes: nucleate, maximum heat flux, transition, minimum heat flux and film boiling were reported. The total cooling time from a room temperature of about 298K to the liquid nitrogen temperature of 77K was varied from 7hr for 51cm thick slab to 2 min for 0,05cm thick slab. The film boiling took most of the cooling period. Cooling time was observed to be roughly linear with copper thickness. This led them to the conclusion that the boiled liquid nitrogen hydrodynamics has more pronounced effect than conduction, thus conduction is not the controlling mechanism. They have also pointed out that the result could be different for other liquid-solid combination. During quenching, the changes in temperature are most rapid around the maximum heat flux area. Considering the time required to pass over the top 10% of the boiling curve as a criterion for assuming quasi steady state to exist; a limiting time of 1sec for a minimum thickness of 2,5cm could be taken to consider quasi-steady state. If a thinner slab is used the maximum heat flux is observed to be lower.

Moreover, in film boiling region a good agreement with steady state boiling curves was obtained for thickness larger than 0.4cm. Thinner blocks had much lower heat flux, thus minimum thickness of 1.3cm was determined to be a limiting condition for permitting quasi steady state assumption in transition and nucleate boiling regimes excluding values close to maximum and minimum heat flux. Below the given thickness the curves were observed to shift towards higher $\Delta T$. They mentioned uncertainties to give conclusion on the Leidenfrost point. Nevertheless, they found out that the Leidenfrost point for quenching is determined by temperature instead of heat flux. Overall, the transient quenching experiment showed a quasi-steady approach for the whole boiling curve of thickness above 2.5cm. The Biot number at maximum heat flux is calculated to be 0.9.

Hendricks and Baumeister cited in Westwater et al (1986) supplied a model for film boiling and it showed that small spheres give larger heat fluxes than large spheres. Then Leinhard (1973) came up with the same conclusion and defined very small diameter to be a diameter smaller than the hydrodynamic wavelength. Based on his hypothesis, Westwater suggested, to attain quasi steady state behaviour, the limiting diameter of 5cm for all metals in all ordinary liquids. [Westwater Hwalek, and Irving (1986)]

Lin and Westwater (1982) reported a decrease in critical heat flux with corresponding shift towards higher superheat in their research to examine the effect of metal thermal properties on the maximum and minimum heat flux points. Their experiment includes five different metals: Zinc, lead, aluminum, bismuth and copper with liquid nitrogen. For a transient data to approach the quasi steady state condition, a minimum Biot number of 0,9 was suggested.

Generally it can be said that the commonly accepted method for determining the "true" boiling curve, q Vs $\Delta T$, for a liquid is to measure the heat flux and surface-to-liquid temperature driving force during a series of steady state tests. However this method is not always applicable. For instance, with fluids having high boiling points, film and transition boiling is difficult to obtain with conventional steady state apparatus due to burn out or lack of secondary fluid with high enough temperature. In such circumstances, transient quenching experiment is the right choice since the experiment is traversed in reverse direction of the boiling curve. Besides, the use of quenching techniques to determine the boiling curves has been proved to be a more rapid and easier method than the steady state method.

In their film boiling study, many of the researchers employed transient calorimeters and have assumed that their data are comparable to data that have been derived from steady state boiling curves from a similar surface – fluid combination. Thus transient quenching is found to be suited for the study of film boiling over spheres in subcooled liquid pool, which is to be conducted in this thesis.

### 3.2.1 Surface Effect

<u>Roughness</u>

In a study conducted by Bernardin and Mudawar (1996) inspection made before and after each heat-quench cycle revealed considerable changes in surface roughness, in turn dependent on initial surface finish of the specimen. The transient cooling curve was shifted to a shorter quench period followed by a rise in Leidenfrost temperature as the test was repeated. This was speculated to be the effect of the surface roughening, which happened during heat-quench cycle. Most of the roughening was expected to be the result of a hydrogen diffusion phenomenon from the break down of water molecules during high temperature oxidation of the aluminium surface. Al-1100 samples had this effect that leads to creation of surface pits and blisters on the polished and particle blasted surface. On the other hand, Al-2024 samples with polished, particle blasted, and extruded surface finishes did not show measurable change in surface roughness during heat treatment. The authors explained this as the result of low solution heat treatment temperatures and effect of alloying elements.

A large number of studies have showed the effect of a roughen surface. In most of the studies, there is consensus on the fact that a better heat transfer at a given superheat temperature can be obtained with roughening the surface. Nucleate boiling heat flux is observed to be improved by roughness if consistent roughening technique is used. However, researches showed that the effect to be confined only to nucleate boiling region. Surface roughness and wettability had different results; this is why the earliest known boiling enhancement effort done by Jacob and Fritz and by Sauer, as cited in Bernardin and Mudawar (1996) end up in rapid deterioration of the boiling heat transfer with time. Roughness has a very understandable positive effect on the number of active nucleation sites as observed in the nucleate boiling region. Direct access of the liquid to the surface during nucleate boiling renders this boiling regime most sensitive to micro-surface geometry. Liquid access is much more limited during the transition boiling regime due to an intermittent vapour blanket between the liquid and the surface, rendering any surface roughness features which are smaller than the thickness of the vapour film ineffective at promoting nucleation. This blanket becomes fairly continuous during film boiling where the effect of surface roughness is less clearly realized.

<u>Oxidation</u>

Chowdhury and Winterton (1985) reported a clear effect of surface. They did a quenching experiment with aluminum and copper cylinders in water or methanol. The surface wettability effects were presented in terms of solid-liquid contact angles determined by solid and liquid surface energies. They observed an increase in heat flux with decrease in contact angle for all the specimens in transition boiling region. No effect is seen in nucleate region. The effect improvement observed with lower contact angle was not limited to

transition boiling region, it also covered the critical heat flux and minimum film boiling heat flux. In conclusion they remarked, a lower contact angle has the effect of extending the nucleate boiling region giving a higher critical heat flux and also it extended the transition boiling region by increasing the minimum film boiling heat flux and the associated temperature. They suggested that the effect observed has a possible practical application in that if improved heat transfer during quenching is required, this might be obtained with a low contact angle surface.

Berenson cited in Bergles and Thompson, in his data of measured contact angle showed lower contact angle had improved heat transfer rate. Oxidized surface had the effect of increasing the wettabilty (lower contact angle) implied that the surface chemistry is more important than the roughness. It was also observed that transition boiling heat transfer be improved with decreasing contact angle

In the experiment of Bergles and Thompson, scaling was pointed out as a reason for mismatch of the results of quenching tests and steady state runs. Freon tests showed porous layer of carbon covered the surface. They discussed how the quenching curve displaced to higher superheat. They explained the effect as the roughness caused by the carbon introduced disturbance in the film increasing the chance of liquid touching the wall. The liquid spreads fast due to the good wetting characteristics of Freon. Besides, the carbon showed additional effect of increasing the nucleation site during transition boiling resulting in higher heat flux in this regime. Thus the usual way of linearly connecting the maximum and minimum heat flux points to define the transition curve was no more appropriate. The effect is even more pronounced in quenching curves than steady state as quenching time are greatly influenced. In general, they concluded that early destabilization has resulted in transition and nucleate region to have a lower $q''_{max}$ and higher superheat values than steady state. For water the oxide layer on copper affected the $q''_{min}$ about 4 times the value predicted caused by increase of surface wettability. The carbon deposited in Freon tests caused film destabilization at approximately 10 times the $q''_{min}$ predicted for clean surface. Finally they summarized suggesting strict controlling of surface conditions is required if transient quenching experiment is desired to produce a reliable boiling curve.

## 3.3 Film Boiling

Liu and Theofanous (1994) made a comprehensive survey on the film boiling heat transfer. They have covered the theoretical and experimental studies carried out prior to their study. All the film boiling category and their correlations are also included in their literature survey.

Here in this section, a brief review is made on those film boiling studies, which have significant to the study. A table that consist of the selected correlations is included in the appendix.

## 3.3.1 Pool Film Boiling

Nusselt (1916) laid the first groundwork for film boiling study. He brought the idea that condensation is controlled by heat conduction through the falling liquid film and developed a model of laminar film condensation on vertical surface. Then Bromley [1950] applied his idea and presented a correlation to saturated pool film boiling from cylinders that include radiation effect. The correlation presented by Bromley did not include the diameter effect. Breen and Westwater (1962) then take into account the diameter parameter and applying Berenson's critical wavelength formulated a semi-empirical correlation for saturated film boiling over a wide range of diameter. Berenson (1962) applied Taylor-Helmhotz Hydrodynamic Instability concept to replace the tube diameter with the critical wavelength.

Sparrow and Cess (1964), described subcooling as an enhancement to film boiling heat transfer. Employing a boundary layer type analysis and with a rigid wall assumption at the vapor-liquid interface, they pointed out five parameters that define the heat transfer coefficient:

$$\underline{\mathrm{Pr}_{v}}, \ \underline{\mathrm{Pr}_{l}}, \ \underline{Cp_v * \Delta T_w / h_{fg}}, \ \underline{Cp_l * \Delta T_{sub} / h_{fg}}, \ \underline{\left[((\rho\mu)_v /(\rho\mu)_l)^2 * (\rho_v/\rho_l) * (Cp_l / \beta h_{fg})\right]^{1/4}}$$

Later applying the non slip condition at the interface for the shear stress and the velocity, Nishikawa and Ito (1966) added one more parameter, $(\rho\mu)_v /(\rho\mu)_l$.

A laminar analysis was also applied by Frederking and Clark (1963) to a natural film boiling. Next Frederking and Hoppenfeld (1964) obtained heat transfer coefficient for the high and low subcooling cases.

On their study of subcooled film boiling heat transfer from vertical plates, Frederking et al. demonstrated in 1965 that it is possible to treat vertical plates, spheres and horizontal cylinders using the same expression multiplied only by a numerical constant to characterize one of the geometries.

Baumeister and Hamill (1967) developed a theoretical model for pool film boiling from small diameter wires. Following the same principle, Hendick and Baumeister (1969) characterize the size of the vapour dome using the critical wavelength $\lambda c$ and applied the principle of maximum rate of entropy production. Nishikawa et al (1976) introduced continuities of velocity and shear stress at the vapour-liquid interface and performed a theoretical analysis for subcooling film boiling heat transfer from a vertical plate and horizontal cylinders.

Grigoriew, Klimenko and Stephen (1982) combined the two approaches (1/4th and 1/3rd power law) to account for the diameter and the turbulent effect. For small diameter they used laminar film boiling (1/4 law) and for large diameter

22

turbulent film boiling (1/3$^{rd}$ law). Their correlation fits well with the data from 11 research groups, which include five liquids and different size sphere diameters 0.25 to 96 mm range. Irving and Westwater (1986) indicated that when d/$\lambda$c >7.8, the heat transfer coefficient will no more depend on the diameter of the sphere.

Sakurai et al (1990) presented an accurate numerical solution verified against extensive set of data for cylinders and spheres. It included saturated and subcooled water at atmospheric and elevated pressure with consideration of radiation effect. They have also introduced an empirical diameter correction factor to account for the diameter effect on their correlations. In the same manner Liu and Theofanous (1994) proposed a similar correlation after comparing with an extensive database.

Tou and Tso (1995) proposed an improved analytical model for film boiling over sphere. The model is pretty much similar to Frederking and Clark model [Frederking and Clark (1963)] except spherical coordinate is employed. The result of their model showed the Nusselt number to approach a value of 2 as the Rayleigh number goes to zero instead of zero. They also got a constant C that varies from 0.586 to 0.828, which is in the same range with Dhir's experimental constant (C=0.8) and Leinhard's suggestion (C=0.67).

Kolev (1998) formulated a semi-empirical film boiling model for vertical plates and spheres that permits separation of the different effects of radiation, subcooling or superheating and computes the heat flux components. The comparison between the predicted and the calculated heat transfer coefficient for all the data from Liu and Theophanous showed an error band of $\pm$ 30%.

## 3.3.2 Forced Convection Film Boiling

Forced film boiling heat transfer is not well studied as pool film boiling. The first analytical work goes to Witte (1963), who made a simple analysis for film boiling on sphere with a given averaged vapor velocity of the potential flow. He suggested that a constant of 2.98 should be used for the saturated film boiling on spheres. Again assuming a potential flow distribution for the liquid velocity field, Wilson (1979) did a theoretical study of film boiling in a sphere in forced convection. He employed Pohlausen's integral technique on the vapor boundary layer and analytically integrated the ordinary differential equation for low and high subcooling cases.

Koboyasi (1965) studied forced convection film boiling heat transfer over a sphere. Linear temperature profile and non-linear vapor velocity profile was assumed. His assumption of non-linear velocity profile was later found to be a better prediction after compared with Witee and Orzco (1984) data.

Epstein and Hauser (1980) considered two extremes: slight subcooling and large subcooling and obtained a theoretical Nusselt number for saturated film boiling in forced convection, employing similarity boundary theory and the perturbation method to model the forced convection film boiling in the

stagnation region of a sphere or cylinder. They also obtained an explicit solution for film thickness. Shigechi and Ito (1983) extended Ito et al (1981)'s study for saturated forced film boiling for subcooled case. The integral method was applied to both liquid boundary layer and vapour film layer to get differential equations.

Fodemski (1992) formulated a model that took into account the forced convection film boiling in the stagnation region of a molten drop and tried to predict the film thickness in his calculation.

Bang (1994) emphasizes the relevance of considering buoyancy term in the theoretical model. He observed that the buoyancy term might not be neglected in the liquid velocity range up to 7m/sec. Generally; his model underestimated the experimental data of Dhir and Purohit. That was reported to be the result of the fact that the model did not account the wavy vapor-liquid interface and it is unable to solve the area beyond the flow separation point. Nevertheless, an improved correlation for the convective heat transfer to the bulk liquid in subcooled film boiling of a sphere in water is proposed for use in predicting vapor generation rate.

## 3.3.2 Experimental Studies

There are no as much reliable experimental data compared with the investigations conducted in the film boiling as the theoretical works. The typical experiments performed are reviewed in this section.

A film boiling experiment was first conducted by Motte and Bromley (1957) with 0 to 40°C subcooled ethyl alcohol, benzene, carbon tetrachloride and hexane from electrical heated graphite tubes (D=9,8-16,2mm) at atmospheric pressure. From the experiment they studied the turbulence effect.

Merte and Clark (1964) did quenching experiment of a heated sphere in liquid nitrogen under different gravity conditions and correlated their data in 1/3 power law. They assumed the transition from laminar to turbulent increased the power from the 1/4 to the 1/3, this happened at a Rayleigh number of about $5x10^7$. The effect of subcooling has been studied using the experiment conducted by Bradfield (1967); he obtained film boiling cool-down transient curves by quenching 59mm diameter pure copper sphere in water at a temperature of 95, 53 and 27 and at atmospheric pressure.

Rhea and Nevins cited in Liu and Theofanous (1994) conducted an experiment with liquid nitrogen, and Schmidt and Witte (1972) did an experiment in Freon-11 and both end up in the same correlation. Marschall and Farrar (1975) obtained the heat transfer coefficient by a partially submerged inconel sphere of 18,75mm in diameter.

Dhir and Purohit (1978) studied the subcooled pool and forced film boiling theoretically and experimentally. The heat transfer analysed theoretically

24

under predicted the experimental data obtained from quenching of 19 and 25.4mm steel, copper and silver sphere in subcooled water. This could be due to the heat loss from the support contributed a large portion in the total heat transfer. Secondly their experiment was operated at the "minimum film boiling temperature state" implying the boiling may be partially in the transition-boiling region. Thus their experimental data may over estimate the film boiling heat transfer from sphere. Toda and Mori (1982) measured the vapour film thickness, heat transfer rates and minimum film boiling temperature in the experiment they performed in a horizontal wire and sphere.

Recently, Liu and Theofanous conducted an experiment that considered the heat loss through the support with transient quenching utilizing induction furnace and suggested a general correlation for all the film boiling category.

### 3.3.3 Effects of Subcooling

In the study made in this thesis an experiment is conducted in highly subcooled liquid and it applied correlations to verify if the experimental procedure followed the right approach. Therefore a brief review of the correlations that take the subcooling in to account will be inevitable. Thus some of the correlations surveyed by Liu and Theophanous are repeated here.

Basically two approaches have been developed to consider the effect of subcooling and radiation. Some of the studies followed Hamill and Baumeister's idea (1967) that applied the addition law in which the general solution enables the total heat transfer coefficient to be evaluated by summing the saturated pool film boiling coefficient ($h_{sat}$), radiation heat transfer ($h_r$), and the subcooled turbulent convective heat transfer ($h_{nc}$) contribution term, which is given by:

$$h_t = h_{sat} + 0.88h_r + 0.12h_{nc}{}^* \Delta T_{sub}/\Delta T_{sup}\dots\dots\dots\dots\dots\dots(3.7)$$

Siviour and Ede (1970) cited in Liu and Theofanous studied highly subcooled film boiling from horizontal cylinders and correlated their experimental data following the addition law:

$$Nu_t = Nu_{sat} + JNu_r + Nu_{nc}(Sc/Sp)(\mu_f/\mu_v)\dots\dots\dots\dots\dots(3.8)$$

$$Nu_{sat} = 0.613[Ar/Sp]^{1/4}, \qquad Nu_{nc} = 0.59[GrPr_f]^{1/4} Pr_f{}^{1/4}$$

where J is 0.78, $Nu_r = h_r d/\kappa_v$ and $Nu_{nc} = h_{nc} d/\kappa_f$

Bradfield (1967) observed the minimum film boiling point increasing with the degree of subcooling. In his experimental study of subcooled film boiling over copper sphere of 60.3mm diameter for every 10K increase in subcooling a wall temperature raise of 70K was measured.

25

A number of researchers, Farahat, Eggen and Armstrong (1972, 1974, 1975) cited again in Liu and Theofanous's study used the addition law, in the study of film boiling from spheres in subcooled sodium and water and correlated their data as

$$Nu_t = Nu_{sat} + 0.88Nu_r + KNu_{nc} \ (Sc/Sp) \ (\mu_f/\mu_v) \dots \dots \dots (3.9)$$

$$Nu_{nc} = 0.75[GrPr_f]^{1/4},$$
$$K=11.9(\Delta T_{sub})^{-0.7} \qquad \text{for d = 25.4mm}$$
$$K=11.9(\Delta T_{sub})^{-0.65} \qquad \text{for d = 19.13mm}$$

In their investigation of subcooled pool boiling, Dhir and Purohit (1978), also applied addition law. Their study showed the minimum film collapse temperature to increase with the liquid subcooling, however flow velocity and properties of the sphere didn't show any effect. Their correlation written as:

$$Nu_t = Nu_{sat} + C_r \ Nu_r + Nu_{nc}(Sc/Sp)(\mu_f/\mu_v) \dots \dots \dots (3.10)$$

Where $\qquad Nu_{sat} = 0.8[Ar/Sp]^{1/4}, \ Nu_{nc} = 0.9[G_rPr_l]^{1/4}$

Others emphasized that: for subcooled film boiling it is the ratio, that is significant, not the difference between the subcooled and the saturated film boiling Nusselt numbers. For instance, Shih and El-Wakil (1981) carried out an analysis for pool film boiling from sphere by using integral method and put their correlation as:

$$Nu/Nusat = 1 + 13,91[ScAr/Gr]0,39 \dots \dots \dots (3.11)$$

They showed that their correlation is supported by experiment with stainless steel spheres of 3.2, 4.8, and 6.4mm in diameter in Freon-11 and Freon-113 with 0-20C subcooling.

Michiyoshi, Takahashi and Kikuchi (1988) also followed the ratio law, and obtained a universal correlation for subcooled pool film boiling from vertical plate, horizontal plate and sphere by an analysis made with integral method.

$$Nu = K(Ar/Sp')^{1/4}M_c^{1/4} \dots \dots \dots (3.12)$$

The correlation was noted to agree well with their data for water and potassium. They conclude that, this will be suitable for characterizing pool film boiling in various non-metallic liquids especially for water.

Shigechi et al (1988) proposed an integral approach of laminar boundary layer in their study of the effect of radiation. They showed the radiation effect is more pronounced with rise in the degree of subcooling. In the analysis, the buoyancy term was taken in to account, however the inertia term in the vapor momentum equation was neglected and also a linear vapor temperature profile was considered. After analysing the effect of different assumptions

regarding vapor velocity profile in the final solution, they reported their result and it fitted well with the data from experiment done on ethanol.

Sakurai et al (1990a, b) formulated a theoretical pool film boiling model that includes the radiation contribution for the case of horizontal cylinder and carried out a rigorous solution. Their study indicated that a rigorous solution is in a good agreement with the simple analytical solutions, which is the same as obtained by Michiyoshi (1988). Subsequently they performed a systematic experiment in a wide range of system pressure, liquid subcooling, surface superheat and cylinder diameter with electrical heated platinum cylinders in various liquids including water, ethanol, isopropanol, Freon-113, Freon-11, liquid Nitrogen and liquid argon. Introduced a diameter depending empirical function K(d') on the right hand side of the correlation and a factor $(1+2/Nu)^{-1}$ on the left hand side (only effective when Nu is very small), they modified their analytical solution based on their experimental out come. Their correlation was given as

$$Nu/(1+2/Nu)=K(d')(Ar/Sp')^{1/4}Mc^{1/4} \dots\dots(3.13)$$

where

Mc is the same as with the Michiyosh's

$K(d')= 0.44d'^{(-1/4)}$,        for d' < 0.14

$K(d')= 0.75/(1+ 0.28d')$,        for 0.14 < d' < 1.25

$K(d')= 2.1d'/(1+3.0d')$,        for 1.25 < d' < 6.6

$K(d')= 0.415d'^{1/4}$,        for d' > 6.6

### 3.3.4 Comparison of Correlations

Liu and Theofanous have made a comparison of film boiling heat transfer correlations as shown in fig 3.1. It included, theoretical correlation of Bromley's, Breen's, Baumeister's, Sakurai's, Hendricks's, and Grigoriev's and experimental data's of: Bradfield, Toda, Aziz, and Dhir. They indicated that in the l'/d range of 0,2 to 1,0, all correlations are well agreed in a band less than 10% except Hendricks's correlation which is about 20 % higher than the others. Bromley's correlation is applicable in this range, but out of this range, Bromley's under predicted the pool film boiling heat transfer. For big diameter case, all correlations tend to depart from Bromley's at the l'/d value of about 0,15 and then keep at a constant level in a band about 13 %. On the other hand for small diameter all the correlations start to deviate from Bromley's at the l'/d value of about 2,0 to 10,0. Hendricks's and Breen's correlation are about 30% higher than Baumeister's and Sakurai's. Under other system pressure than 1 bar and superheat conditions the comparison is little bit different not significant as such.

27
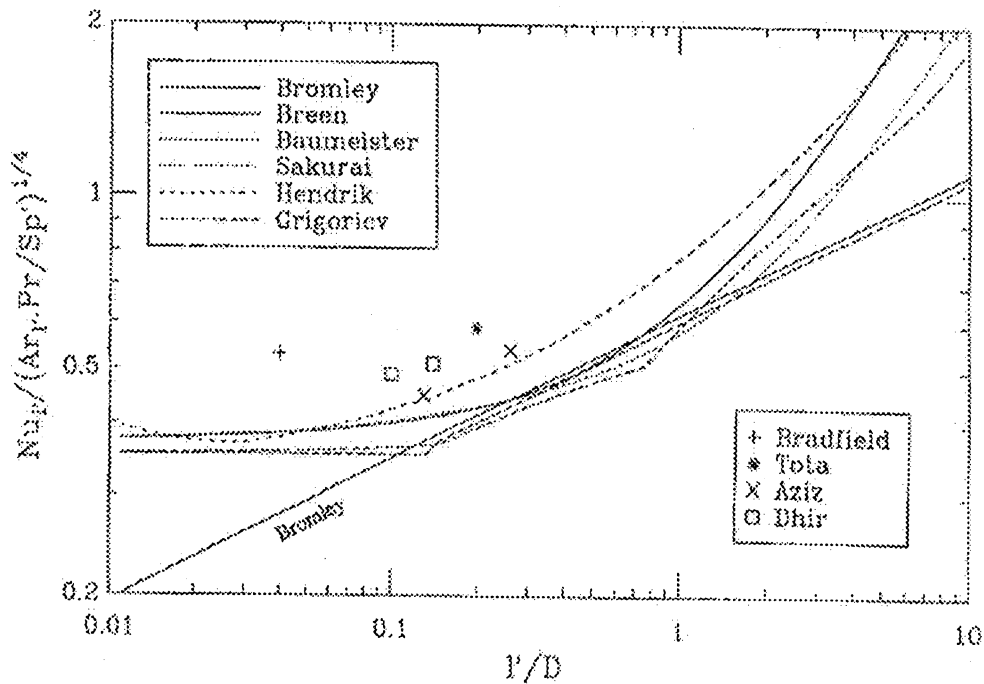
**Figure 3. 1** *Comparison of pool film boiling correlations for saturated condition data with experimental data [Liu and Theofanos (1994)]*

With their experimental database at the condition of 1 bar system pressure, 660C sphere superheat and 9.53 mm in diameter, they also did comparison of pool film boiling correlations at subcooled conditions [Fig. 3.2]. According to the comparison they made Michiyoshi's, Sakurai's, and Dhir's correlation gave fairly consistent prediction except in the low subcooling case in which Dhir's is a bout 15% higher than the other two. Both correlations in ratio form and addition form showed similar trend: Nu increasing with liquid subcooling approximately linearly. The two correlations are also compared at system pressure of 1,10 and 50 bars. It is noted that the increase in pressure has much more effect on the correlation in ratio form than in addition form. Since the correlation in ratio form has been verified by experiment at high pressure as claimed by Sakurai (1990 b), the correlation in addition form with a fixed constant is only valid at certain pressures (for this case it is atmospheric pressure).
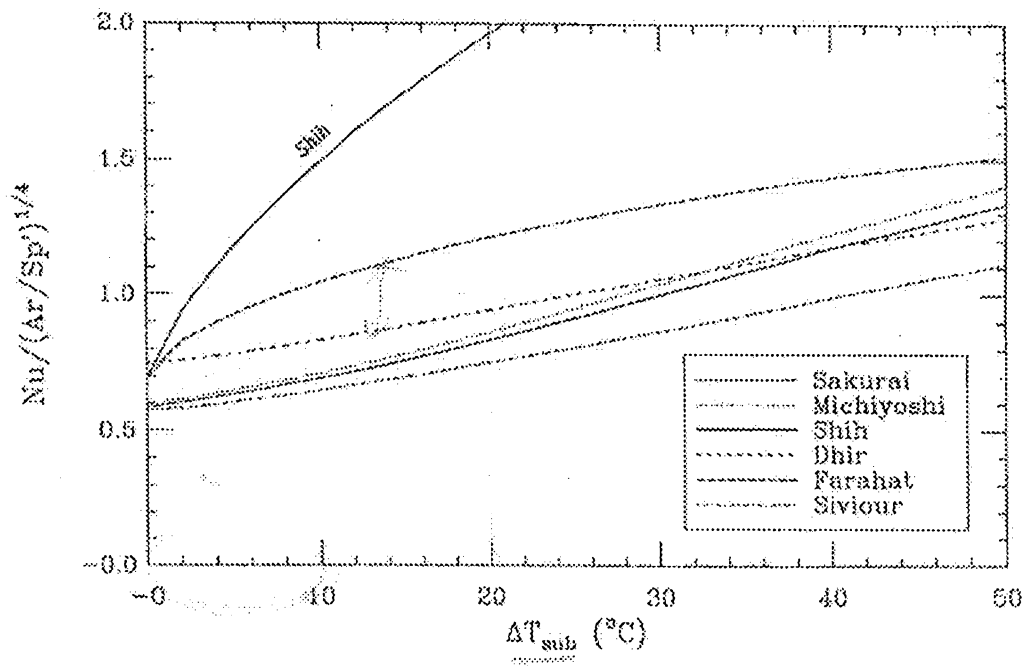
**Figure 3. 2** *Comparison of pool film boiling correlation at subcooled condition (with superheat of 660K at 1 bar Pressure) [Liu and Theofanos (1994)]*

As a concluding remark, they underlined the correlations in ratio form to be likely valid for various of liquids and a wide range of liquid subcooling, surface superheat and system pressure, while the correlation in addition form is only valid in certain conditions.

Most of the film boiling experiments have been conducted with fast cool down transient method, passing a sphere through a still water pool in short time. The sphere traveling time is so short that the thermal response of the sphere and the entrance effect will limit the accuracy of the experimental data. Orzco and Witte (1986) heated their test sphere by circulating Dowtherm G through a passage in a hemisphere sphere. Although this technique avoids the short transient problem it may be difficult to account for the heat loss at the backside of the sphere. Recently Liu and Theofanous's experiment has made advancement in the experiment methodology avoiding the drawbacks and also came up with a correlation that can combine saturated and subcooled film boiling and all the other regimes.

# 4. REVIEW OF THEORETICAL FILM BOILING MODELS

It was planned to devise a model that considered the Buoyancy, and inertia effects that has been neglected in most of the analytical works in formulating a correlation. Therefore theoretical model study has been carried out in the beginning of the thesis, which could help in a sensitivity analysis and the parametric study of the new fluids. However, due to time limitation and the focus was turned to experimentally investigating the effect of nanofluids in film boiling, the task of theoretical study will be pursued in the next step. Here is a review of the theoretical studies made at the beginning.

Extensive studies have been done from theoretical aspects for the film boiling. However they are limited to specific conditions and the analysis was made with simplified assumptions.

Several numerical solutions with simplifying assumptions are also available. Sakurai proposed the most accurate correlation for cylinder geometry. This forms a good approximation of the accurate numerical solution and compares favourably with experimental data for saturated and subcooled water at atmospheric and elevated pressure with radiation effect also considered. Liu and Theofanous have recently recommended the same correlation after comparison with an extensive experimental database. A numerical solution of the combined natural and forced-convection film boiling problem for spheres in saturated, subcooled or superheated water with radiation is possible as demonstrated in the literature, but requires very large amount of computation effort if implemented in system computer codes. To analyse the interaction of fragmenting liquid metal in water, a simple method is needed which has the capability: (a) to reproduce the available data for the heat transfer coefficient for natural and forced convection, (b) to separate the effect of radiation, sub cooling or superheating in order to compute the heat flux component consumed to cool the hot structure, to heat or to cool the liquid, and to produce steam [Kolev (1998)]. Most of the analytical and numerical investigations conducted so far didn't consider either of the points, and neglected most of the parameters that is the driving force for the need of a new model.

## 4.1 Liu & Theofanous Model (1994)

Assumptions
- Two phase boundary layer
- Steady laminar boundary layer

- Density of vapour is negligible.
- Inertia and convection terms are neglected from momentum and energy equations respectively of vapour film layer. (Effective latent heat of vaporization is used to compensate the effect).
- Radiation heat transfer is not considered

Under the above assumptions the fundamental equations are

## For the vapour regime

### Continuity equation

$$\frac{1}{r}\frac{\partial u_v}{\partial \theta} + \frac{\partial v_v}{\partial y} + \frac{u_v}{r}\cot\theta = 0 \tag{4.1}$$

### Momentum Equations

$$0 = -g\rho_v\sin\theta - \frac{1}{r}\frac{\partial p_v}{\partial \theta} + \mu_v\frac{\partial^2 u_v}{\partial y^2} \tag{4.2}$$

### Energy Equation

$$0 = k_v\frac{\partial^2 T_v}{\partial y^2} \tag{4.3}$$

## For the liquid boundary layer
### Continuity equations

$$\frac{1}{r}\frac{\partial u_l}{\partial \theta} + \frac{\partial v_l}{\partial y} + \frac{u_l}{r}\cot\theta = 0 \tag{4.4}$$

### Momentum Equation

$$\frac{u_l}{r}\frac{\partial u_l}{\partial \theta} + v_l\frac{\partial v_l}{\partial y} = g\beta_l(T_l - T_\infty)\sin\theta + \frac{9}{8}\frac{U_\infty}{r}\sin 2\theta + \frac{\mu_l}{\rho_l}\frac{\partial^2 u_l}{\partial y^2} \tag{4.5}$$

### Energy Equation

$$\frac{u_l}{r}\frac{\partial T_l}{\partial \theta} + v_l\frac{\partial T_l}{\partial y} = \frac{k_l}{c_{pl}\rho_l}\frac{\partial^2 T_l}{\partial y^2} \tag{4.6}$$

## Boundary conditions
Two boundary layers are assumed (velocity and thermal)
The boundary conditions and the compatibility conditions at the vapour interface are:

y=0 $\qquad\qquad u_v = v_v = 0$ $\qquad\qquad\qquad$ (4.7)

$\qquad\qquad\qquad Tv = T_w$ $\qquad\qquad\qquad\qquad$ (4.8)

y=δ $\qquad\qquad u_v = u_l = u_\delta$ $\qquad\qquad\qquad$ (4.9)

$$\mu_v\left(\frac{\partial v_v}{\partial y}\right)_\delta = \mu_l\left(\frac{\partial u_l}{\partial y}\right)_\delta \tag{4.10}$$

$$\rho_v\left(v_v - \frac{u_v}{r}\frac{d\delta}{d\theta}\right)_\delta = \rho_l\left(v_l - \frac{u_l}{r}\frac{d\delta}{d\theta}\right)_\delta \tag{4.11}$$

$$T_v = T_l = T_s \tag{4.12}$$

$$-k_v \left(\frac{\partial T_v}{\partial y}\right)_\delta = -\dot{m} h'_{fg} - k_l \left(\frac{\partial T_l}{\partial y}\right)_\delta \qquad (4.13)$$

y=δ + δ$_v$ $\qquad u_l = u_l \qquad \delta_v = \frac{3}{2} U_\infty \sin\theta \qquad (4.14)$

$$\left(\frac{\partial u_l}{\partial y}\right)_{\delta_v} = 0 \qquad (4.15)$$

y= δ + δ$_T$ $\qquad T_l = T_\infty \qquad (4.16)$

$$\left(\frac{\partial T_l}{\partial y}\right)_{\delta_T} = 0 \qquad (4.17)$$

In order to carry out analytical solutions further assumptions are made

- The buoyancy term is neglected
- The thickness of the momentum boundary layer is assumed to be the same as that of the thermal boundary layer in liquid phase

The results of the governing equations are presented as follows

The Nusselt No is formulated as:

$$Nu = Co \left(\frac{Ar}{Sp^1}\right)^{\frac{1}{4}} Mc^{\frac{1}{4}}$$

$$(4.18)$$

Where:

$$Mc = \frac{E^3}{\left[1 + \frac{E}{(Sp^1 P_{rl})}\right]\left(RP_{rl}Sp^1\right)}$$

$$E = \left(A + CB^{\frac{1}{2}}\right)^{\frac{1}{3}} + \left(A - CB^{\frac{1}{2}}\right)^{\frac{1}{3}} + \frac{1}{3}Sc^*$$

$$A = \frac{1}{27}Sc^{*3} + \frac{1}{3}R^2 Sp^1 P_{rl} Sc^* + \frac{1}{4}R^2 Sp'^2 P_{rl}^2$$

$$B = \frac{-4}{27}Sc^{*2} + \frac{2}{3}Sp' P_{rl} Sc^* - \frac{32}{27}Sp' P_{rl} R^2 + \frac{1}{4}Sp'^2 P_{rl} + \frac{2}{27}Sc^{*3} / R^2$$

$$C = 1/2 R^2 Sp^1 P_{rl} \qquad R = \left[(\mu\rho)_v / (\mu\rho)_l\right]^{\frac{1}{2}} \qquad Sc^* = C_{pl}\Delta T_{sub} / h_{fg}^1$$

$$h_{fg}^1 = h_{fg} + 0.5 C_{pv}\Delta T_{sup} \qquad Sp^1 = C_{pv}\Delta T_{sup} / (h_{fg}^1 P_{rv})$$

$$Co = 2^{-\frac{3}{2}} \int_0^x \frac{\sin\phi}{I(\phi)} d\phi = 0.696$$

And the thickness of the film could be described as:

$$\Delta = I(\phi) \left\{ \left(\frac{f + \xi}{f + 4\xi}\right) \left[\frac{16 R \mu_v k_v \Delta T_{sup}}{g(\rho_l - \rho_v)\rho_v h'_{fg}} - \frac{16 R \mu_l k_l \Delta T_{sub}}{g(\rho_l - \rho_v)\rho_v h'_{fg}\xi}\right] \right\}^{\frac{1}{4}}$$

$$(4.19)$$

$$I(\phi) = \frac{\left[\int_0^\phi \sin^{5/3}(\phi)d\phi\right]^{1/4}}{\sin^{2/3}\phi}$$

$$\xi = \left(W_1 + W_2^{1/2}\right)^{1/3} + \left(W_1 - W_2^{1/2}\right) + \frac{k_l \Delta T_{sub}}{3k_v \Delta T_{sup}}$$

$$W_1 = \left(\frac{C_2}{3C_1}\right)^3 + \frac{2C_2C_3}{2C_1^2 f} + \frac{C_3}{2C_1}$$

$$W_2 = \left(\frac{C_3}{2C_1}\right)^2 + \left(\frac{C_3}{C_1}\right)\left(\frac{C_2}{3C_1}\right)^3 + \left(\frac{C_3^2}{fC_1^3}\right)\left[\frac{2C_2}{3} - \frac{4C_2^2}{27fC_1} - \frac{64C_3}{27f^2}\right] \qquad f = \frac{\mu_l}{\mu_v}$$

$$C_1 = \frac{12\mu_v k_v \Delta T_{sup}}{g(\rho_l - \rho_v)\rho_v h'_{fg}} \qquad C_2 = \frac{12\mu_v k_l \Delta T_{sub}}{g(\rho_l - \rho_v)\rho_v h'_{fg}} \qquad C_3 = \frac{6\mu_v k_l}{g(\rho_l - \rho_v)\rho_l C_{pl}}$$

## 4.2 Tou and Tso Model (1997)

An analytical model for stable film boiling heat transfer from a sphere is derived following the classical approach of Frederking and Clark but they used spherical coordinates instead,

Assumptions:
- Laminar boundary layer
- Constant vapour density in the film layer
- Viscous heating is negligible and conduction is dominant in the film
- Inertia effects are negligible
- Fluid properties are constant and surface tension is negligible
- Film layer remains attached on the entire surface with out separation
- Radiation heat transfer is negligible and there is no sub cooling in the liquid
- The effects of waves at the interface are negligible

The governing equations for the film layer in spherical coordinate system after taking the above assumptions in to consideration are the following:

Continuity Equation

$$\frac{\partial}{\partial \theta}(v_\theta \sin\theta) = 0$$

(4.20)

Momentum Equation

$$\frac{\mu_v}{\rho_v r^2}\frac{\partial}{\partial r}(r^2\frac{\partial v_\theta}{\partial r}) + g\frac{\rho_l - \rho_v}{\rho_v}\sin\theta = 0$$

(4.21)

Energy Equation

$$\frac{1}{r^2}\frac{\partial}{\partial r}(r^2\frac{\partial T}{\partial r}) = 0$$

(4.22)

Boundary conditions

Two different types of boundary conditions were considered, which represent two extreme cases. Case 1 assumes that the fluid is immovable and no-slip applies. Whereas case 2 assumes friction is negligible at the interface

The boundary conditions for the film layer are

At θ=0,                                         δ=0                    (4.23)

At r=R                                  $v_\theta$=0,   T= Tw          (4.24)

At r=R+δ                                   T=Ts                         (4.25)

At r=R

$$k_v dA(-\frac{\partial T}{\partial r})_{r=R} = h_{fg}dw_i,$$

dA=2πR²sinθdθ          (4.26)

At the vapour-liquid interface, two cases are taken representing the upper and lower bands

When r=R+δ

Case 1:        $v_{\theta,v} = v_{\theta,l}$    the fluid is immovable and no slip applies

Case 2:        $\tau_v = \tau_l = -v_v(\frac{\partial v_\theta}{\partial r})_i = 0$    friction is negligible at the interface

The results represented in terms of the film thickness and Nusselt no are:

For Case 1

$$\frac{\delta}{R} = 2\left[\frac{8C_p\Delta T_{sup}}{(Ra)h_{fg}}\right]^{1/4}(1+\frac{\delta}{R})\frac{\left[\int_0^\theta \sin^{5/3}\theta d\theta\right]^{1/4}}{\sin^{2/3}\theta}$$

(4.27)

$$Nu = 0,586\left[\frac{Ra}{Ja}\right]^{1/4} + 2 \qquad Ja = \frac{C_p\Delta T}{h_{fg}}$$

(4.28)

Applying the case 2 boundary condition the result reported was

$$\frac{\delta}{R} = \left[ \frac{32 C_p \Delta T}{(Ra) h_{fg}} \right]^{1/4} \frac{\left[ \int_0^\theta \sin^{5/3} \theta d\theta \right]^{1/4}}{\sin^{2/3} \theta}$$

(4.29)

$$Nu = 0,828 \left[ \frac{Ra}{Ja} \right]^{1/4} + 2 \qquad Ja = \frac{C_p \Delta T}{h_{fg}}$$

(4.30)

## 4.3 The Present Model based on Bang's Model
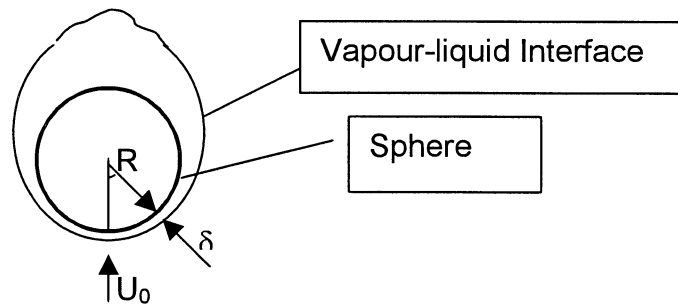
Model Formulation



**Figure 4 1** *Sketch of the assumed model*

The basic flow model is shown in the figure. The models are based on the following assumption.

- Pure, incompressible liquid and vapour
- Smooth liquid vapour interface with laminar vapour and liquid flows
- Uniform surface temperature
- Thin vapour film compared with the size of the sphere
- Constant thermo physical properties
- Thermal absorption is included only at the liquid-vapour interface

The fundamental governing equations are

Vapour region
Continuity Equation

$$\frac{\partial r u_v}{\partial x} + \frac{\partial r v_v}{\partial y} = 0$$

(4.31)

Momentum Equation

$$u_v \frac{\partial u_v}{\partial x} + v_v \frac{\partial u_v}{\partial y} = U_0 \frac{dU_0}{dx} + v_v \frac{\partial^2 u_v}{\partial y^2} + \frac{\Delta \rho}{\rho_l} g_0 \sin\left(\frac{x}{a}\right)$$

(4.32)

Energy Equation

$$u_v \frac{\partial T_v}{\partial x} + v \frac{\partial T_v}{\partial y} = \alpha_T \frac{\partial^2 T_v}{\partial y^2}$$

(4.33)

35

Liquid regime

Continuty Equation

$$\frac{\partial r u_l}{\partial x} + \frac{\partial r \upsilon_l}{\partial y} = 0$$

(4.34)

Momentum Equation

$$u_l \frac{\partial u_l}{\partial x} + \upsilon_l \frac{\partial u_l}{\partial y} = U_0 \frac{dU_0}{dx} + \upsilon_l \frac{\partial^2 u_l}{\partial y^2}$$

(4.35)

Energy Equation

$$u_l \frac{\partial T_l}{\partial x} + \upsilon_l \frac{\partial T_l}{\partial y} = \alpha_T \frac{\partial^2 T_l}{\partial y^2}$$

(4.36)

Boundary conditions

$$u_{liq} = u_{vap}$$   Continuity of tangential velocity

$$\mu_l \left( \frac{\partial u}{\partial y} \right)_{liq} = \mu_\upsilon \left( \frac{\partial u}{\partial y} \right)_{vap}$$   Continuity of the tangential shear stress

$$\rho_l \left( u \frac{d\delta}{dx} - \upsilon \right)_{liq} = \rho_\upsilon \left( u \frac{d\delta}{dx} - \upsilon \right)_{vap}$$   Continuty of mass-flow crossing the interface

$$T_l = T_v = T_{sat}$$   Interface temperature

$$y=0:$$     $$u=v=o$$     $$T=T_w$$
$$y \to \infty:$$     $$u \to U_0$$     $$T=T_0$$

Applying Falkner-Skan transformation variables

$$\eta = y \sqrt{\left( \frac{U_0}{v_v x} \right)}$$      $$f(\eta, \xi) = \frac{\psi}{\sqrt{(v_v U_0 x)}} \quad \xi = \frac{x}{a}$$

$$\theta(\eta, \xi) = \frac{T - T_{sat}}{Tw - T_{sat}}$$

Rearranging

$$f'(\eta_\delta)\xi\frac{d\eta_\delta}{d\xi}+\frac{1}{2}f(\eta_\delta)(1+M+2R)+\xi\frac{\partial f}{\partial\xi}\bigg|_{\eta_\delta}=$$

$$\frac{Ja_v}{\Pr_v}[-\theta'(\eta_\delta)]-\frac{Ja_l}{\Pr_l}[-\Theta'(0)]\sqrt{\left(\frac{\rho_l\mu_l}{\rho_v\mu_v}\right)}+\frac{Nu_r}{\sqrt{(\mathrm{Re}_v)}}\left(\frac{Ja_v}{\Pr_v}\right)\sqrt{\left(\frac{\xi}{2(u_0/u_\infty)}\right)}$$

$$\dots\dots\dots\dots\dots\dots\dots\dots\dots\dots\dots\dots\dots\dots\dots\dots\dots\dots\dots\dots(4.37)$$

$$Nu=\sqrt{(2\mathrm{Re}_v)}[-\theta'(0)]\sqrt{\left(\frac{u_0/u_\infty}{\xi}\right)}+Nu_r \qquad\dots\dots\dots\dots\dots\dots\dots(4.38)$$

The free stream velocity was taken from the potential flow result, which is $\dfrac{u_0}{u_\infty}=\frac{3}{2}\sin\xi$

The above equations are solved numerically to get film thickness and Nusselt number. However before computing the result numerically the experimental approach was pursued and this task is postponed to the future work of the study.

# 5. EXPERIMENTAL APPROACH

Quenching experiment of stainless steel spherical ball was conducted in a pool of various liquids. The study investigate the ranges of liquid subcooling used to cool the heated sphere plunged at higher temperature. Two different size spherical SKF bearing balls, RB-10/G20W and RB-20/G20W with sizes of 10 and 20 mm in diameter respectively, were used in the experiments. The sphere is chosen due to its geometry, since the geometry of molten metal in the theoretical analysis of single drop modeling is represented by spherical geometry. The other advantages of selecting a spherical geometry are: The uncounted heat does not pose any problem. Besides it is a proper geometry to ensure all the heat from the heated sphere is transferred to the surrounding liquid.

The test is made to investigate the effect of the different liquids in the film boiling heat transfer. The experimental conditions are tabulated in table 5.1

**Table 5. 1** *Experimental Conditions*

| Type of liquid | • Distilled and De-ionized water<br>• 33nm $Al_2O_3$<br>   o 5, 10 and 20 vol. % in pure water<br>• 300 nm $Al_2O_3$<br>   o 5 and 10 vol. % in pure water and surfactants (Laurent salt) |
|---|---|
| Liquid subcooling (k) | 10 ~80 |
| Initial sphere temperature (k) | 1000~1450 |
| Sphere diameter (mm) | 10, 20 |

Schematics of apparatus employed to perform the test is presented in Fig 5.1
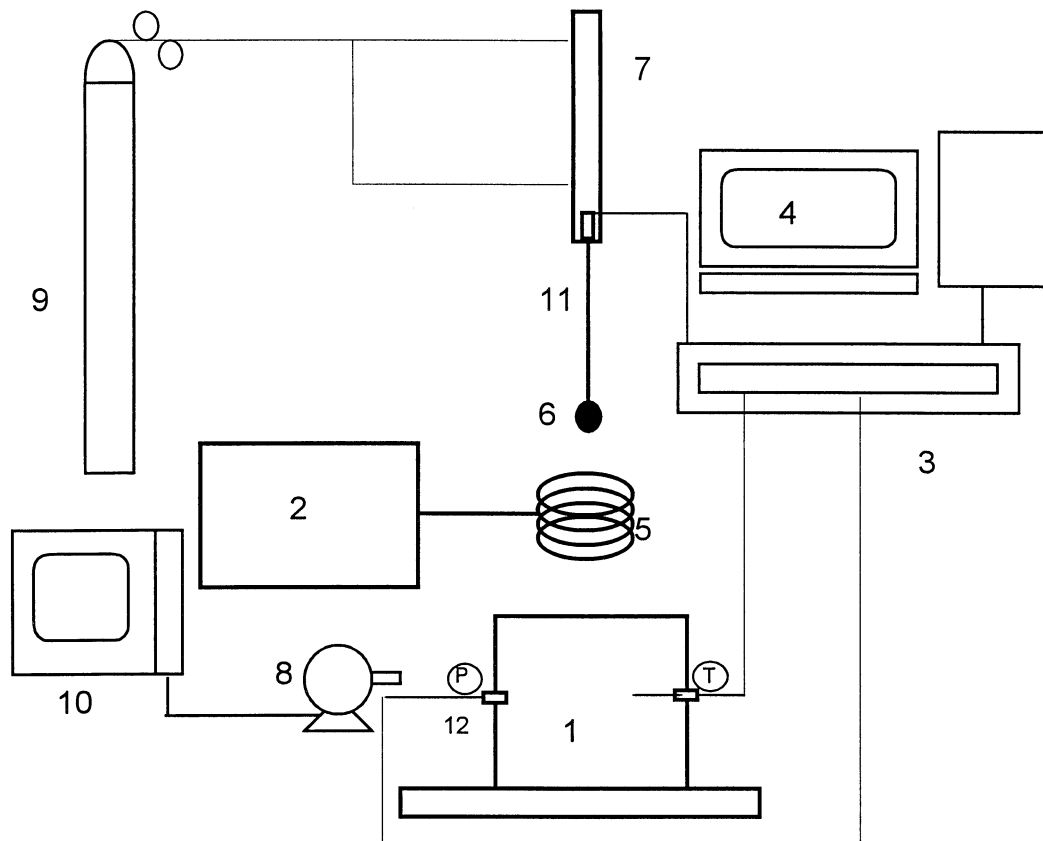
1. Test Chamber
2. Induction Furnace
3. DAS
4. Computer for Data Processing
5. Magnetic Copper Coil
6. Sphere
7. Pneumatic Cylinder
8. High Speed Camera
9. Argon Cylinder
10. Motion Scope
11. Thermocouple Support system
12. Pressure Transducer

**Figure 5. 1** *Schematics of the Experimental Set up*

## 5.1 Description of Experiment Apparatus

The experiment set up involved different apparatuses, such as: heating furnace, sphere and its support system, Argon system, pneumatic cylinder, test vessel, data acquisition system, video camera, high speed camera, motion scope and thermocouples. A very brief description of their contribution and concurrence in the test will be illustrated for the main apparatuses. Detail specification of the apparatuses is listed in the appendix

### 5.1.1 Heating Equipment

There are different ways to heat the sphere ball; direct (surface or internal) electric heating or convective heating (passing a hot fluid through the sphere), are some of the common techniques that have been used. To support a stable film on a heated sphere with highly subcooled liquid requires higher initial temperature of the sphere. Magnetic induction heating is employed to heat the sphere in these experiments. The construction of the copper coils for the magnetic field generation was; 4 turns of 6mm outer diameter copper tube made in to a coil with inner diameter of 50mm. It is held 180 mm from induction furnace by the same copper pipe budding straight from it. Cold water is made to pass through the copper pipe to keep it cold; means there was no any heat went to the bulk liquid from the heating system. The sphere is placed in the centre of copper coil hanged by the thermocouple support system so that a uniform heating to a required higher temperature will be possible in short time. The induction furnace generator used was GT-6 type (HeatTek) that is capable supplying up to 6 kW power with easy control.

### 5.1.2 Test Section

The test section is 100 mm x 100 mm rectangular vessel having depth of 150 mm. It is made of plexi glass, for visual observation from the outside and videotaping. Besides, it will eliminate the possibility of heating the test section by the induction furnace.

Two holes on opposite sides of the test section was drilled, one is to put in a K-type thermocouple in the liquid pool for regulating its temperature. It is positioned in a way that the average temperature of the bulk liquid could be recorded. The other hole was to plug a pressure transducer that will be in use to measure peak pressure, produced when the vapour film collapsed. The liquid is filled to 12 cm height of the vessel and the sphere is dipped to a depth of 6cm during the experiment.

### 5.1.3 Sphere Support System

The thermocouple stem was arranged to support the sphere. This way the heat loss from the support system will be minimized. The thermocouple

inserted in the sphere acquires the transient cooling temperature history of the centre of the sphere besides supporting the sphere.

Hole was drilled on the sphere in the centerline up to half the diameter and the sheathed thermocouple was then inserted. Only one thermocouple for each sphere was employed again not to loose heat through the support system. For the smaller sphere (10mm diameter), a 0.5mm OD and 305 mm long K-Type Inconnel sheathed ungrounded thermocouple (OMEGA) was used. This is then put in to a 0.9mm OD steel tube fixed at the other end of the thermocouple. Roughly 40mm from the sphere, the tube is reinforced by another steel tube 3.1 mm OD. The assembly is sketched in Fig 5.2. In the case of the larger sphere (20mm diameter), stainless steel sheathed ungrounded K-type thermocouple (1,5mm OD and 305 mm long) (OMEGA) was used. The thermocouple stem is reinforced by a steel tube 4mm OD 47mm from the sphere as shown in Fig 5.3

The thermocouple support stem should have a negligible thermal capacitance to minimize the effect of the support on the vapour film. Though it will ensure good contact, the option of slot in a layer of solder between the walls of the hole drilled on the sphere and the thermocouple sheathe is excluded. This is due to the possibility of loosing the joint owing to melting point limit as it was supposed to go temperatures over $1000^{\circ}C$ .The consequence of using a weld joint was the effect that the excess weld on the surface would have on the heat loss and the corollary of interfering with the collapse of the vapour film.

In examination made to assess the effect of welding the thermocouple with the sphere. Susan (1993) in her thesis had showed that the possibility of the film collapse to begin from the joint for welded joint. The other drawback with welding the sphere to the thermocouple was the thickness of the thermocouple sheath has thickness of 0.2mm; in which case welding couldn't be convenient for joining the smaller sphere support system. Thus, a friction joint was employed to connect the small sphere. The thermocouple assembly was force fitted in the hole drilled on the spheres. Heating of the sphere once; made the shrink fit enough to support the sphere due to the thermal expansion and contraction. In the beginning of the experiment, the large sphere was welded with the sheathed thermocouple. Later for both spheres friction joint was utilized. This will give the possibility of using thin thermocouple support (low heat capacity) increasing the chance of minimizing the premature collapse of the vapour film on the sphere caused by interference with the joint.

Only one thermocouple was assumed to be enough for each sphere to minimize disturbance of the flow and fast film collapse of the rear portion by the thermocouple stems. Liu and Theofanous tested the effect of using three thermocouples and found out that the heat loss increased by 20% compared with a single thermocouple.

The ratio of the support diameter to the sphere diameter used in the present experiment was 0,09 and 0,07 for the 10 and 20mm sphere respectively.
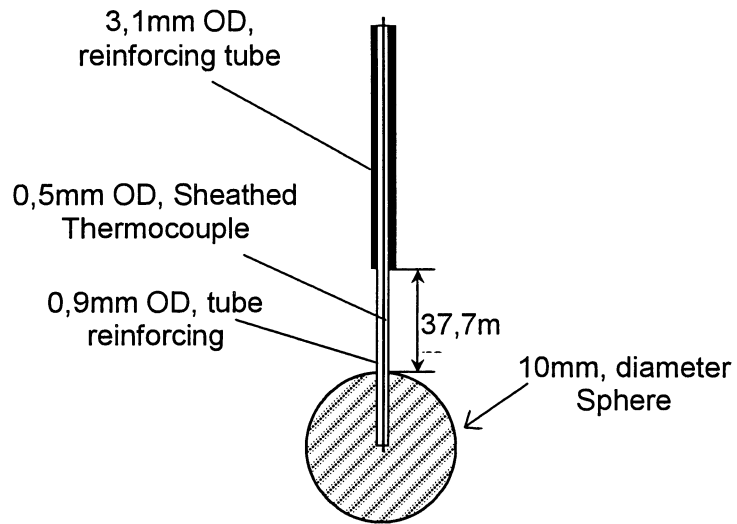
3,1mm OD,
reinforcing tube

0,5mm OD, Sheathed
Thermocouple

0,9mm OD, tube
reinforcing

37,7m

10mm, diameter
Sphere

**Figure 5. 2** *Thermocouple-Sphere Support Sketch for the 10mm in diameter Sphere*



4mm OD,
reinforcing tube

1,6 mm OD, Sheathed
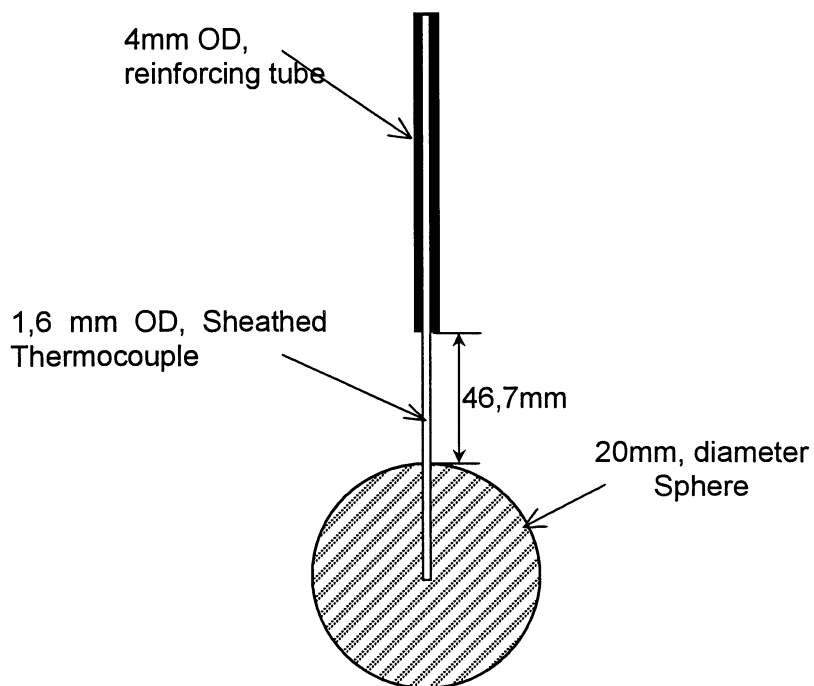Thermocouple

46,7mm

20mm, diameter
Sphere

**Figure 5. 3** *Thermocouple-Sphere Support Sketch for the 20mm in diameter Sphere*

## 5.1.4 Pneumatic Cylinder

The sphere support system is fixed to the end of a piston rod. A pneumatic double acting cylinder actuates the rod with bore diameter $\phi$ 20mm and stroke 160mm long, which can handle a maximum of 10 bars. Pressurized argon cylinders were used to operate the sphere support structure and the system pressure of the argon was varied to control the speed of the ball. In any case, the effect of varying the speed of the ball is negligible to the experiment, because after few seconds it was real that the ball will come to stop inside the liquid, i.e. when the piston in the pneumatic cylinder reaches the top dead centre. Thus for longer period of the test the ball stays stationary in the liquid. Large portion of the film boiling regime, and all the rest boiling portions (transition, nucleate, natural convection) is conducted with the ball being standstill. Anyhow to attune the speed of the ball, equation that correlates speed of the ball with the argon pressure was necessary. Consequently, a successive test varying the pressure was conducted by the pneumatic cylinder, which was attached to the ball through the support system. A high-speed camera was employed to determine the downward speed of the ball. The result is tabulated in table 5.1

**Table 5. 2** *Pressure of the Argon with Corresponding Velocity of the Piston rod*

| Pressure ($Kp/Cm^2$) | Velocity (m/sec) |
|---|---|
| 2 | 0,781 |
| 3 | 0,862 |
| 4 | 0,926 |
| 5 | 1,000 |
| 6 | 1,087 |
| 7 | 1,190 |
| 8 | 1,316 |
| 9 | 1,470 |

## 5.1.5 Data Acquisition System

Transient test data were recorded via centrally located thermocouple, data acquisition system (HP SCXI-1102) and employing Lab View software. The thermocouples inserted to the sphere and the test vessel continually measured the centre temperature of the sphere and the liquid bulk temperature, respectively.

The thermocouple wires are plugged in to a NI A/D Converter after the signal is amplified; the data is fed into a PC. The data sampling was ranging 100~250 scans per second. The data sampling frequency is fast compared with the thermocouple response time.

A high-speed camera with a capability of 8000 frames per second and Video with 230 frames per second are employed to monitor the configuration of the film and process the image.

## 5.2 Experiment Procedure

A number of experiments have been conducted under different fluids. The first couple of experiments were conducted only with highly subcooled distilled water to verify experimental methodology by comparing with the known correlations and experiments conducted earlier. Later, the type of fluid, diameters of sphere and the degree of subcooling is varied to investigate their effect. The procedure of the experiment can be briefly expressed as follows.

- The test vessel was filled with liquids;
- The Argon cylinder was open to let Argon in the systems & to purge the sphere while heating
- The sphere was positioned in the centre of the coil and the coil is covered with insulation
- The tap water was led through the induction furnace copper coil And the furnace is made in the ready mode
- The data acquisition system was started recording the temperatures.
- When the temperature of the centre of sphere reached the required higher temperature the induction furnace turned off to reach a steady state level
- Then the sphere was plugged in to the pool of liquid with 60 mm depth of immersion
- The data recording was continued till the sphere temperature became close to the liquid bulk temperature (i.e. end of natural convection)

## 5.3 Nanofluid Preparation

As mentioned in the literature survey preparations of nanofluids require: even suspension, stable suspension, durable suspension, low agglomeration of particles, and no chemical change of the fluid. To prepare suspensions different techniques have been in use: to change the pH value of suspensions, to use surface activators and/or dispersants, and use Ultrasonic vibrators. In this study, nanofluid was prepared by the dispersion of nano size $Al_2O_3$ particle powders into de-ionized distilled water using an ultrasonic vibrator. Figure 5.4 shows a TEM (Transmission Electron Microscopy) image for the $Al_2O_3$ nanoparticles and the corresponding particle size distribution used is presented in figure 5.5. The average particle size and size distribution were obtained from the TEM images for the samples using an image analysis program by measuring the diameters of at least 500 particles. Perfectly spherical $Al_2O_3$ nanoparticles with an average diameter of 33.1 nm were found.
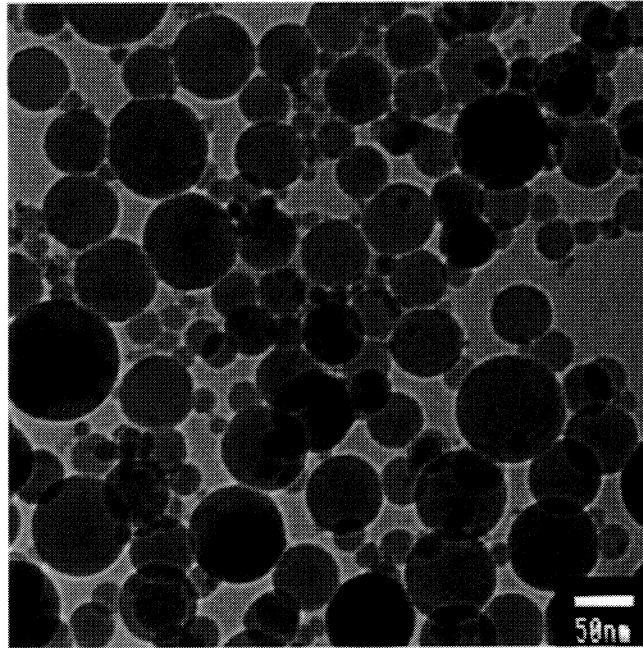
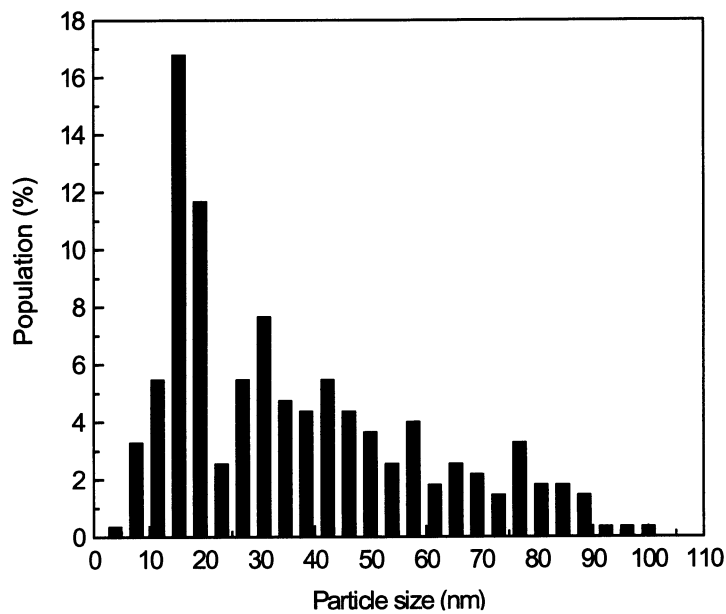**Figure 5. 4** *Transmission electron microscopy (TEM) image*



**Figure 5. 5** *Size distribution histogram of Al2O3 nanoparticles in nanofluids*

Ultrasonic vibration was found to be effective for suspending the smaller size nanoparticles with out changing the pH or adding surfactants. Many studies showed that addition of surfactants has effect in the boiling characteristics of the fluid. To avoid this influence no surface activator was added in the effort made to investigate nanofluid effect. However for the curiosity and sense of completeness another solution that utilized Laurent salt (surfactant) as an

additive to suspend the particles was prepared with 5 vol. % $Al_2O_3$ nano particles for the 300nm in diameter particles.

In this study, the $Al_2O_3$ nanoparticle was chosen because the majority of the previous works on heat transfer in nanofluids were carried out employing this nanoparticle. The nanofluids with the 5, 10, 20 volume percent of the nanoparticles were tested at various nanofluid temperatures

## 5.4 Experimental Observations

Pool quenching experiments of a stainless steel sphere balls of diameter 10mm and 20mm with highly subcooled liquids were conducted. The liquid subcooling was ranged from 10K ~ 80K for the various fluids. The tests were made at higher initial sphere temperature, varying from $750^0C$ to $1150^0C$.

As most of the experiments were conducted at highly subcooled liquids, getting a stable film was very unlikely. The sphere to carry stable film the initial temperature has to be higher. However heating the sphere to higher temperature for long period will lead to another surface effect i.e. adverse oxidation will take part. Thus selecting the right initial temperature was necessary. Much higher initial temperatures led to unsuccessful exertion to get film. Instead the quench time is observed to be short. Difficulties had been encountered in obtaining film boiling at higher subcoolings in the preliminary experiments.

The cause for it was not probable to observe a stable film for experiments conducted at higher initial temperature of the sphere might be due to the non-uniform oxide layer formed over the surface of the sphere interfered with the vapour/liquid interface layer leading to fast collapse. The oxide layer observed was thick at higher temperature, this had enormous effect in changing the surface roughness and chemistry of the sphere, which in turn easily interfered the thin vapour layer affecting the stability of the interface leading to partial or full collapse. The film thickness in highly subcooled liquid case was so thin (in micro meter range) that it is highly susceptible to slight roughness caused by over hanged scales of oxide. Thus liquid directly contacts the surface and transition or direct contact boiling become prominent which is characterized by increased heat flux, longer period of transition region (covering the expected film region too), and uneven vapour distribution over the whole surface.

Susan (1993) made attempts to obtain film boiling in highly subcooled fluids, the sphere temperature was increased to higher and higher values, however film boiling was observed once in a while up to the subcooling of 60K, but not beyond that. For half-inch diameter spheres, film boiling was readily obtained for subcoolings up to 40K. In Dhir and Purohit experiment, when the sphere was oxidized or its surface had pits or protrusions (i.e. where the stem was welded or brazed to the sphere) a premature contact of the liquid with sphere surface was observed to happen. That was leading to either a partial collapse of the film or pulsation of the film prior to complete collapse. For this reason the observation on these spheres was limited to low subcoolings. They have

expressed their surprise writing "it is interesting to note that for a sphere surface temperature of 473K, it is impossible to support a vapour film when the liquid subcooling is greater than about 25k."

However in the present experiment, tests were made at highly subcooled ~80k and was managed to obtain a stable film for some of the experiments typically for the 10mm diameter sphere. To balance the effect of oxide formation and the lowest temperature that can sustain the high subcoolings, a number of tests have been performed in the beginning at higher and lower initial sphere temperature covering a range of ($750^0C$~$1100^0C$). It was possible to obtain a stable film boiling for some of the experiments only for the smaller sphere. The initial temperature of the sphere at which it became practicable was $930^0C$ ~$940^0C$.

However attempts done to obtain a stable film on the large sphere (20mm diameter) didn't succeed due to oxide layer interference. On larger spheres the vapour film travels a greater distance  that disturbance at the vapour-liquid interface also have greater opportunity to grow. Furthermore, during high subcooling vapours generated collapsed fast in the bulk liquid. This may be due to much heat is lost from the vapour than the hot surface can supply to the vapour. In another say, the convective heat transfer in the liquid side is more effective than the film boiling heat transfer.

When early collapse is happening, the film boiling region is predisposed by the transition and direct contact boiling regime. A similar observation is also reported by Dhir and Purohit with a 38mm copper sphere. The vapour film was found to be more susceptible to premature collapse especially when the liquid subcooling was greater than 10K. The reason was postulated to be during heating the sphere took longer time to reach the desired temperature, which in turn led to a higher degree of oxidation of the sphere.

Many researchers have investigated surface effects; a survey on this is presented on the literature study. A few of the important aspects are stated here for explanation of the observations. It has been noted that, ageing, contamination, oxidation or improving wetting to advance the post critical heat flux heat transfer (i.e. to produce a higher heat flux at a given superheat temperature)

In Burgles and Thompson experiment presented in the literature survey, surface effects were expected to be the reason for the deviation in the boiling curves from quenching method and steady state data. Specimens to be quenched usually have surface contaminations, which will act to destabilize film boiling thereby reducing the characteristic "slow cooling" portion of the quench. Nevertheless, surface chemistry rather than roughness is the important consideration. When the quenched piece is preheated the surface is oxidized and the wettability increases. This will result in film collapse at higher temperature and heat transfer.

Generally if the surface is slightly oxidized the observed $\Delta T_{min}$ may be higher than expected for clean spheres. Therefore a method has to be devised to lessen the unwanted phenomenon as surface effects (surface oxidation, roughness) so that experimental condition could generate reliable data. As long as the sphere surface was very smooth and relatively clean. The thermo physical properties of the sphere have insignificant effect. The first couple of experiments were informative for the improvements done later to avoid the listed effects. Thus the heated sphere was continually purged with an Argon gas to minimize the oxidation of the surface at elevated temperatures.

The point here is to give emphasis on the influence of surface condition. Its effect is observed to be significant and one has to make a careful consideration of the phenomena if a reliable experimental result is expected. This is also supported by Burgles and Thompson observation, they concluded unless surface conditions can be strictly controlled the transition and nucleate boiling regions are greatly distorted. Even with cryogen the difference between quench and steady state boiling curves are sufficient to suggest that the quenching experiment may not provide accurate transition and nucleate boiling data, due to these effects.

## 5.4.1 Observation Of Film Configuration

The experiment is also configured to observe film configurations. The film boiling process was video taped, and a screen capture was taken to analyze the film thickness.

Observation

Its been observed that a long period sustained film was possible over the small diameter sphere than the larger. This might be due to the reason explained earlier to this section that non uniform oxide formation and roughness of the surface affecting the stability of the film, as a result quick shift to transition region is taking over.

Film configuration

The experiment set up was convenient in that every process of the film boiling phenomena can be observed from the outside. Thus video camera was utilised to film the quenching process of the ball and visualize the film boiling in a close look.

A high speed camera with speed of 8000 frames/ sec was also used. To process the image and possibly to measure the film thickness variation around the sphere 'OPTIMAS' software was employed.

The visualization is made only to distill water tests at high and low degrees of subcooling. In the experiment with nanofluid, video taping the film boiling process was not possible because of the opaqueness of the fluid. It was not possible to see any thing through the milky solution of nanofluids. In the future

it is intended that x-ray radiography will be employed for film boiling visualization and to understand the quenching process of nanofluids. The facility is already prepared and the study is underway.

In highly subcooled tests, the vapour film observed was a smooth vapour/liquid interface with little dome at the rear of the sphere as shown in fig 5.4. The vapor film is almost perfectly spherical and because of the large degree of subcooling the vapor is being condensed at the liquid-vapor interface in the wake region at approximately the same rate as it is being formed around the front of the sphere. As a result there is no large trail. As the temperature of the sphere is decreasing, the film is getting thinner and smoother. Finally when it passed the minimum film boiling temperature the film collapsed producing pop sound.



**Figure 5. 6** *Film Configuration of A highly Subcooled film boiling test*
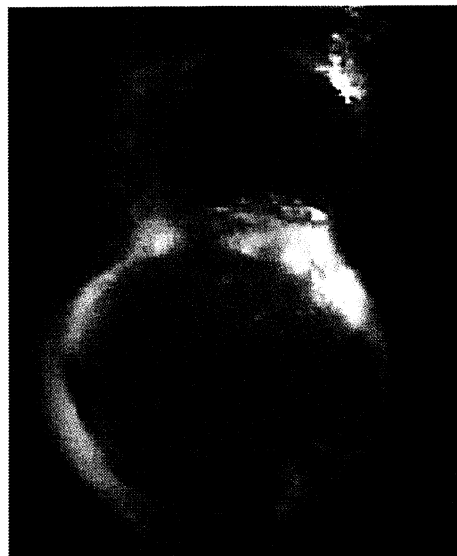


**Figure 5. 7** *Film Configuration of A low subcooled film boiling test*

In case of low degree of subcooling the vapour dome in the rear region detaches periodically. The film is thick plus the frequency is higher at higher temperature. As a result of periodic detachment the vapour/liquid interface is wavy. As the temperature is decreasing the, the film tends to become stable the interface became smoother and the film get thinner. Then eventually it collapsed, when the temperature of the surface became so low that the sphere is not able to carry the film.

# 6. DATA REDUCTION METHODODLGY

During quenching experiments with spheres the measuring junction must not be attached to the outside surface of the sphere because that disturbs the fluid flow and the heat flow. Thus temperature measurements are taken from the centre of the sphere as it is also inconvenient to place thermocouples in the surface of the sphere and increases the fining effect. Apparently this brings another effort to predict the sphere surface temperature and the corresponding surface heat flux. There are different ways to address the problem. Here are some models to approximate the surface temperature and surface heat flux from the measured center temperature of the sphere.

## 6.1 Exact Solution Model

Exact solution model is developed analytically solving the differential energy equation for the sphere. Adiabatic boundary conditions at the centre and a convective boundary condition at the surface will be applied. The temperature distribution inside the material in terms of the dimensionless parameter is described as follows.

$$\theta = \sum_{n=1}^{\infty} A_n \cdot \exp\{-\lambda_n^2 \tau\} \frac{\sin(\lambda_n r^*)}{\lambda_n r^*} \qquad (6.1)$$

with $$A_n = \frac{4[\sin(\lambda_n) - \lambda_n \cos(\lambda_n)]}{2\lambda_n - \sin(2\lambda_n)} \qquad (6.2)$$

$$1 - \lambda_n \cot(\lambda_n) = Bi$$

The dimensionless parameters, temperature, spatial position and time are:

$$\theta = \frac{T(r,t) - T_\infty}{T_i - T_\infty} \qquad (6.3)$$

$$r^* = \frac{r}{R}$$

$$\tau = \frac{\alpha t}{R^2}$$

$$Bi = \frac{hR}{K}$$

If the dimensionless time is not too small ($\tau > 0.2$), the above exact solution can be approximated by taking only the first term of the series solution.

$$\theta = \sum_{n=1}^{\infty} A_1 \cdot \exp\{-\lambda_1^2 \tau\} \frac{\sin(\lambda_1 r^*)}{\lambda_1 r^*} \qquad (6.4)$$

And at the centre of the sphere,

$$\theta_0 = A_1 . \exp\left\{-\lambda_1^2 \tau\right\}$$

However, the above model assumes constant convective heat transfer coefficient, which is not the case in the present study.

## 6.2 Inverse Heat Conduction Problem Method

The other way to approximate the surface temperature from the measured centre temperature time history is applying the so-called Inverse Heat Conduction Problem (IHCP).

This is extrapolating the measured temperature to the surface temperature by solving the inverse heat conduction problem numerically. Then the surface heat flux can be determined from the temperature gradient at the surface and applying the Fourier's first law of heat conduction.

It has been pointed out the necessity of a specimen with negligible internal resistance if accurate assessment of instantaneous average heat transfer is desired in a quenching experiment,

Merte and Clark (1964) used temperature measured near the surface of the sphere in a finite difference calculation of the one dimensional inverse heat conduction to estimate the instantaneous heat flux obtaining the internal temperature distribution of the specimen. They found it to be accurate if the thermocouples are positioned precisely.

Solving the one dimensional transient heat conduction problem numerically, Chen and Liu (1999) compared the results they obtained with the experimental measured center temperature. A surface temperature measurement was also taken and the model was verified to accurately describe the problem.

Inverse heat conduction problem employs the one dimensional transient heat conduction.
The fundamental equation is:

$$\frac{\partial T}{\partial r}\left[k(T)\frac{\partial T}{\partial r}\right] + \frac{2}{r}\frac{\partial T}{\partial r} = \rho C(T)\frac{\partial T}{\partial t} \qquad (6.5)$$

Subject to the boundary conditions,

At the center

$$\left[\frac{\partial T}{\partial r}\right]_{(0,t)} = 0, \text{ i.e., symmetry applies at the center of the substance}$$

or

T (0, t) = measured centre temperature history

At the surface,

$$-K(T)\left[\frac{\partial T}{\partial r}\right]_{(R,t)} = h(t)[T(R,t) - Tsat] \qquad (6.6)$$

## 6.3 Lumped Capacitance Assumption

More often, the task of converting the measured centre line transient temperature to the surface temperature and corresponding heat flux has been simplified by assuming constant temperature through out the material, i.e. the lumped capacitance assumption model. Then the temperature solution may be given as:

$$\frac{T(t) - T_\infty}{T_i - T_\infty} = e^{-bt} \qquad (6.7)$$

Where,

$$b = \frac{hAs}{mCp}$$

$$t = -\frac{1}{b}\ln\left\{\frac{T(t) - T_\infty}{T_i - T_\infty}\right\}$$

$$Bi_{lumped} = \frac{L_C h}{k}, \quad Lc \text{ is the characteristic length, written}$$

$$Lc = \frac{V}{As}$$

For a sphere of radius R, The lumped Biot number is $\quad Bi_{lumped} = \dfrac{hR}{3K}$

The instantaneous heat flux in this case is give as

$$q = -\frac{m_s Cp(T)}{\pi D^2}\frac{dT}{dt}$$

In some studies the applicability of the lumped parameter assumption method has been tested. It is considered to be accurate for Biot number less than 0.2, for the maximum heat flux case [Bergles and Thompson (1970)]

Peyayopanakul and Westwater (1978) reported the validity of the method for Biot numbers less than 0.45, after comparing the boiling curve obtained from lumped parameter assumption with the numerical solution of one-dimensional transient equation using finite difference scheme. However, there are cases, which the internal thermal resistance cannot be neglected. As a result investigators have developed a data reduction technique, which accounted the internal temperature gradient in the sphere.

In most cool down transient test the sphere temperature is assumed uniform through out the body. However this assumption is not always correct. Usually at the front stagnation point, the heat flux is higher and the temperature is lower than any other part of the surface. The centre temperature is higher that the surface temperature. Cases with high liquid velocity and larger subcooling are sensitive. It has been roughly analysed for stainless steel sphere with a liquid velocity of ~2m/s and a subcooling of ~30K. The result showed the temperature difference between the sphere centre and the surface turned out to be 20% of the superheat [Liu and Theofanous (1994)].

The uniform temperature assumption is considered when the temperature difference with in the material is small especially when the thermal conductivity of the material is large and the convective heat transfer coefficient is lower and the superheat is higher. For instance transient cool down test of stainless steel sphere (lower thermal conductivity) in saturated liquid film boiling the temperature difference between the front stagnation point and the centre of the sphere is only 50K, which is less than 10% of superheat. In case of brass sphere the difference is about 10 times smaller than this.[Liu and Theofanos (1994)]

Thus the assumption of a uniform temperature distribution inside the sphere is realistic.for the film boiling portion in which case the heat transfer coefficient is relatively lower. Thus temperature measured at any location in the sphere could be used as a characteristic sphere temperature. Moreover the calculated Biot Number is smaller than 0.4. Therefore a lumped capacity mode is assumed for the present data analysis of the film boiling test.

# 7. PREMILINARY DATA ANALYSIS

Each experiment of the new fluids is preceded by a couple of distilled water experiments under the same experimental condition. During comparison, this cleared the uncertainty that additional effects might show up and therefore the measured result will elucidate the effect of a single parameter only. The pure water data will be first analysed and compared against known film boiling correlations. This will reveal if the right experimental approach in this thesis is employed. It will be assurance mainly for the new fluid tests since the trait of these fluids are not well understood.

## 7.1 Overview of The Transient Quenching Plots

A brief outline of the complete boiling curve from the quenching experiment in water that comprises the transient temperature and heat flux plots will be presented. This is to demonstrate the differences in the curves for cases where a film boiling region is dominated by transition boiling regime and to compare qualitatively with the tests that produce stable film boiling.

In cases with highly subcooled liquid (~Tsup=80K), to establish film boiling the temperature of the solid sphere has to be higher (above $700^0C$). A typical transient temperature and heat flux versus superheat temperature plots (when no film boiling is observed) are presented in Fig. 7.1 and 7.2 respectively.

For cases with no stable film boiling region as the figures indicate, the temperature decreases fast with time. Consequently, the heat flux becomes abnormally high at higher superheat temperature (approximately, 2-7 times higher than the critical heat flux obtained from conventional steady state tests). This could be due to the dominating direct contact or transition boiling heat transfer.

Peyayopank and Westwater (1978) observed similar behavior in the study made to obtain a data from quenching experiments consistent with those of the steady state experiment. They reported variations in the minimum film boiling heat flux at higher quench rates but not in the minimum film boiling superheat. The effect of increasing quench rate is also manifested in increasing the superheat value at the critical heat flux. In their critical heat flux superheat observations, it was postulated that the minimum film boiling superheat has been shifted to the right as the initial sphere temperature was increased. Finally, they pointed out the quench rate should remain low if a matching result is desired.

Such results can be obtained due to the adverse effect of oxidation at higher temperature of the solid in addition to the difficulty to support stable film at higher subcooling. This promotes early film collapse and dictates a shifted boiling curve. It was also seen that both surface oxidation and addition of

wetting agent (oleic acid) destabilized film boiling at a higher heat flux and wall superheat. This early destabilization produces an ill-defined peak heat flux condition. Kovalev cited in Burgles and Thompson (1970) showed that $q''_{min}$ was elevated over a factor of two by continuous exposure of the Nichrome heater to saturated water at high pressure. In general, the value of $q''_{min}$ predicted analytical considered as a lower limit which can be frequently exceeded for engineering surfaces. Furthermore the transition regime of the boiling curve is considerably different from that obtained by the usual procedure of linearly connecting up the steady-state $q''_{max}$ point with $q''_{min}$. This difference becomes particularly significant in quenching since the quench times are greatly affected.

In Burgles and Thompson experiment of Freon, five successive quench runs were taken without removing the carbon scale, which started to form during the first run. The result indicated the quench times decreased with increased scaling and the boiling curves were shifted considerably.

.
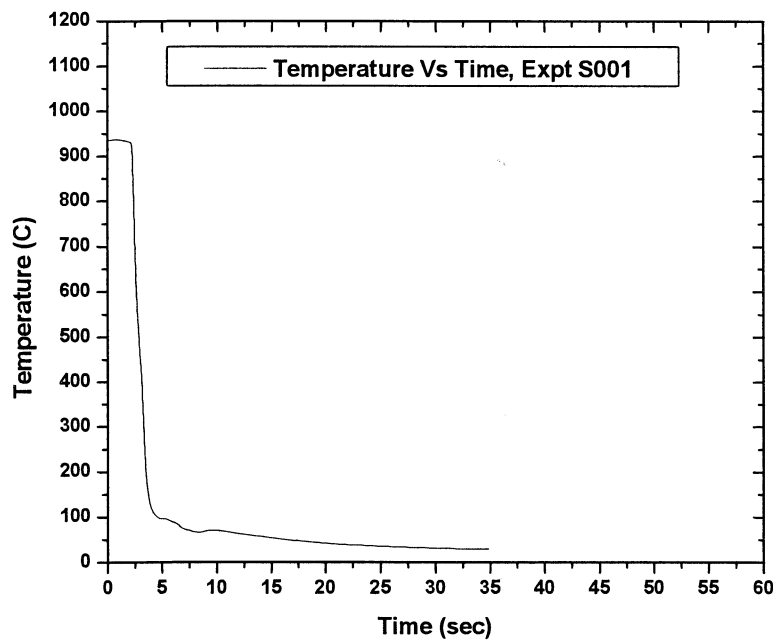


Figure 7. 1 *Temperature history of the 10mm diameter sphere for $T_{sub}=80K$, at atmospheric pressure*
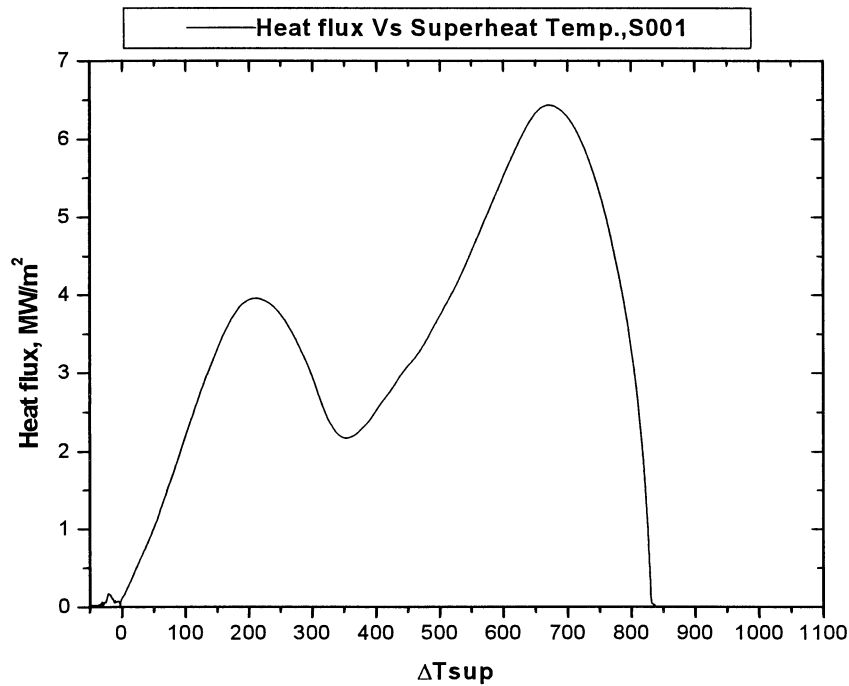
**Figure 7. 2.** *Heat Flux Vs superheat plot for the whole boiling regime, for 10mm sphere ball ($\Delta T_{sub}$=80K) at atmospheric pressure,*

With high subcooling, e.g., $\Delta T_{sub}$=80K, the boiling curves shown in Fig. 7.2 showed the characteristics of transition boiling without film boiling over entire range of the superheating.

The general effect of the oxide scale was to initiate transition boiling at higher heat flux and wall superheat as shown in Fig. 7.2. During additional experiments the scale thickened until it fell off whereupon the next quench reverted back toward a longer quench time with a relatively longer period film covering. Typical quenching curves when a stable film boiling was observed are presented in the Figs. 7.3 and 7.4.

During tests with highly subcooled liquid, unlike cases of near saturation tests the vapour blanket is not initiated right at the beginning of surface-liquid contact, instead direct contact heat transfer preceded the film boiling. As a result, the minimum film boiling point is shifted to the left. Usually minimum film boiling temperature increases with degree of subcooling as discussed in Dhir's study, however that conclusion was made from an experiment conducted a few degrees of subcooling. In the present experiment, it is realized that the vapour film will not collapse early, rather a stable, long time sustained, film boiling regime could be obtained for relatively high subcooling.
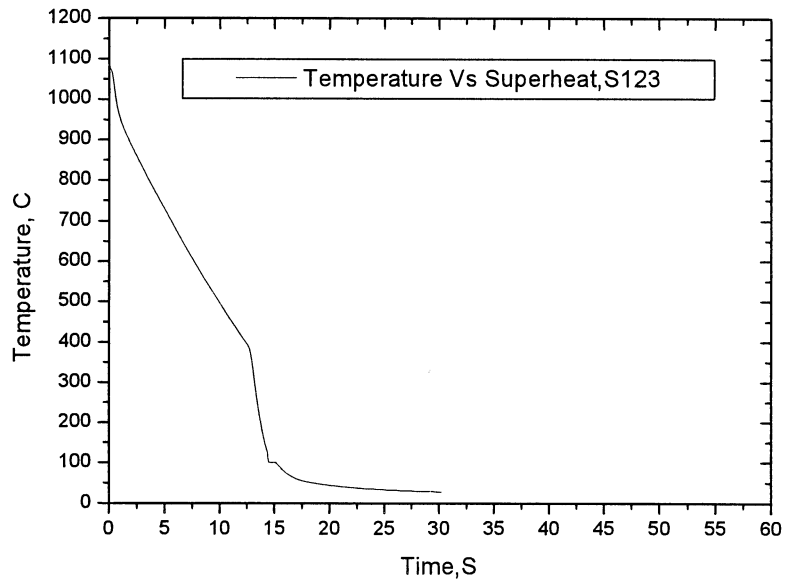
57

**Figure 7. 3** *Temperature history of 10mm diameter sphere, at Tsub=80K,*
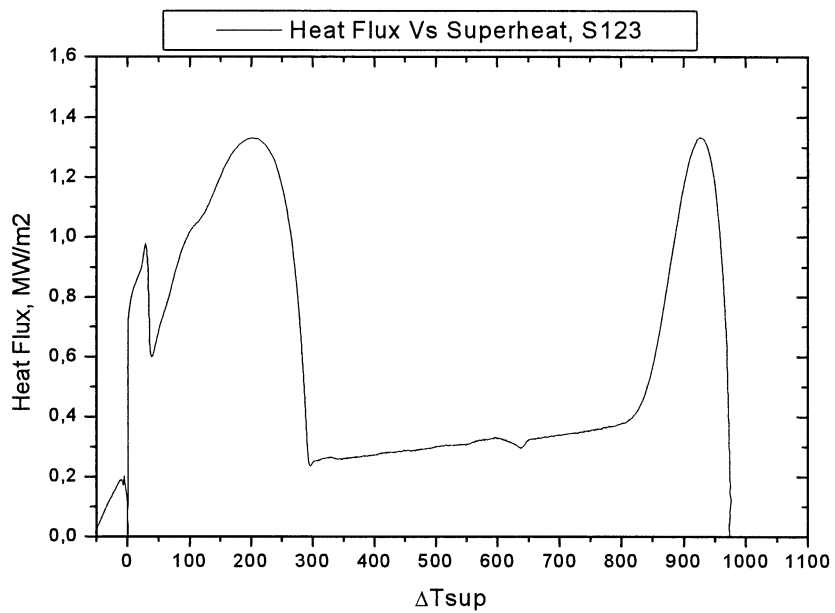$P_{amb}$



**Figure 7.4** *Heat Flux Vs Superheat plot at $T_{sub}$=80K for 10mm Sphere*

It was unlikely to have stable film in highly subcooled tests for the 20mm diameter sphere. This is because the diameter becomes relatively large to the vapour thickness and thus any surface defect due to the formation of oxide scale disturbs the stable vapour film to collapse. In the present experiment, it was not possible to get a film boiling that stayed long at any initial temperatures in highly subcooled cases with distilled water. It is noted that quenching without film boiling may be beneficial for heat treatment. Therefore highly subcooled baths or surface defects would cause early destabilizing of vapour film.

## 7.2 Correlating Water Data based on Existing Film Boiling Correlations

Further analysis on film boiling was made on the water experiment data and discussed using the subcooled pool film boiling correlations presented in the literature survey section of this thesis. Two basic approaches are usually followed. One is termed as "addition law" which depict the total heat transfer coefficient or Nusselt number as the sum of the saturated pool film boiling coefficient, radiation heat transfer coefficient and the subcooled turbulent convective heat transfer. Another is the "ratio law" which correlates the film boiling in the form of the ratio of the effects.

A comparison of the existing subcooling studies summarized for addition and ratio laws, such as Liu's (1994), Sakurai's (1990a), Michiyoshi's (1988), Dhir's (1978) and Siviour's (1970) in the literature was carried out with the present experimental data. This is plotted in Figs. 7.5 and 7.6 for high and low subcooled water respectively.

For high subcooled condition showed in Fig. 7.5, the experimental data are well correlated by the Michyoshi's and Sakurai's correlation for superheat temperature less than ~750 K. Beyond 750 K, they overestimated the entire data. Liu and Theofanous correlation has slightly overestimated the experimental data. The correlation that follows the addition principle, i.e. Siviour's correlation has generally underestimated the present data. Dhir's correlation predicts the data in similar way to those that employed the ratio law, except has slightly overestimated the data at higher superheat temperature. It is noted that his correlation is derived from an experiment conducted with highly subcooled liquid.

At low subcooling case (Fig. 7.6), Michyoshi's correlation estimated the data well for low superheat temperature less than 600 K. Above this temperature it overpredicts the data. Sakurai also followed the same trend as Michyoshi's. At higher superheat temperature it approximates the data better than Michyoshi. Liu and Theofanous correlation has a gain to some extent overestimated the entire data.

Unlike the high subcooling case, Dhir's correlation has underestimated the entire data in the whole range of superheat the similar to Siviour's.
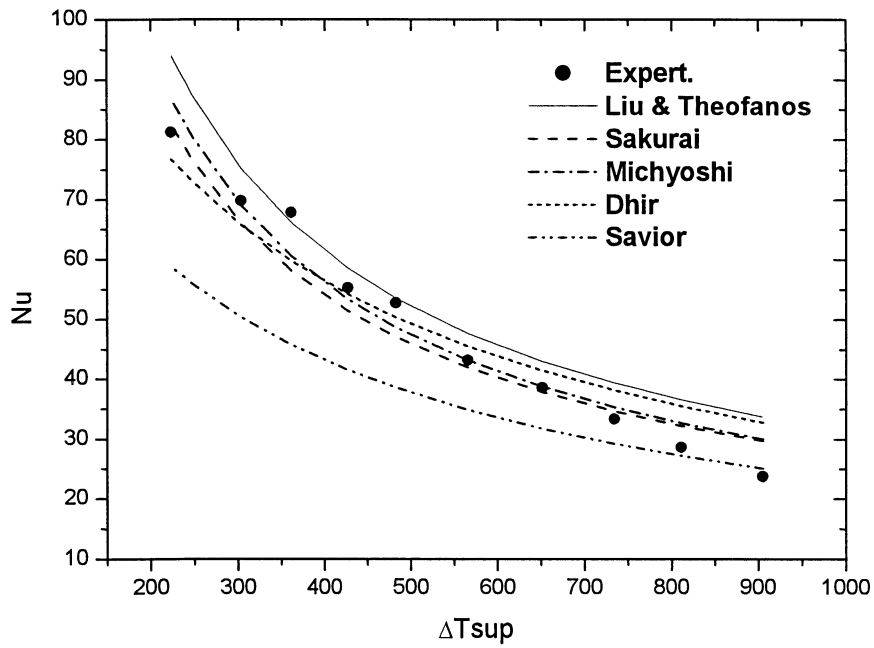
59

**Figure 7. 5** *Comparison of different correlations with a highly subcooled water test ($\Delta T_{sub}$= 80K) and atmospheric pressure*
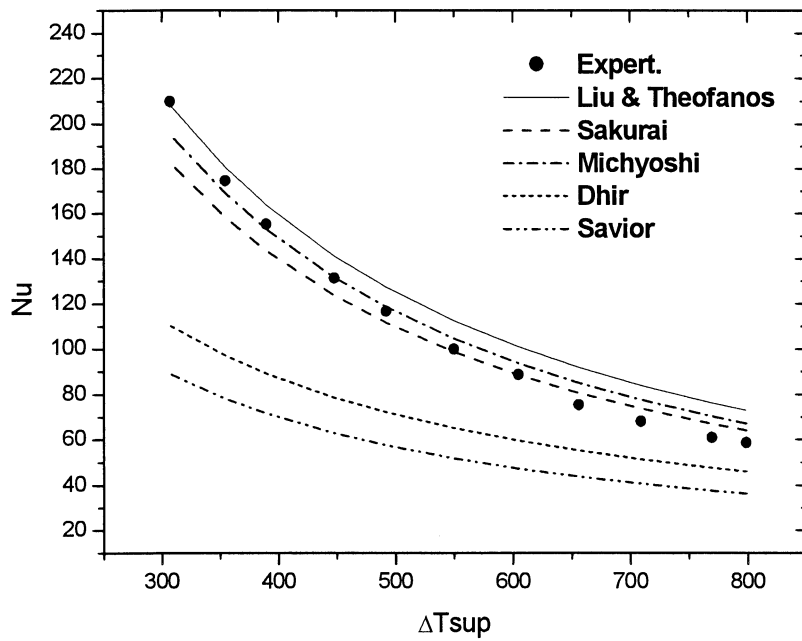


**Figure 7. 6** *Comparison of different correlations with relatively low subcooling water data ($\Delta T_{sub}$= 10K)*

From the above comparison, three different correlations are selected to analyse the present experimental data from distilled water. Two of them are applied to the saturated pool film boiling of the total heat transfer coefficient. They are termed as 1/3 and 1/4 power laws. The third correlation reflects the recent ratio concept on subcooled pool film boiling analysis. For this purpose the well-known Michyosh's correlation is selected. The constants (coefficients) based on all the three different correlations are evaluated and plotted to select the correlation, which predicts the data better.

The total heat flux obtained from the experiment presents all the effects together, such as the radiation effect.

$$q_c = q_t - Jq_r \qquad (7.1)$$

$$q_r = \varepsilon\sigma\left[Tw^4 - Ts^4\right]; \qquad (7.2)$$

$J$ = 7/8, from Bromley. The Nusselt number for the film boiling becomes,

$$Nu = \frac{q_c D}{\Delta T_{sup} Kv} \qquad (7.3)$$

## 1/3-Power law

$$Nu = C_{sat,(1/3)}\left\{Ar/Sp'\right\}^{1/3} \qquad (7.4)$$

## 1/4 power law

$$Nu = C_{sat,(1/4)}\left\{Ar/Sp'\right\}^{1/4} \qquad (7.5)$$

## Michyoshi's correlation

$$Nu = C_{Mch}\left(Ar/Sp'\right)^{1/4} Mc^{1/4} \qquad (7.6)$$

Where

$$Mc = \frac{E^3}{\left[1 + \frac{E}{\left(Sp^1 P_{rl}\right)}\right]\left(RP_{rl}Sp^1\right)}$$

$$E = \left(A + CB^{1/2}\right)^{1/3} + \left(A - CB^{1/2}\right)^{1/3} + \frac{1}{3}Sc^*$$

$$A = \frac{1}{27}Sc^{*3} + \frac{1}{3}R^2 Sp^1 P_{rl}Sc^* + \frac{1}{4}R^2 Sp'^2 P_{rl}^2$$

$$B = \frac{-4}{27} Sc^{*2} + \frac{2}{3} Sp' P_{rl} Sc^{*} - \frac{32}{27} Sp' P_{rl} R^2 + \frac{1}{4} Sp'^2 P_{rl} + \frac{2}{27} Sc^{*3} / R^2$$

$$C = 1/2 R^2 Sp^1 P_{rl} \quad ;$$

$$R = [(\mu\rho)_v / (\mu\rho)_l]^{1/2} \quad ; \qquad Sc^{*} = C_{pl} \Delta T_{sub} / h_{fg}^{1}$$

$$h_{fg}^{1} = h_{fg} + 0.5 C_{pv} \Delta T_{sup} ; \qquad Sp^{1} = C_{pv} \Delta T_{sup} / (h_{fg}^{1} P_{rv})$$

$$C_{Mch} = 0.696$$

The data are plotted in terms of the 1/3-power law in Fig. 7.7. For all the superheat temperatures, the constant $C_{sat,(1/3)} = Nu / (Ar/Sp^1)^{1/3}$ in the equation (7.4) ranges from 0,33 to 0,56, with mean value of 0.42 and standard deviation of 0.079. The constant is higher compared with Merte and Clark (1964), which is 0,15.

Fig. 7.8 showed, the data presented in the form of the 1/4 power law the constant, $C_{sat(1/4)} = Nu / (Ar/Sp')^{1/4}$, the value is not the same for the entire superheat temperatures. It varies from 1.2 to 2.4; the average value of the constant is 1.68 with a standard deviation of 0.42. Comparing this average value with the Bromley's experimental constant of 0.62, Dhir's experimental constant 0.8, and Frederking and Clark's theoretical constant, 0.586. The present experiment constant is considerably larger than all the other, however it should be noted that these data are from the experiment conducted at highly subcooled distilled water, while the correlation takes only the saturation heat transfer effect.

Afterwards, the data for $\Delta T_{sub} = 80K$ were plotted in form of Michyoshi's correlation in Fig. 7.9. It showed that the constant to range from 0,62 to 0.75, which is in agreement with Michyoshi's theoretical value of 0.696 from Michyoshi analysis

Michyoshi's analysis employed the ratio concept and the effect of subcooling is well included in the correlation. This could be the reason for the major deviation observed in comparison with the first two correlation, which are basically suited for saturated film boiling heat transfer while the data was from highly subcooled test.
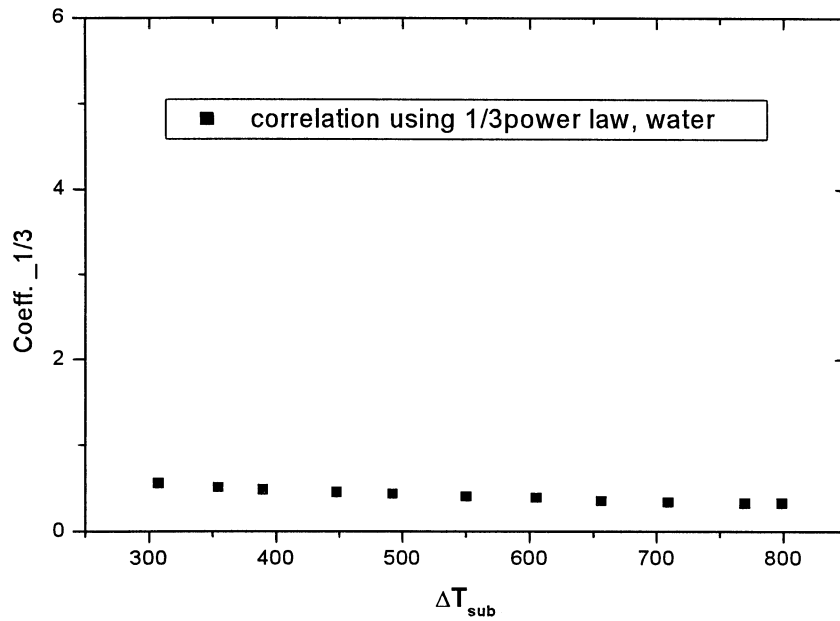
**Figure 7. 7** *Highly Subcooled water ($\Delta T_{sub}$= 80K) data plotted according to 1/3 power law*
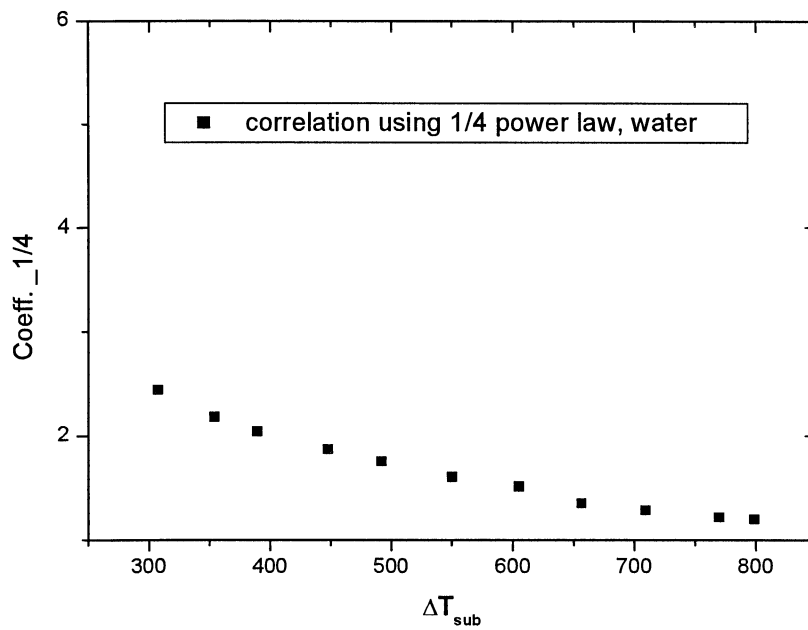


**Figure 7. 8** *Highly subcooled ($\Delta T_{sub}$= 80K) water data plotted with the 1/4 power law*
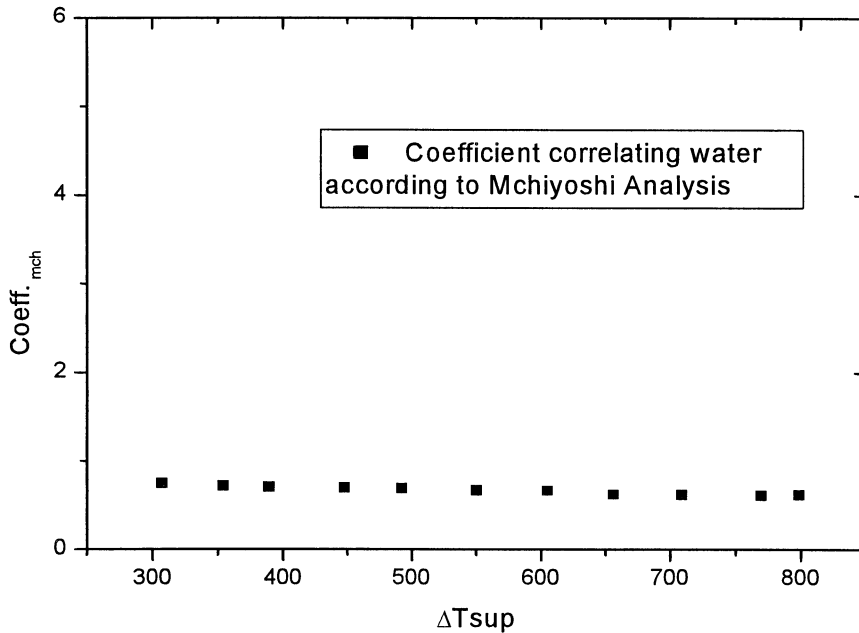
**Figure 7. 9** *Highly subcooled data plotted in form of Michyosh's Correlation*

In the aforementioned three plots, Figs. 7.7, 7.8 and 7.9 considering the variation of the coefficients of the correlations with the degree of superheat value, it can be deduced that the ratio approach predicts the experimental data (without incorporating the effect of superheat in the constant), better than the other two. Therefore a good prediction of the present experimental data is made by Michyoshi's correlation. Further analysis is carried out to understand the sensitivity of these correlations with the degree of subcooling.

## 7.2 Effect of Subcooling

It is already discussed in the literature study that, subcooling affects the film boiling heat transfer considerably. Subsequently, a number of correlations are presented which takes in to account this effect. The data plotted earlier showed the variation of the coefficients used in the correlations with surface superheat, however all plots were made at a constant subcooling value. Figs. 7.10, 7.11 and 7.12 show the effect of the subcooling in heat flux; heat transfer coefficient, Nusselt Number and correlation coefficients will be presented.
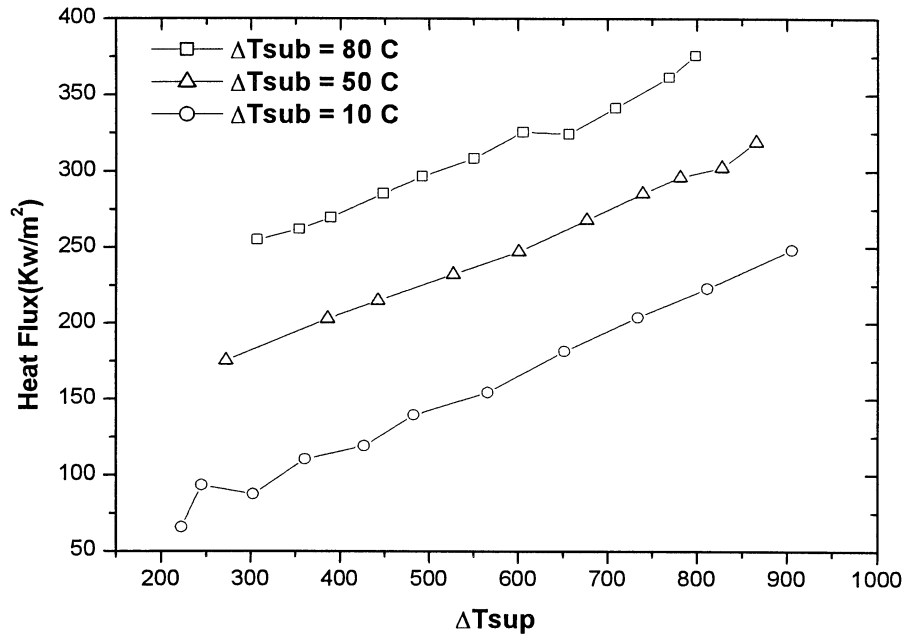
**Figure 7. 10** *Heat Flux Vs superheat temperature at different degree of subcooling for distilled water*
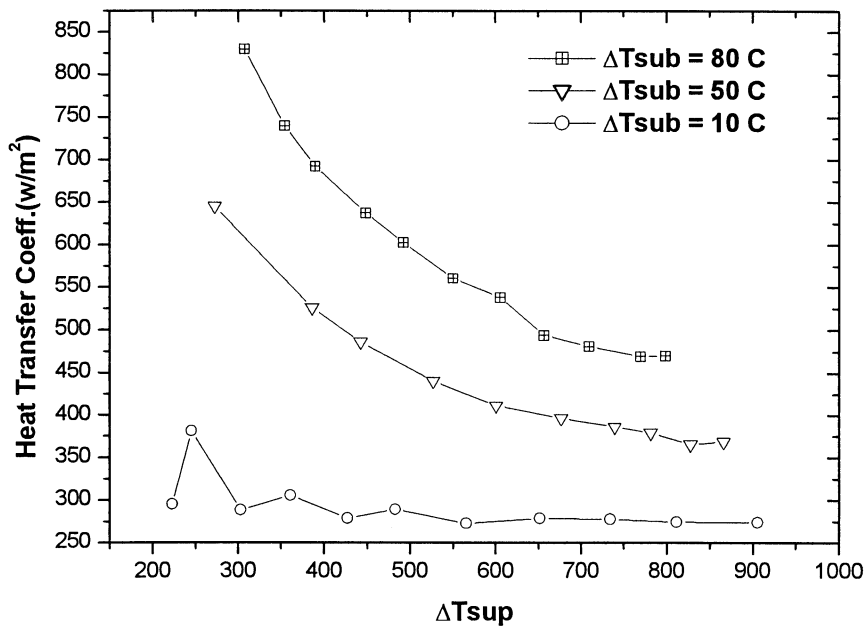


**Figure 7. 11** *Heat Transfer Coefficient Vs Superheat temperature at different degree of subcooling for distilled water*

In Fig 7.10 the heat flux increases with degree of subcooling following the same trend in its variation with superheat. Minimum film boiling point heat flux and the corresponding superheat temperature also increased with liquid subcooling.

Fig. 7.11 shows that the heat transfer coefficient increases with degree of subcooling. For near saturation case, heat transfer coefficient remains almost constant (approximately 280 $w/m^2K$) with the degree of superheat temperature.

The total Nusselt number, which includes the radiation heat transfer contribution is plotted in Fig. 7.12.This also revealed similar effect as showed in the heat transfer coefficient. The deviation in the Nusselt number between different degrees of subcooling is narrower than that showed in heat transfer coefficient plot.
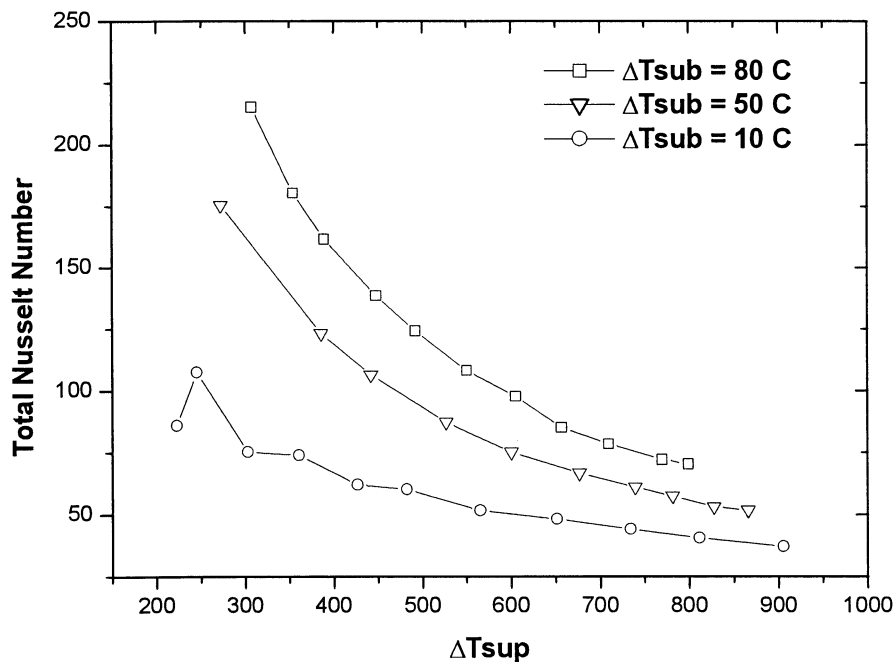


**Figure 7. 12** *Total Nusselt number Vs Superheat temperature at different degree of subcooling for distilled water*

The sensitivity of the correlation coefficients (evaluated from 1/3 power, 1/4 power and Michyoshi) to changes in the degree of subcooling is described in Figs 7.13, 7.14 and 7.15. The degree of superheat is also incorporated. It helps to identify the correlation that predicts the experiment data well. This investigation is presented in Figs. 7.13, 7.14 and 7.15, respectively of 1/3-power, 1/4-power and Michyoshi correlations.
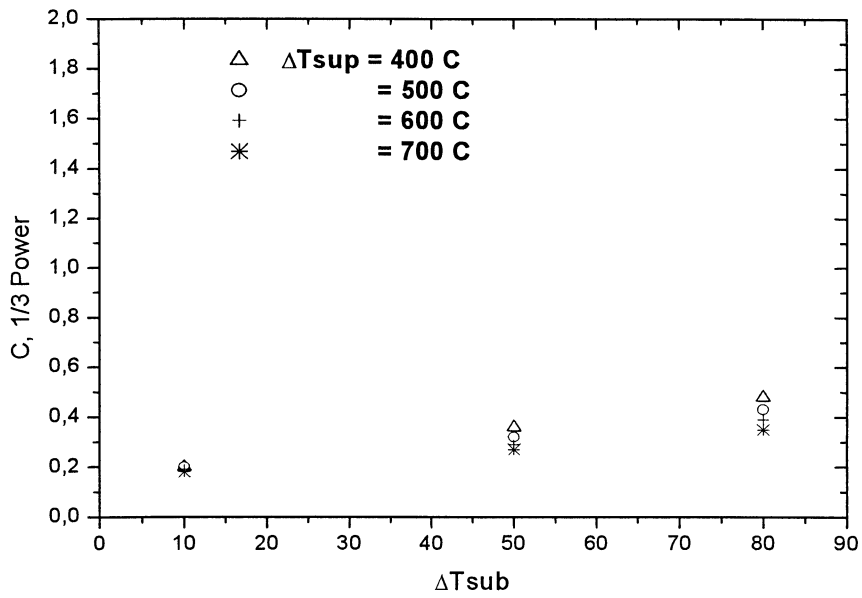
**Figure 7. 13** *The effect of subcooling in the correlations presented in form of 1/3 power law*
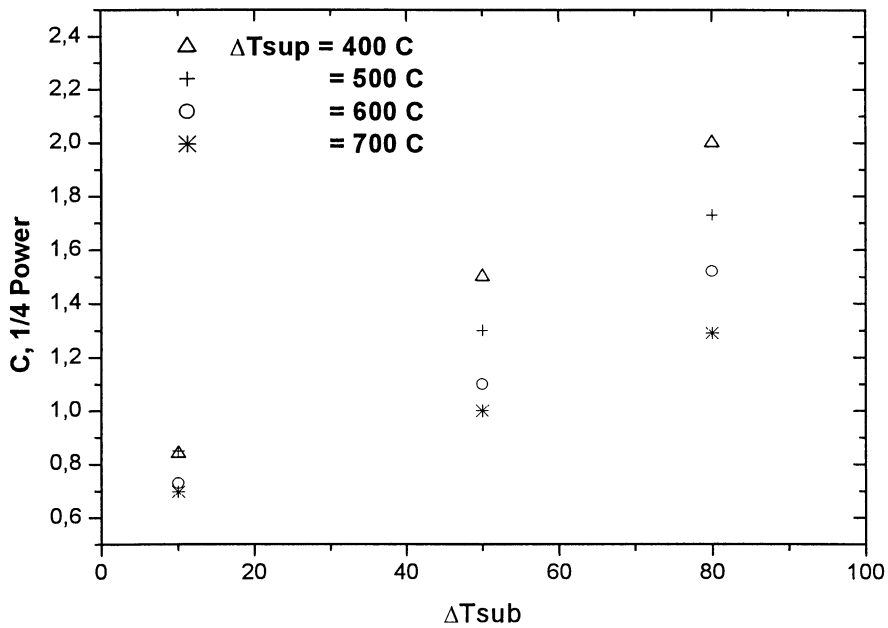


**Figure 7. 14** *Effect of subcooling on the correlation presented in form of ¼ power law*
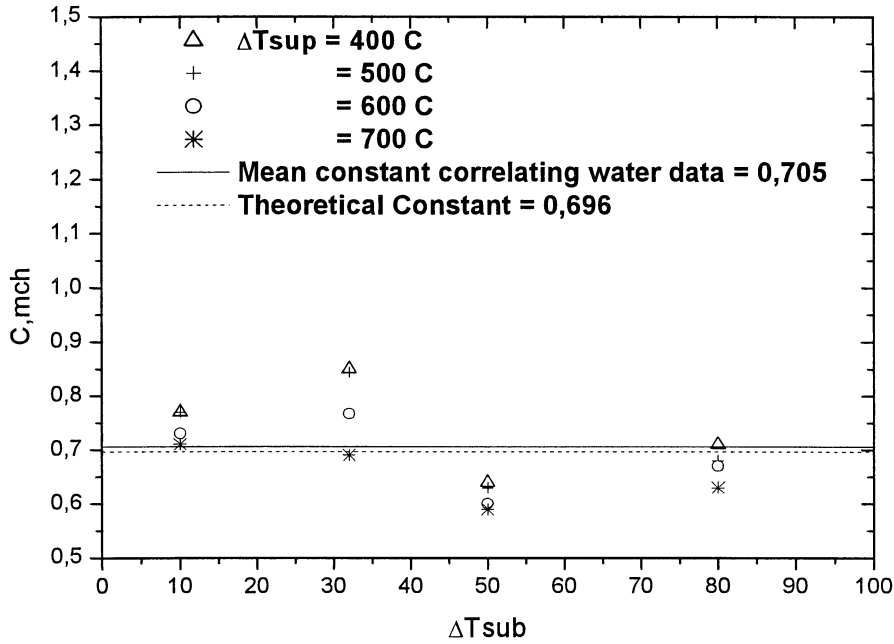
**Figure 7. 15** *Effect of subcooling on the Michyoshi's correlation constant*

Figs. 7.13, 7.14 and 7.15 shows that the experimental data is well correlated by the Michyosh's correlation using an average constant of 0.677 with a standard deviation of 0.04.

For different subcooling and superheating conditions the Michyosh's equation has estimated the data better than the others. Michyoshi correlation can be suggested (with the use of a constant C=0,705) to correlate the present experimental data for the distilled water test with good accuracy. Thus the equation 7.6 can be applied with a constant of 0,705 to correlate all the experimental data of distilled water.

Finally it will be interesting to see the water experimental result plotted for all the cases in the form of equation 7.6. Therefore the data of the ditilled water experiment are plotted in Fig 7.16 in terms of Michyosh's equation and it shows agreement within ±18% error band.

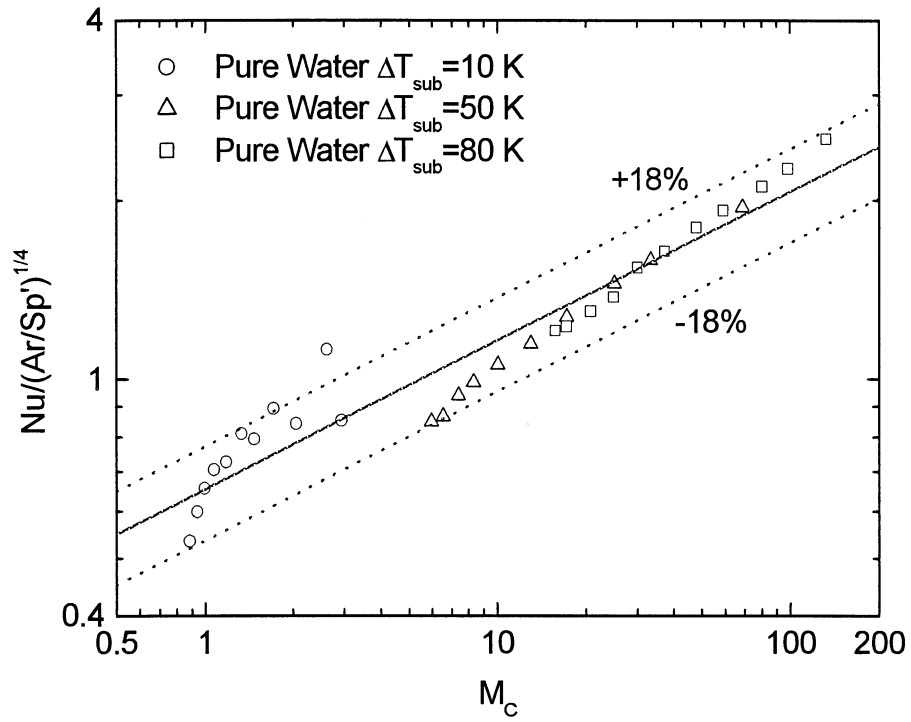**Figure 7. 16** *Water data for different subcooling plotted in form of equation 7.6, atmospheric pressure*

# 8. RESULTS AND DISCUSSION

The preliminary analyses presented in the previous section for the water experiments confirmed that the experimental approach was appropriate and was compared with the existing works. The same experimental approach for the next experiments was employed to perform the next series of experiments with different types of liquids. In this section the result of the film boiling phenomena for different types of fluids will be presented.

## 8.1 The Effect of Changing Fluid Type

The three different fluids were employed:
- Distilled water,
- 5 volume %, $\approx$ 33 nm diameter $Al_2O_3$ particles suspended in a distilled water, prepared only with ultrasonic vibration, and
- 5 volume %, 300 nm diameter $Al_2O_3$ particles suspended in distilled water, prepared by adding laurite salt (surfactant) after ultrasonic vibration

As mentioned in the literature, there are different techniques to suspend the particles in the fluid. In this study, two methods are employed separately. For the smaller size nanoparticles ($\approx$ 33 nm), only ultrasonic vibration technique was employed. As for the 300nm nanoparticles, laurite salt (additive) was used to obtain suspension. Laurent salt was added after ultrasonic vibration, to assist the particles suspend well. Surfactants have recognized effect on the different boiling regimes. To avoid the confusion this additive could bring in the result of the nanofluid analysis, the fluid prepared without surfactant addition was used as a basis for comparison with distilled water. Moreover ultrasonic vibration was observed to suspend the particles well without any addition of surfactant during the 33nm-$Al_2O_3$ nanofluid preparations. However, for completeness, comparison of the result of the nanoparticle suspension with the surfactant is also presented.
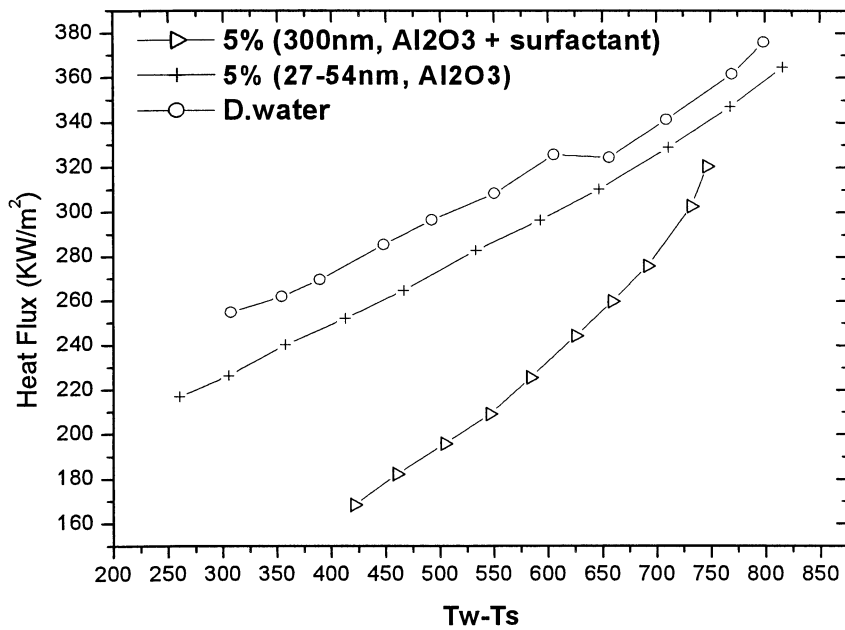
**Figure 8. 1** *Heat Flux Vs Superheat temperature, for the different highly subcooled fluids at atmospheric pressure*

It can be clearly seen from the Fig. 8.1 that the addition of suspensions has resulted in lowering the heat flux at each superheat compared to the base fluid (distilled water). For superheat temperature roughly above 650K, compared with distilled water the nanoparticle ($\approx$33nm) suspension has resulted in a constant degradation of the heat flux by about 14 kW/m$^2$ (3.8 $\sim$ 4.5 %) for each superheat temperature. Below 600K, the constant reduction in heat flux becomes larger. It showed approximately 24 kW/m$^2$ (7.5 $\sim$ 10.5 %) for each superheat. In contrast, the nanoparticle with the surfactant signify deterioration of the heat flux curve. It gives lower heat flux, 18 to 80 kW/m$^2$ lower than pure water.
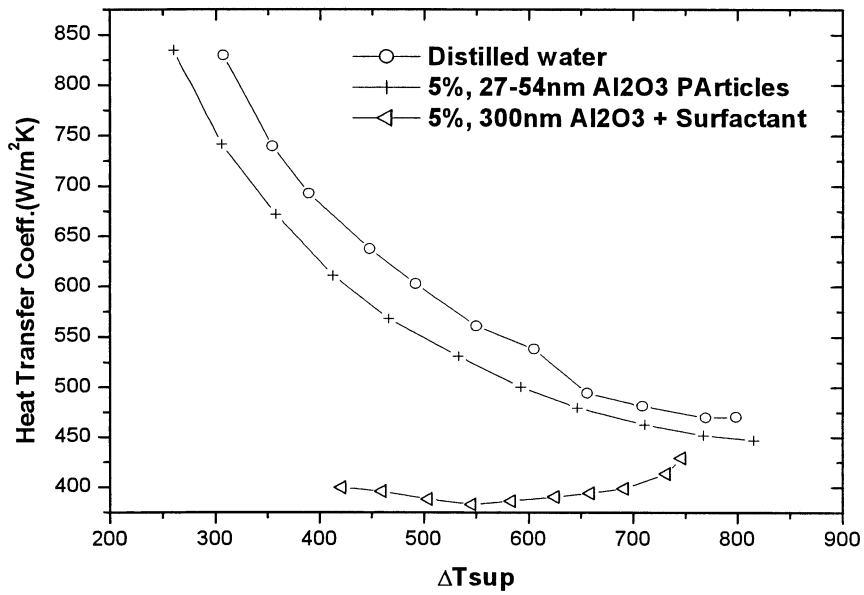
**Figure 8. 2** *Heat Transfer Coefficient Vs Superheat temperature for highly subcooled fluids ($\Delta T_{sub}$= 80K) atmospheric pressure*
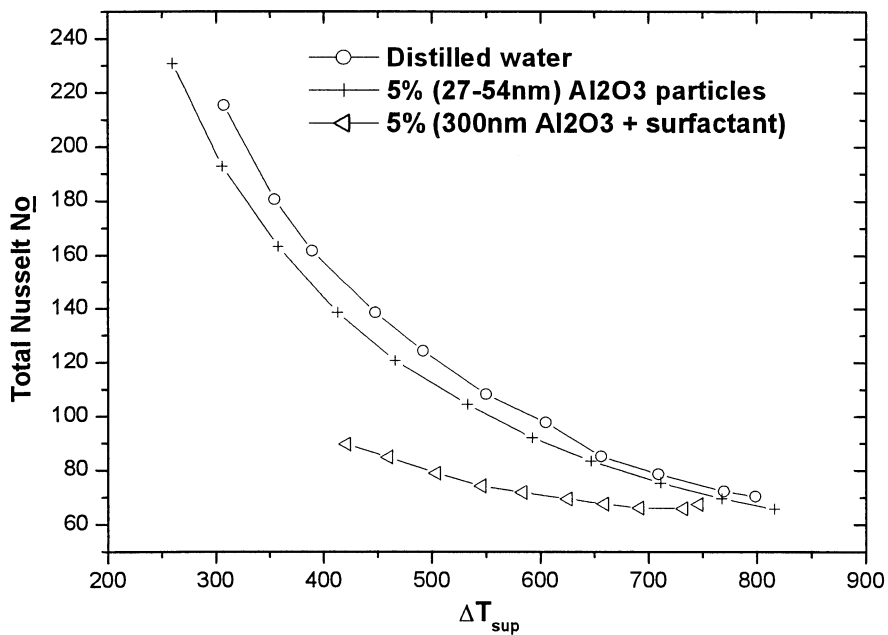


**Figure 8. 3** *Total Nusselt Number Vs Super heat temperature for highly subcooled case ($\Delta T_{sub}$= 80K), at atmospheric pressure*

The heat transfer coefficient presented in Fig. 8.2, also conveys the same result as the heat flux curve. The percentage degradation in the heat transfer coefficient of the nanofluid (without surfactant) based with the pure water is evaluated and plotted in Fig 8.4. The plot demonstrates that the deviation in heat transfer coefficient between the two liquids becomes wider as the superheat decreases. It can be linearly correlated to predict the heat transfer coefficient from the corresponding value for the basic liquid at the same superheat temperature. The relation can be given as

$$\Delta h = 14.05 - 0.013 * (\Delta T_{sup}) \tag{8.1}$$

$$\Delta h = \frac{[h \text{ (base liquid) } -h \text{ (nanofluid, without surfactant)}] * 100}{h \text{ (basic fluid)}} \tag{8.2}$$

where h is the heat transfer coefficient
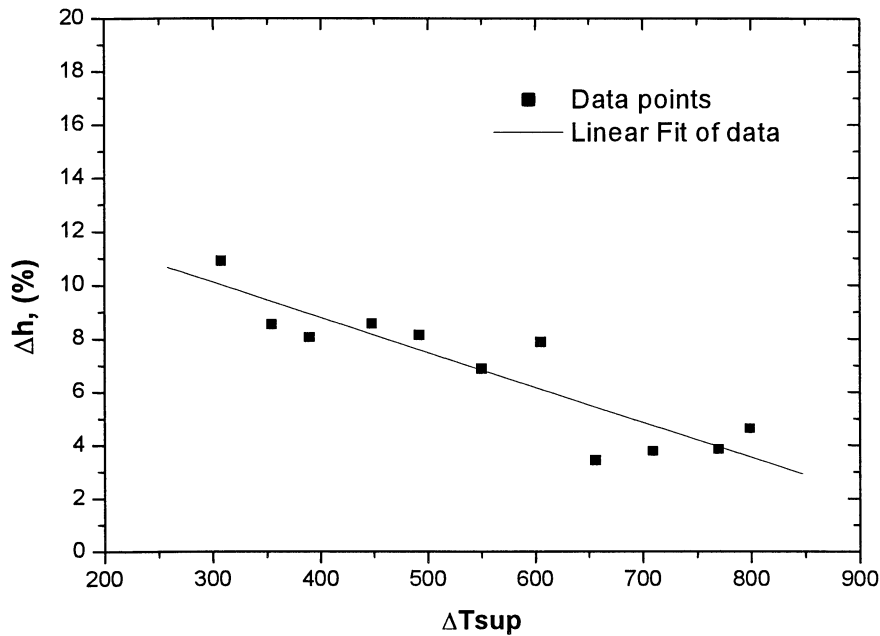


**Figure 8. 4** *Percentage reduction in heat transfer coefficient of the nanofluid (5 Vol. % 33nm Al₂O₃ solution) from the base fluid (distilled water)*

Fig 8.3 shows that at higher superheat region the variation in the total film boiling Nusselt numbers among the three fluids is small compared to the pure water. The variation becomes wider and wider as the superheat temperature decreases.

## 8.2 Effect of the Degree of Subcooling

Changing the degree of subcooling, the effect of nanoparticle suspension in the heat flux and heat transfer coefficient of film boiling heat transfer is analyzed. This was initiated with the assumption that the suspensions may become active in transferring the heat at an increase temperature of the fluid. Fig 8.5 shows the effect at a relatively lower subcooling value.
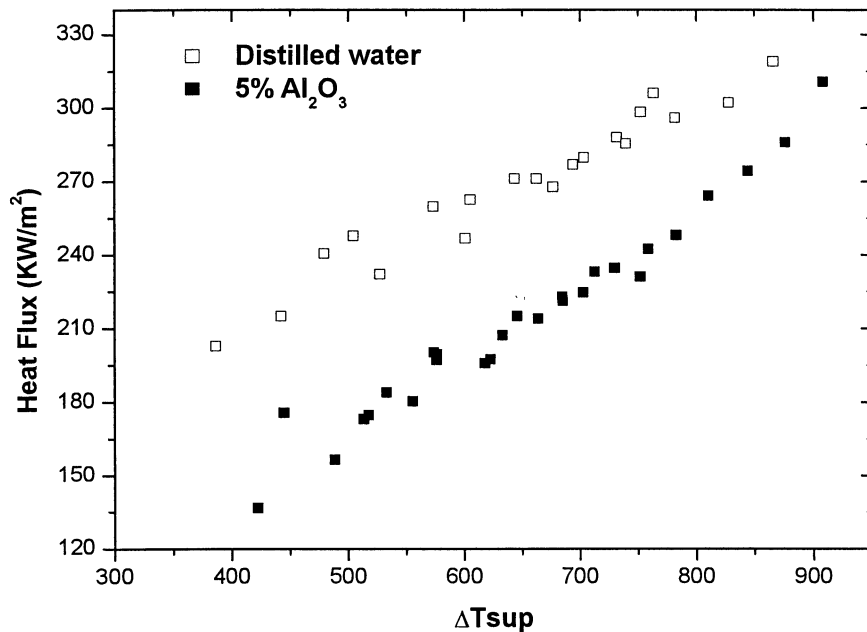


**Figure 8. 5** *Heat Flux Vs Super heat temperature at ($\Delta T_{sub}$= 30K)*

Fig 8.5 revealed decreasing the degree of liquid subcooling, the degradation in film boiling observed for nanofluids is not reverted.

In the heat flux shown in Fig 8.5, in the case of lower liquid subcooling ($\Delta T_{sub}$= 30K), the degradation in heat flux is larger than that observed for the highly subcooling case ($\Delta T_{sub}$= 80K). Unlike the deviation observed in Fig 8.1, which remained almost constant with superheat temperature, at lower degree of subcooling, the variation becomes large with decrease of superheat temperature. It ranged roughly from 30 to 68 kW/m² (10–50 % degradation). Moreover, near elevated superheat radiation heat transfer is more prominent than conduction and convection heat transfer. This might be the reason for lower difference between the two fluids at higher superheat temperature.

The heat transfer coefficient shown in Fig 8.6 indicated a wide gap between the two fluids compared with the highly subcooled condition. The reduction

varies from 38-163 W/m$^2$k as the degree of superheat lowered from 850K to 400K.

At $\Delta T_{sub}$= 30K, the nanofluid resulted with a heat transfer coefficient roughly constant ($\approx$325 W/m$^2$K) with the superheat temperature. For distilled water this phenomenon was observed at relatively lower degree of subcooling ($\Delta T_{sub}$= 10K). This implied that the suspension of nanoparticle has enhanced the generation of vapour making the subcooled fluid to behave the same as distilled water performed in near saturation condition.

In Fig 8.7, the Nusselt number is plotted for the two fluids at lower degree of subcooling. The deviation in the value ranged from 5 to 38 with varying the superheat temperature. Typically, in the heat transfer coefficient plot the variation between the fluids is observed to be much larger, in comparison with the heat flux and Nusselt number plots.

The degradation observed in the three plots for heat flux, heat transfer coefficient and Nusselt number for nanofluids are postulated to be because of the ability of the particles to enhance the vapour generation and making film to be stable and thick. This will be explained later after all the possible plots are presented.
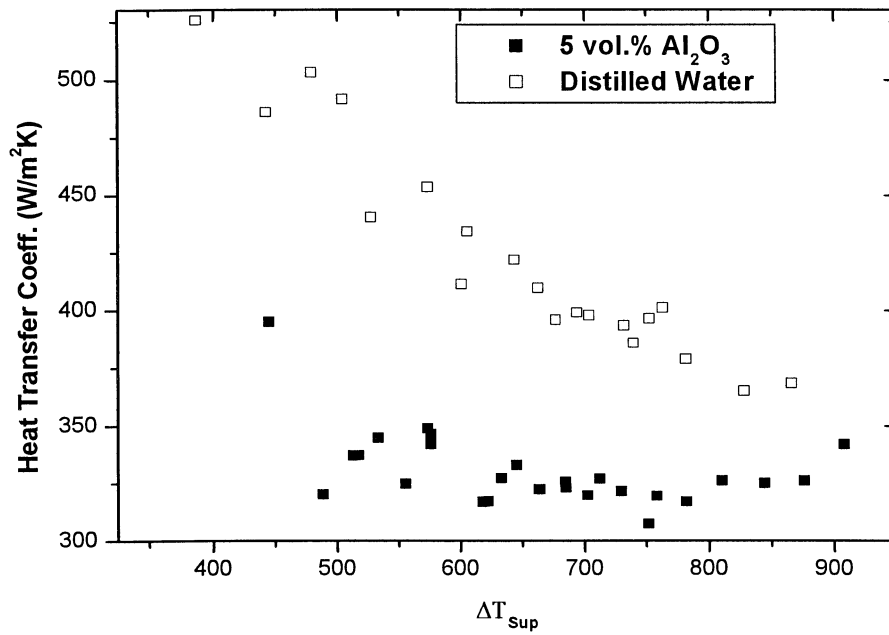
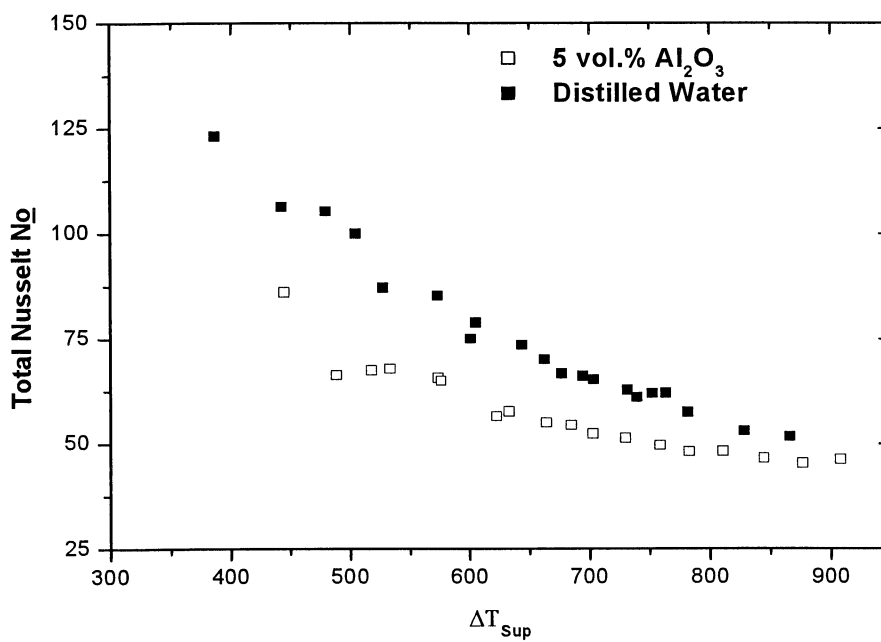**Figure 8. 6** *Heat transfer coefficient Vs Superheat temperature at ($\Delta T_{sub}$= 30K)*



**Figure 8. 7** *Total Nusselt number Vs Superheat temperature at $\Delta T_{sub}$= 30K , atmospheric pressure*

## 8.3 The Effect of Nanoparticle Concentration

The volume percentage of the nanoparticles was increased to investigate the influence of having densely particles in the fluid. The concentrations include 5%, 10%, and 20% volume percentage of $\approx$33 nm $Al_2O_3$. The heat flux, heat transfer coefficient and the Nusselt number plots with superheat temperature are presented in Figs. 8.8, 8.9 and 8.10, respectively.

The results showed that the effect of concentration is not significant after 5% volume. The different concentrations are observed to show almost similar effect. A slight further reduction in heat transfer values was observed with increasing percentage volume. However the variation was not seen to be consistent.

This agrees with the recent study of You and Kim (2003) [Fig. 8.14]. They investigated the effect of a very small concentration of nanoparticles on critical heat flux. They observed that above 0.01g/liter concentration level, no effect of nanoparticle concentration on CHF was noticed. Their observation can be an indication to make the future focus of the study towards low concentration effects.



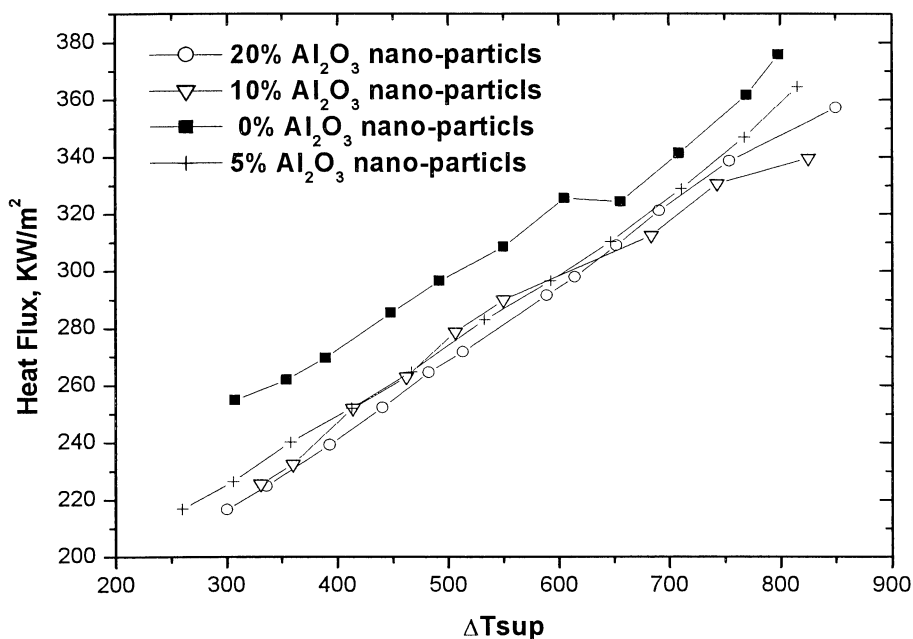**Figure 8.8** *Heat flux Vs Superheat temperature for increasing concentration of nanoparticles, atmospheric pressure*
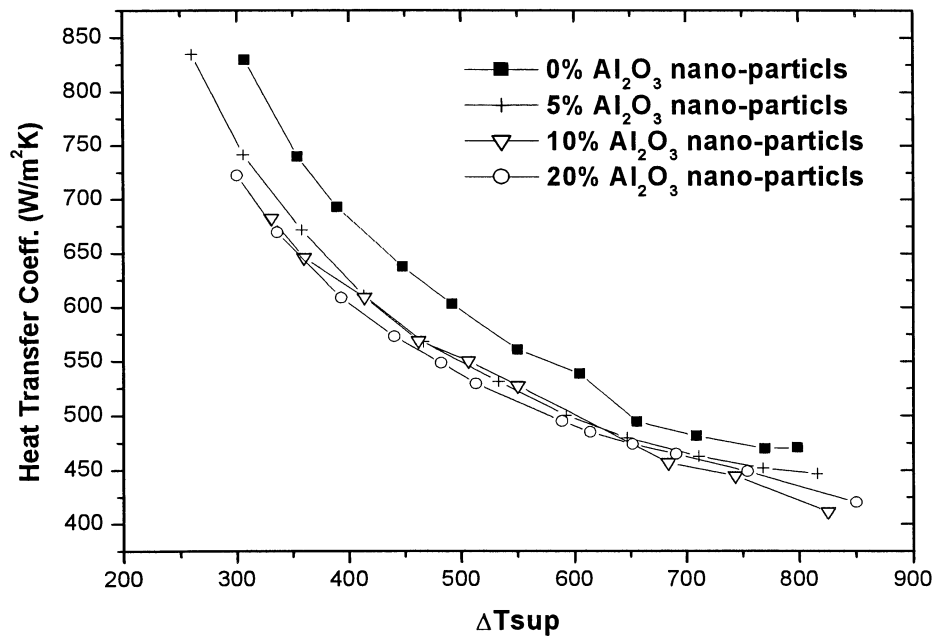
**Figure 8. 9** *Heat transfer Coeff. Vs $\Delta T_{sup}$ with increasing concentration of nanoparticles*
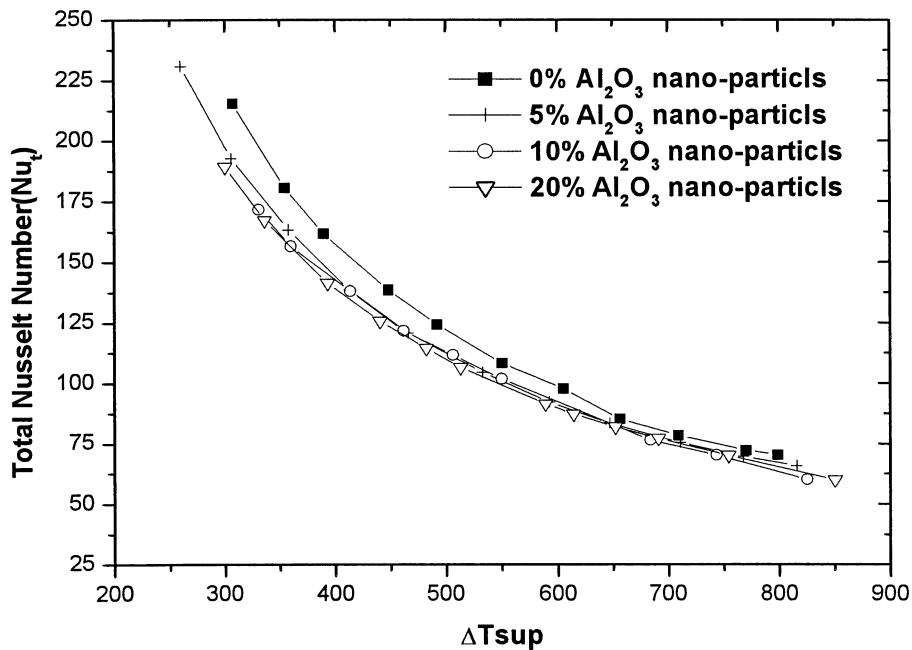


**Figure 8.10** *Total Nusselt number Vs Superheat temperature with increasing Conc. of nanoparticles, atmospheric pressure*

## 8.4 The Minimum Film Boiling Point

Further investigation on the nanofluid experiment was conducted to understand the reason for their degradation of film boiling heat transfer. This includes minimum film boiling heat flux and minimum film boiling superheat temperature for different concentration nanofluids. This specific analysis will have importance in informing whether these fluids have potential to suppress the steam explosion phenomena. The plots are presented in Figs. 8.11 and 8.12.

The minimum film temperature plotted in Fig 8.11 showed that the 5 vol. % nanofluid has a minimum film point temperature less than all the water tests at the same subcooling ($\Delta T_{sub}$=80K). Nevertheless, increasing the concentration of the particles brings back the result similar to those for distilled water. In general it can be said that relatively higher concentrations have no significant change over the minimum film boiling temperature.
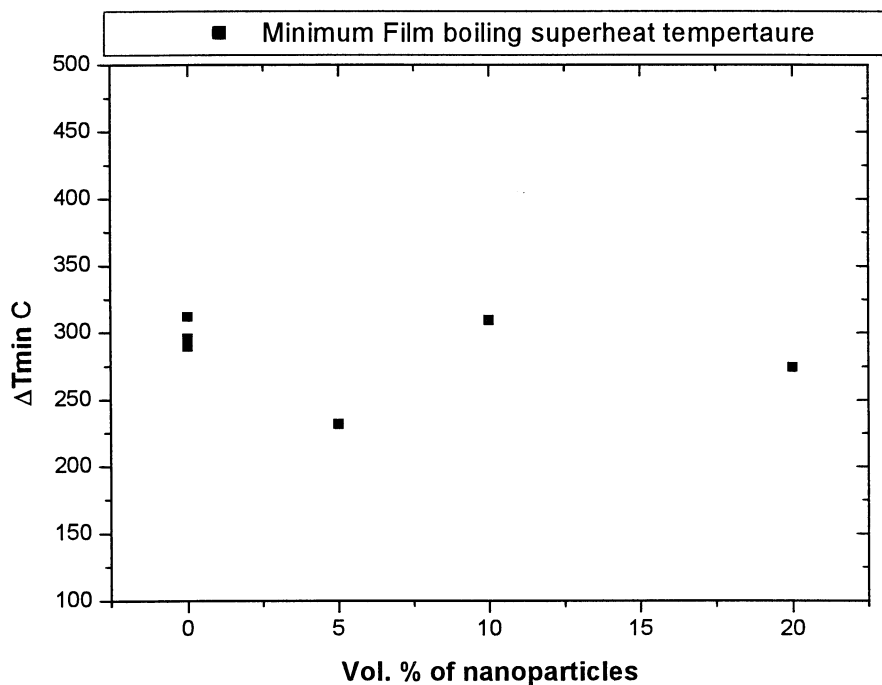


**Figure 8. 11** *Minimum film boiling temperature Vs Concentration of nanoparticles in water, atmospheric pressure, $\Delta T_{sub}$=80K*

The minimum heat flux is also plotted in Fig 8.12. In this figure the nanofluids have given lower minimum heat flux than pure water. The reason for the decline in the minimum heat flux value could be due to the same reason that the nanofluids in general showed a degradation in film boiling heat transfer coefficient.
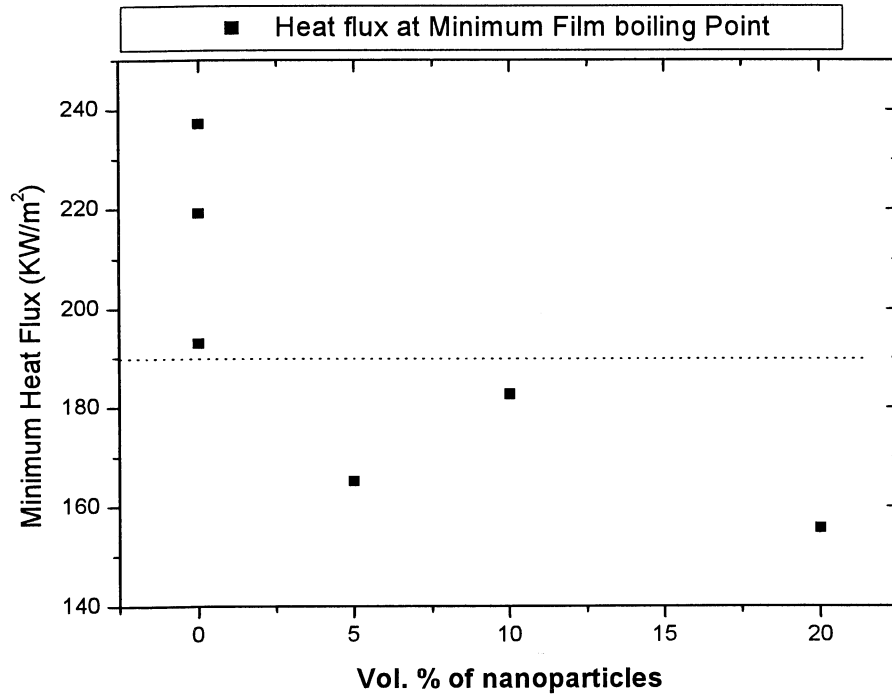


**Figure 8. 12** *Minimum heat flux Vs Concentration of nanoparticles in the basic fluid (water) $\Delta T_{sub}$ =80K, atmospheric pressure*

Finally it was interesting to see a plot as shown in Fig 8.13 that comprises the minimum heat flux and the minimum film boiling temperature together.
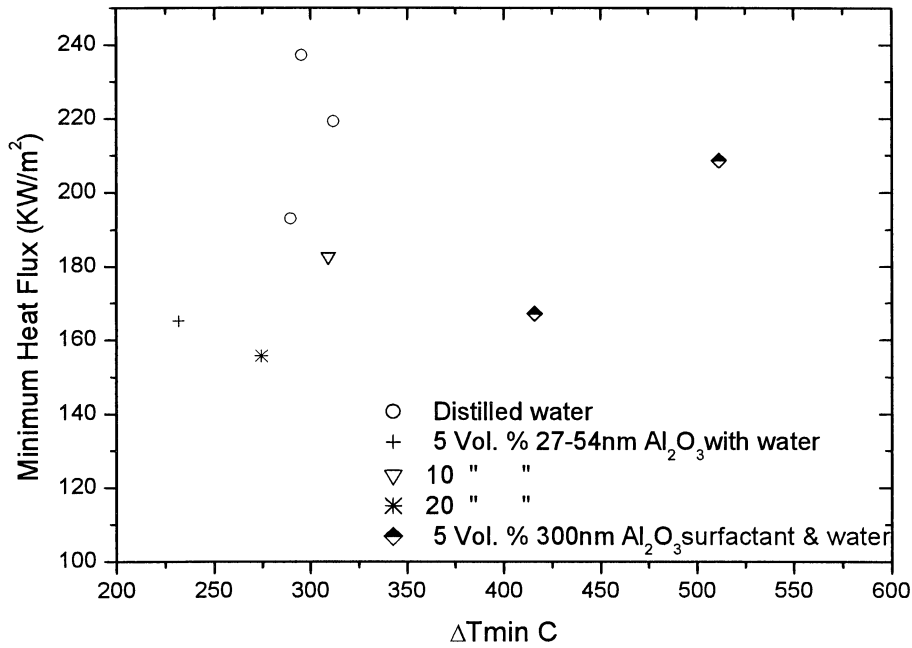
**Figure 8.13** *Minimum heat flux with the corresponding superheat temperature for all fluids*

Fig 8.13 revealed similar trend: this nanofluid could have the tendency of decreasing the minimum heat flux and the corresponding minimum film boiling superheat temperature. That could make this fluid to be candidate for suppressing steam explosion.

Unlike the rest of the liquids, the fluids with surfactant resulted in a higher minimum film boiling temperature. However it is essentially to make a remark that the fluid with the surfactant has suspensions relatively larger in size (300nm) than the main nanofluid ($\approx$33 nm) considered earlier.

## 8.5 Discussion

It is mentioned in the literature survey section that suspending small concentration of nanoparticles has enhanced the thermal conductivity by 10 to 60 % [Eastman (1997), Choi (1995), Xuan (2000), etc]. Furthermore, Xuan has observed the potential of the nanoparticles in advancing the rate of heat transfer in the natural convection. However their effect in the two-phase application i.e. for instance in boiling, typically in nucleate boiling region is found to be insignificant compared with water. One study was mentioned in the literature study, to have reported degradation in nucleate pool boiling with addition of nanoparticles.

Recently studies have interestingly shown a considerable increase in the critical heat flux limit (CHF) with using small quantity of nanoparticle suspensions (Fig. 8.14). You and Kim (2003) have displayed the observation of the bubbles using a camera. From the picture taken for the two fluids, distilled water and diluted nanofluids, the vapours formed for the case of diluted nanofluid solution are larger in size and the departure rate is very less frequent (Fig 8.15).
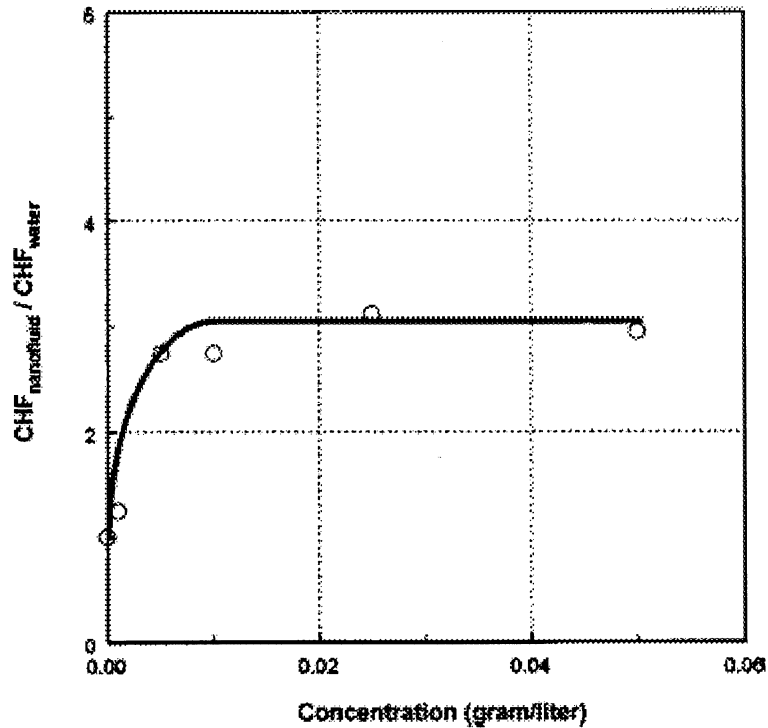


**Figure 8. 14.** $CHF_{nanofluids}$ /$CHF_{water}$ at different concentrations, [You and Kim(2003)].
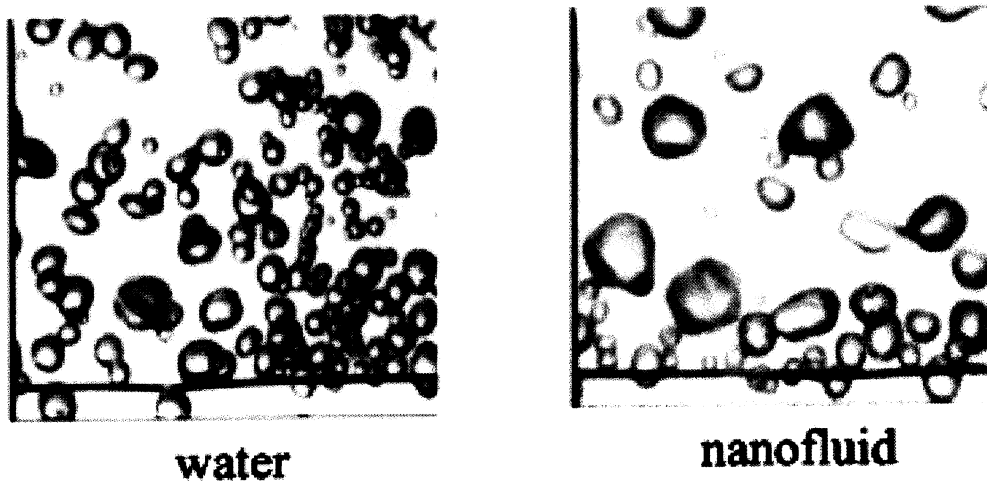
water                              nanofluid

**Figure 8. 15** *Sample Pictures of bubbles from wire (300KW/m²) [You and Kim (2003)]*

Thus the reason to the present observation the nanofluids performance, decline of in the heat transfer coefficient of film boiling region in comparison to distilled water could be hypothesized in different ways. However the author believes that this could be that nanoparticles increase the vapour film thickness, as a result of enhanced boiling process observed in the presented plots. The film thickness might be attributed from either the increased nucleation site density that the particles could create on the vapour liquid interface or the particles could act as local heat generators because of the increased heat capacity.

To further analyse this postulation, the quenching rate (temperature drop to the corresponding elapsed time) and the film boiling region duration were calculated and compared in Figs. 8.15 and 8.16, respectively.

Fig. 8.15 showed the nanofluids for all the concentrations provides minimum quenching rate than pure water. As the quenching rate used here includes all the boiling regions, the next plot in Fig 8.16 was necessary to identify the boiling regime resulted in the decrease of the total quench rate for these fluids compared with water.

The comparison in the duration of film boiling region explained the lower quenching rate could be due to the extended film boiling portion that this fluids showed. In turn this agrees with the earlier assumption that, nanofluids could have a thick stable film, which could be a possible cause for their lower film boiling heat transfer coefficient.

It can be noted that, if these fluids have a tendency of increasing the bubble dimension as illustrated above in the recent studies, thus probably their effect

in increasing the vapour size or film thickness in the film boiling region is a better assumption. This could be a reason for decrease in the heat transfer as the vapor thickness and the Nusselt number has inverse relation ship.

A further study is under way to clarify this postulation. It will employ a technique that helps to measure the film thickness experimentally using processing the image of the film configuration. However, since nanofluids are not transparent unless diluted X-ray radiography can be useful to configure the film around the sphere in these fluids.
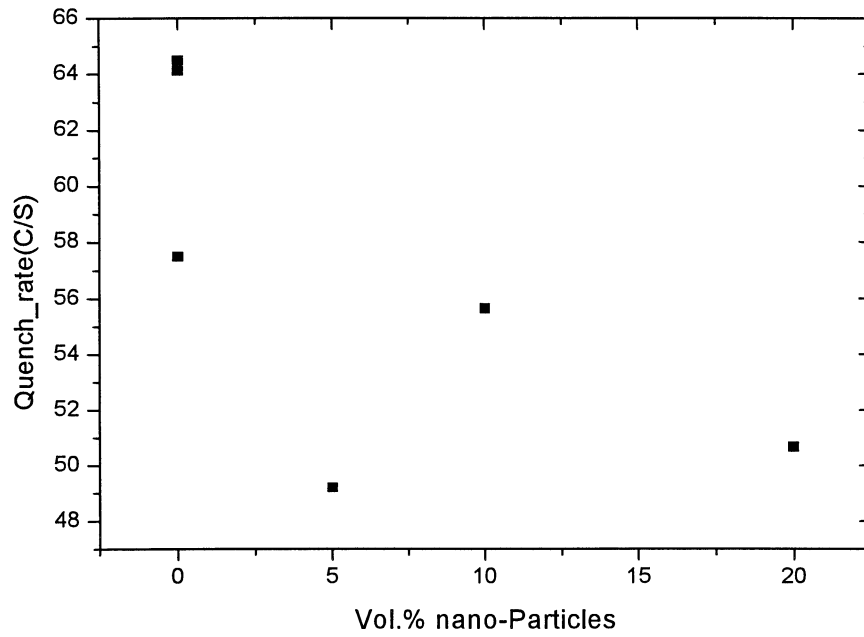
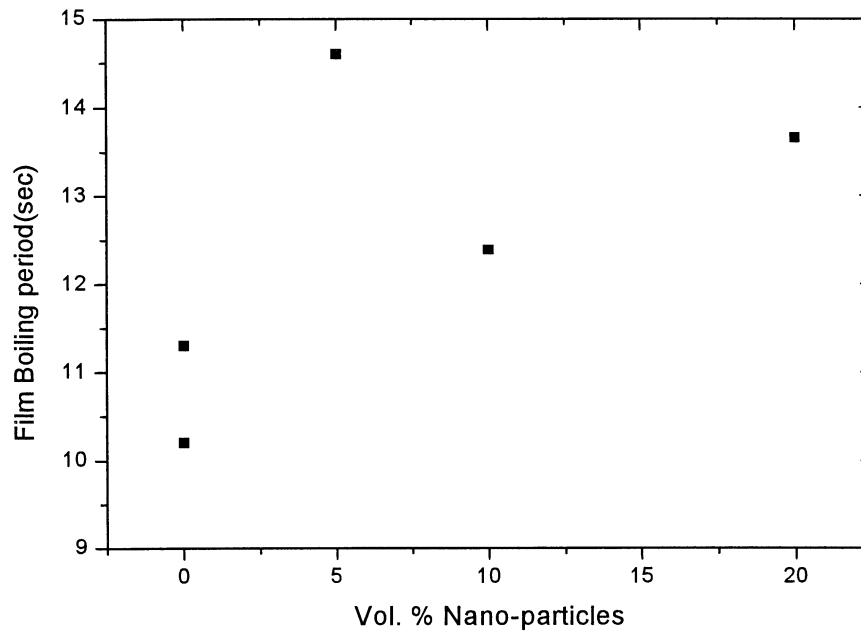**Figure 8. 16** *Quenching rate with concentration of nanoparticles*



**Figure 8. 17** *Film boiling periods with concentration of nanoparticles.*

The other interesting point might be to investigate how the quenching process would be affected by the presence of nanoparticle suspensions in a fluid. It is noted that, an ideal quench is one that proceeds at an infinitely fast rate since this would prevent any massive coalescence of hardening solutes along the grain boundaries. In most practical situations, however, quench rate is slowed by the poor heat transfer effectiveness of the film boiling regime at the onset of the quench. The rate of quenching is slowest during the film boiling regime and undergoes a rapid increase at the Leidenfrost (minimum heat flux) temperature. Unfortunately, it is at temperatures associated with the film boiling regime that much of the detrimental coalescence of solutes occurs along the grain boundaries. To most heat treatment operations, earlier exit from the film boiling regime (i.e. a higher Leidenfrost temperature) is key to attaining a proper alloy microstructure; hence the practice of using additives which facilitate the breakup of the vapor blanket at higher surface temperatures was common practice. A more popular alternative to bath cooling in many heat treating operations is quenching via water sprays. High velocity droplet impact greatly increase cooling effectiveness in all boiling regimes; thus contributing to a faster rate of quenching and superior.

For comparison at the same set up condition, a test with distilled water was conducted before changing the fluid to nanofluids. The fluid is changed and the ball is heated to higher temperature. Subsequently, a trial was made to repeat the experiment without varying any set up at the same concentration. Whenever the sphere was not cleaned for the tests none of the attempts made to obtain a stable film boiling were successful. It was postulated that deposition of nanoparticles in the previous tests altered the roughness or surface condition of the sphere. Therefore, to check if this assumption is true the ball is cleaned lightly and the experiment was repeated again. This time a stable film was obtained.

Fig. 8.17 shows that repeated results of the experiment with and with out cleaning the sphere in terms of quenching rates.

This experiment was conducted under 5 vol. % solution of nanofluid. Then the test was repeated with no sphere cleaning, however it was not possible to see stable film up to test No 4. To check if the event remains same after the liquid pool is replaced by distilled water, No 5 was conducted with that frame of mind, however still it was not possible to get film boiling. Then the ball is cleaned and the experiment is repeated for 10 vol. %, in the same way a stable film is observed only in the first experiment. Altering the fluid to distilled water again gave the same result with no cleaning. If not the ball is cleaned; there was no film observed for the consecutive tests after experiment with nanofluid is carried out.

Those experiment that showed a stable film boiling are characterized here by their corresponding lower quenching rate (expressed by the ratio of temperature drop to the time elapsed). In cases where no film is observed the quenching rate radically increased and it means with in short time it will be possible to take too much heat from the ball. This value is considerably lower

86

when a stable film boiling is occurred compared with experiments that didn't experience the film boiling region.

The analysis showed the new fluid changes the entire quenching rate of the specimen. It is observed that nanoparticles stacked with the surface (when the surface is immersed and then heated) and change the surface characteristic and consequently the quenching rate became dramatically fast. That could arise since the surface effect might decrease the contact angle and the wetting characteristic will raise resulting in high heat transfer and changing the surface roughness and or chemistry of the sphere.

The phenomena might be interesting for metallurgists, as it could open a new opportunity in developing a mechanism to boost the quenching rate. There could be a great possibility of destabilizing the film boiling to get early collapse so that the quench rate will be higher.
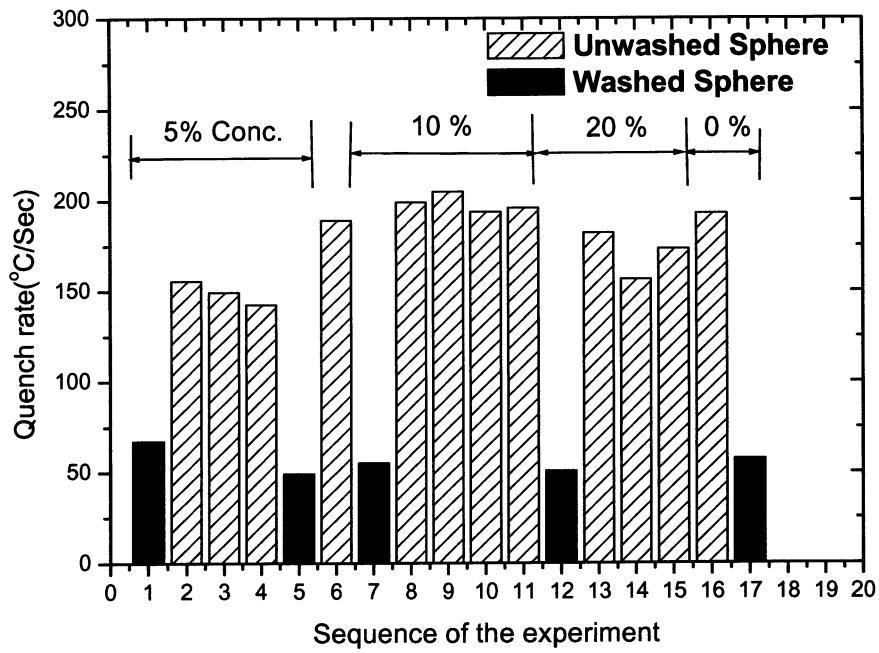
**Figure 8. 18,** *Quench rate for a repeated test in different concentration of nanofluids*
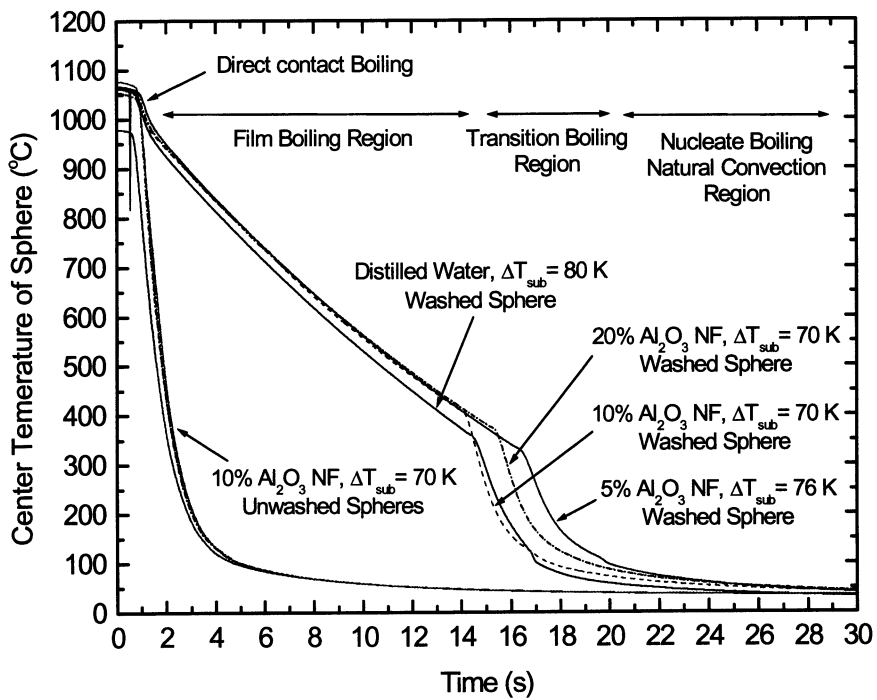


**Figure 8. 19,** *Transient temperature history, with and with out quenching*

## 8.6 Correlating Nanofluid Data (with and without surfactant)

In this section, the nanofluid data are correlated with the selected correlations discussed in the previous section 7, such as 1/3, 1/4-power law and Michyoshi's correlations.

Next the nanofluid data (with and with out surfactant) will be presented in terms of the 1/3 - power law, 1/4-power and the Michyoshi's correlation for different subcooling cases.
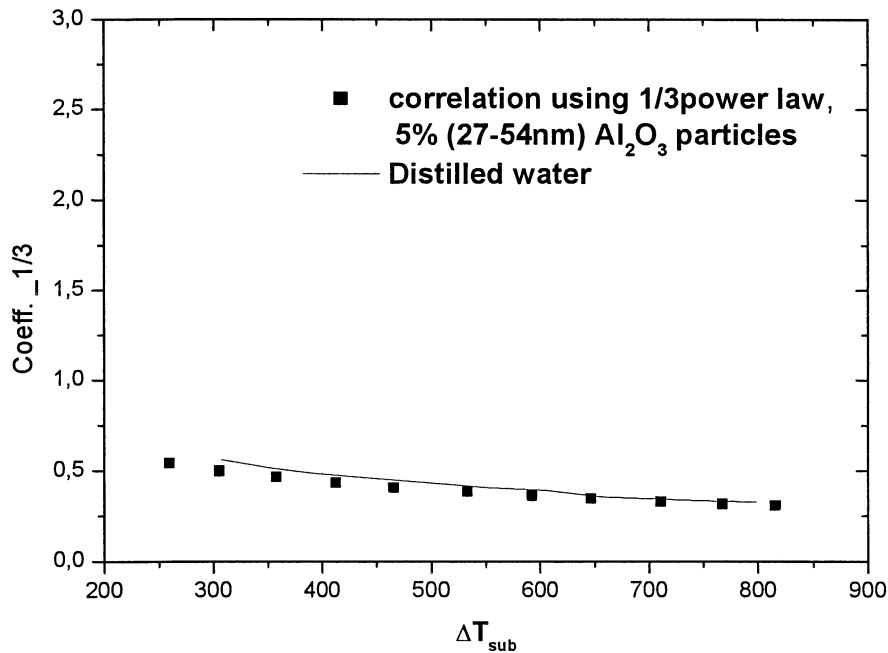
**Figure 8. 20** *Nanofluid data plotted in 1/3-power law form, no surfactant, atmospheric pressure,*
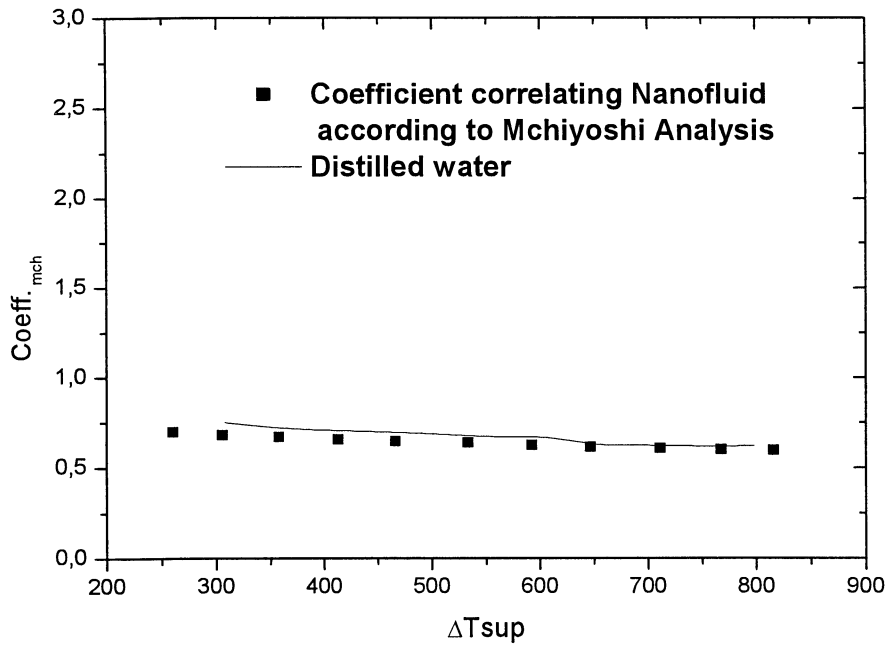
**Figure 8. 21** *Nanofluid data plotted in the form of Michyoshi's correlation*
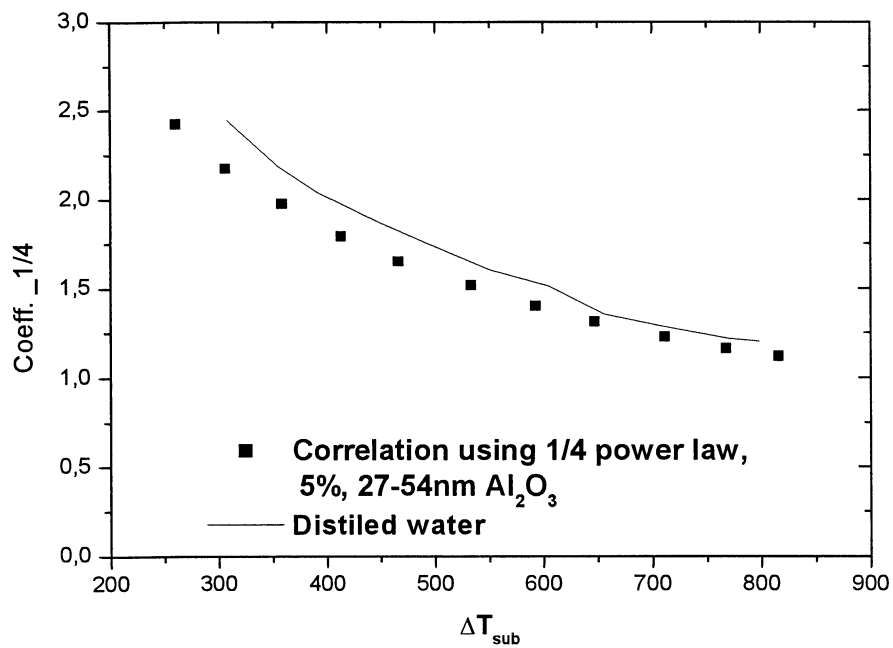


**Figure 8. 21** *Nanofluid data plotted in the 1/4 -power law*

The nanofluid data plotted in the 1/3 power law as shown in Fig. 8.19 resulted in a constant that varied from 0.30 to 0.54, for water it was from 0.33 to 0.56, which is almost the same result as water.

The nanofluid data plotted in the Michyoshi's correlation showed in Fig. 8.20 displayed the constant to vary from 0.60 to 0.70 compared with water results that varied from 0.62 to 0.75. The data in the form of 1/4 - power law (Fig. 8.21) produced constants ranging from1.20 to 2.4 compared with water from 1.12 to 2.42, which is again quite similar with water results. The above plots show more or less the same behavior that shown on similar plots for the water test earlier in the analysis.

There is a possibility of correlating the nanofluids with the same correlations used for water. However, further analysis will be made next to see how the above correlations react to changing degree of subcooling. The nanofluid with a surfactant solution is also repeated to the above plots to see the difference the surfactant caused.
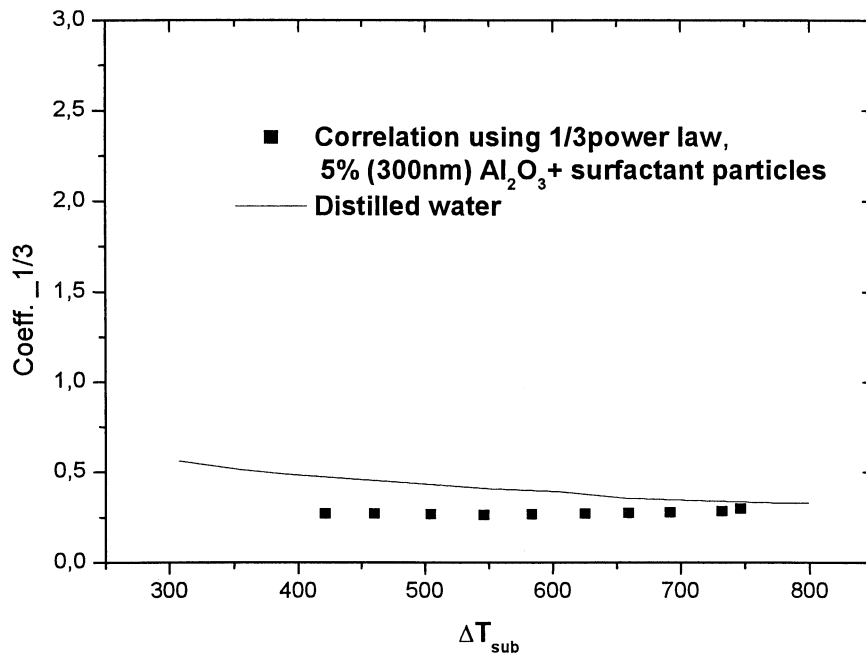


**Figure 8. 22** *Nanofluid with surfactant data plotted in the form of 1/3 power law (High subcooling)*
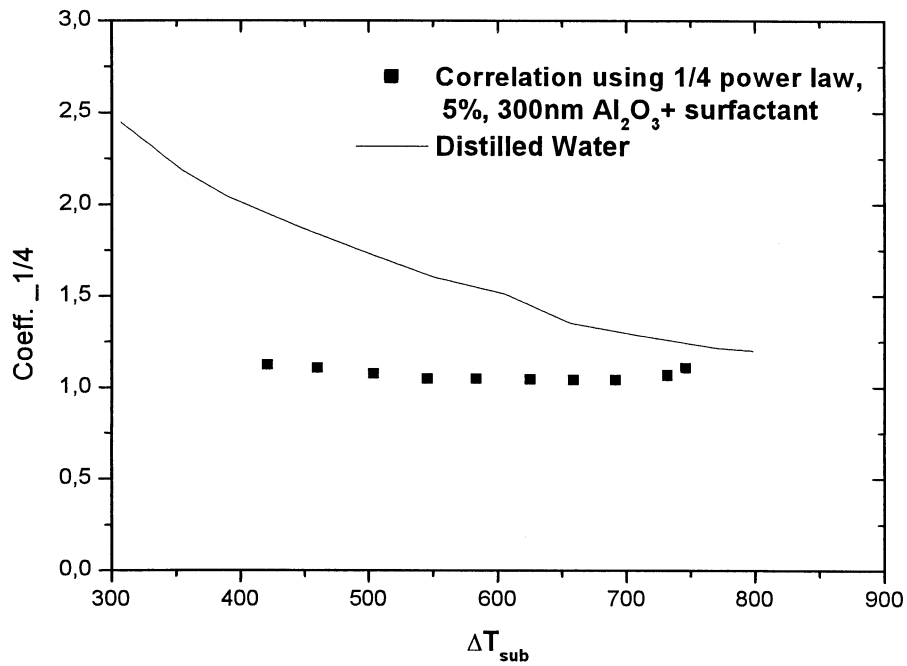
**Figure 8. 23** *Nanofluid with surfactant data plotted in 1/4- power law. (high subcooling)*
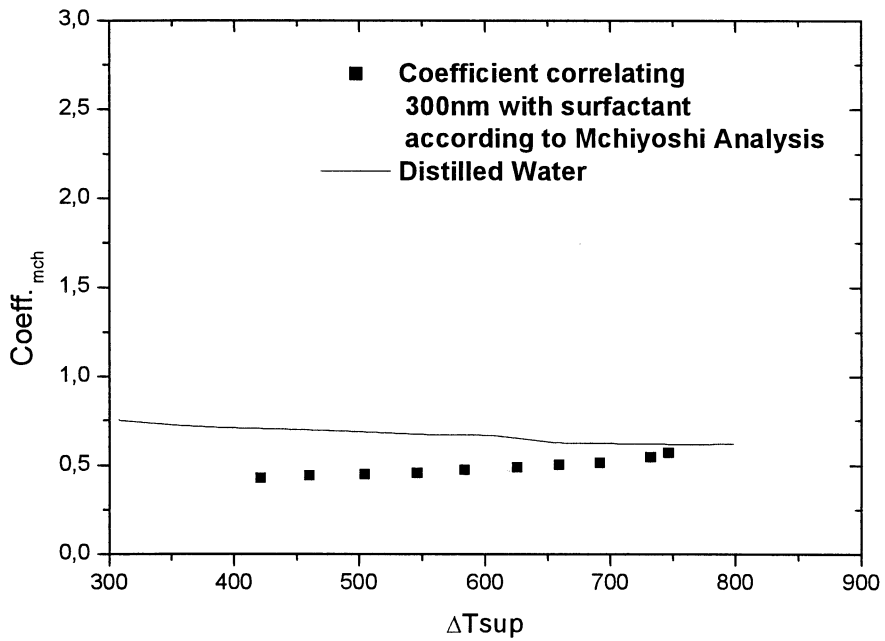


**Figure 8. 24** *Nanofluid with surfactant data plotted in terms of Michyoshi's Correlation, (high subcooling)*

The addition of surfactant does not only deteriorate the film boiling heat transfer rate but also changes the characteristic of the curve. Heat transfer coefficient and Nusselt number plots for the fluid with surfactant revealed the gradient of the curve is almost constant with lowering the superheat temperature. The correlation that I defines the data may vary from the other two fluids.

The 1/3 power law shown in Fig. 8.22 provides the constant to fluctuate from 0.266 to 0.3 with a mean value of 0.276 and standard deviation of 0.01. The variation in the constant for changing the superheat temperature is small compared with the other two fluids. The average value is close to the theoretical value (0.15) recommended in the literature.

The constant that is defined by the 1/4 power-law shown in Fig. 8.23 described a value that is steady with varying the superheat temperature. The value ranged from 1.04 to 1.12 with a mean value of 1.07 and standard deviation of 0.032. Unlike the previous fluids, the correlations with 1/4 and 1/3-power laws (which reflect the saturation effect than the effect of subcooling) could predict the data of the fluid with surfactant.

Michyoshi's correlation shown in Fig. 8.24, described similar difference as with the other fluids. The constant is obtained to diverge with in the range of 0.43 to 0.545. The mean value and the standard deviation are found to be 0.49 and 0.046, respectively.

The effect of subcooling in the nanofluid data presented in terms of the above correlations is also included for nanofluids without surfactant; this will make possible to be accurate in selecting the right correlation for the new fluid. Below the plots of correlation constants against the liquid subcooling is presented in Figs. 8.25, 8.26, and 8.27.
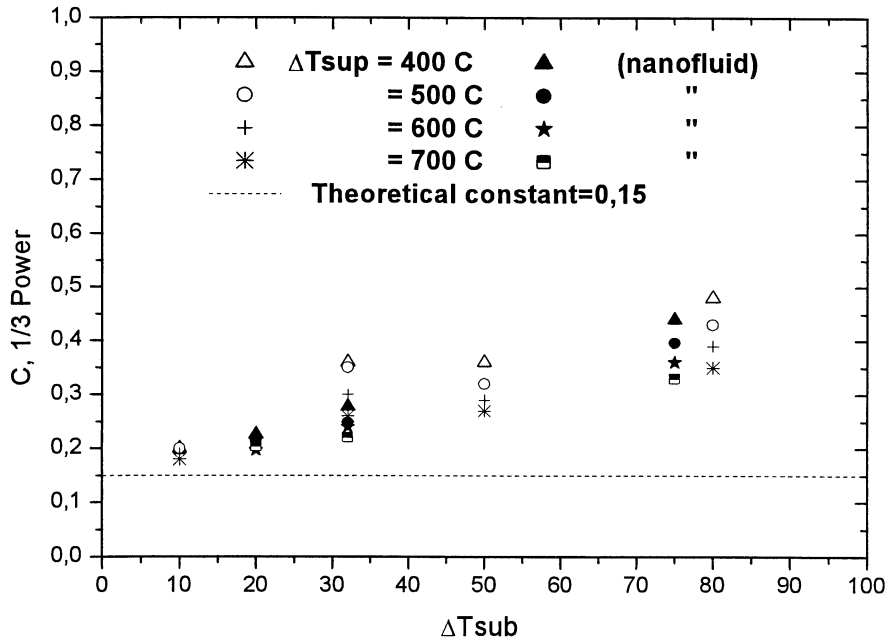
**Figure 8. 25** *Nanofluid and water data plotted in 1/3 power law with subcooling parameter*
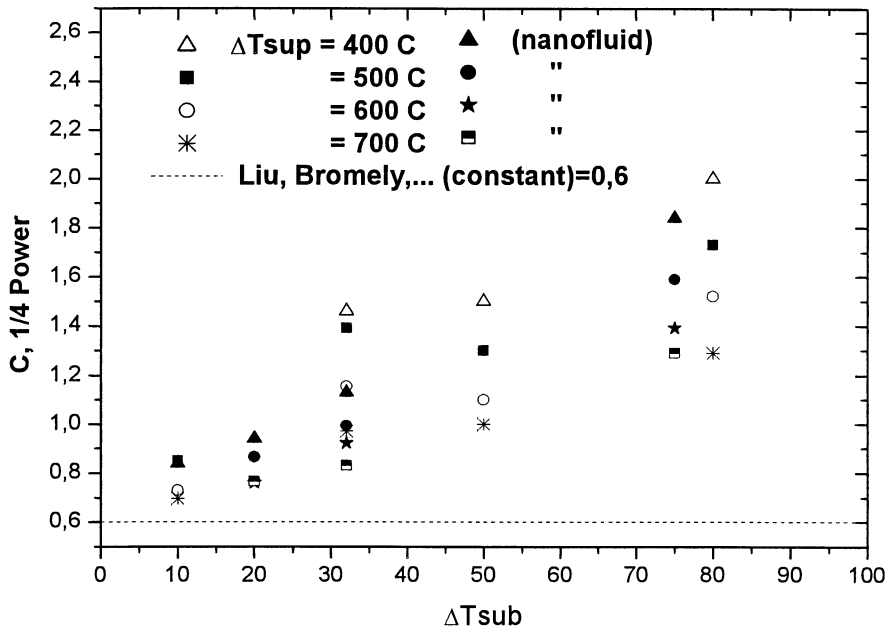


**Figure 8. 26** *Nanofluid and water data plotted in the form of 1/4 power law*
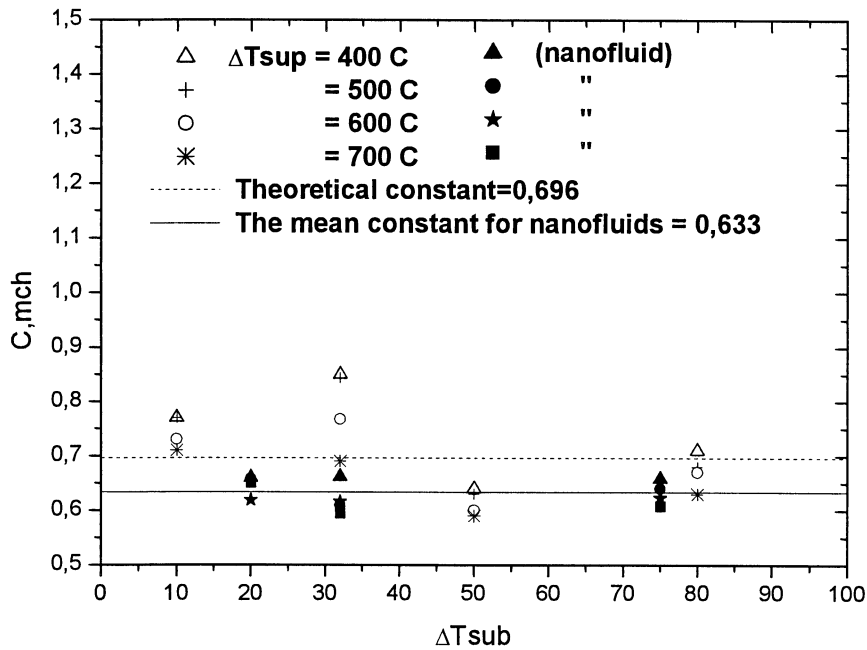
**Figure 8. 27** *The nanofluid and water data plotted in terms of Michyoshi's correlation.*

The three plots clearly show that the constant for 1/3-power law and the 1/4 power law increase with the degree of subcooling. Typically the 1/4 power law diverges more than the 1/3 power law. The trend is the same for water and nanofluids, except the constant for the nanofluid is less than that for water.

On the other hand the constants based on the Michyoish's correlation are almost steady with the degree of subcooling. Here too, the values are less compared to distilled water.

The conclusion is therefore, Michyoshi's correlation as it predicts the water data with a constant 0.695; It can also be taken to correlate nanofluids with out surfactant, constant of 0.633. Thus the nanofluids data can be predicted with equation 7.6.

# 9. SUMMARY AND CONCLUSION

The film boiling study has counted several years, and a number of theoretically and experimental studies have been made since then.

In this thesis, a series of experimental study was conducted (a) to find a new innovative coolant to enhance thermal performance in heat transport system including nuclear power systems, (b) to find a new quenching liquid, which efficiently cool the hot materials including nuclear reactor core during reactor sever accidents, (c) to complete $Al_2O_3$ nanofluid boiling curve studied from the single-phase convection presently up to the critical heat flux and (d) to investigate the feasibility to use nanofluids as a new liquid to suppress the steam explosion during the quenching of high temperature molten material in nuclear sever accidents (if the minimum film boiling point has changed from the distilled water). The experiment includes quenching of a highly heated stainless steel sphere in a pool of three different fluids: 33nm $Al_2O_3$-water, 300nm $Al_2O_3$ -water + surfactant and distilled water.

The result of the experiment showed that fluids with nanoparticle suspensions provided lower film boiling heat transfer compared with the base fluid. Moreover the plots of the heat transfer coefficient and the Nusselt number follows the same trend as for distilled water.

The reason for the degradation in the heat transfer coefficient is supposed to be due the relatively better ability of the suspensions to enhance the vapour generation and resulted in increase of the vapour film thickness. Furthermore, the film boiling period for these fluids is extended leading to a slow quenching rate. The Nusselt number, inversely proportional to the vapour film thickness, declined for these fluids as the film thickness increases.

As mentioned in the literature, additives have been added expecting they will suppress the film vapour explosion completely. From that approach they have been suppressing the explosion to some extent by decreasing the minimum film boiling point.

Therefore the effect of the new fluid as to the explosion of vapour is concerned. Employing nanofluid has lowered the minimum film boiling point slightly, there could be a possibility to use them to suppress steam explosion. They are also more important from quenching point of view in postulated accident nuclear reactors and in heating and cooling appliance, where fast cooling like Iron and steel industries or heat treatment application are required.

The significant of nanofluids in terms of the fast cooling can be explained as due changing of the surface condition they may destabilize the film early so that the quenching process will be held fast with no vapour blanket. It will be necessary to mention the importance of further study in the transition and other boiling regions to investigate their effect

At this point the present study suggests a further surface effect study of these particles when heated with the surface. In that sense this result will be an indication to open a new insight to apply these fluids when an early destabilizing of a vapour film is required.

# 10. REFERENCES

A.E. Bergles and W.G. Thompson, Jr, 1970, The Relationship Of Quench Data To Steady-State Pool Boiling Data, Int. J. Heat Mass Trans. , Vol.13, pp.55-68

Baumeister, K.J. and T.D. Hamill, 1967, Laminar flow Analysis Of Film Boiling from A Horizontal Wire, NASA TN. D. –4035

Bradfield, W.S., 1967, On The Effect OF Subcooling On Wall Superheat In Pool Boiling, J. Heat Transfer, Trans. Of The ASME, pp 269-270

Breen, B.P. and J.W. Westwater, 1962, Effect Of Diameter Of Horizontal Tubes On Film Boiling, Chemical Engineering Progress, Vol. 58, No. 7

Bromley, L.A., 1950, Heat Transfer In Stable Film Boiling, Chemical Engineering Progress, Vol. 46, No.5, pp. 221-227

C. Liu and T.G. Theofanous, 1994, Film Boiling On Spheres In Single and Two Phase Flows, (See kolev)

Cess, R.D. and E.M. Sparrow, 1961, Subcooled Forced Convection Film Boiling On A Flat Plate, J. of Heat Transfer, Trans. Of The ASME, pp 377-379

Cess. R.D. and E.M. Sparrow, 1964, Film Boiling In A Forced Convection Boundary Layer Flow, J. of Heat Transfer, Trans. Of The ASME, pp370-376

Choi U.S., 1995, Enhancing Thermal Conductivity Of Fluids With Nano-Particles, ASME FED 231, 99-103

D.R. Veres and L.W. Florshuetz, 1971, A Comparison Of Transient and Steady-State Pool Boiling Data Obtained Using The Same Heating Surface, J. Heat Transfer, Vol. 93, pp. 229-232

Dhir V.K. and G.P. Purohit, 1978, Subcooled Film Boiling Heat Transfer From Spheres, Nuclear Engineering and Design, Vol. 47, pp. 49-66

Eastman J.A., Choi U.S., Li S., Thompson L.J., Lee S., 1997, Enhanced Thermal Conductivity Through The Development Of Nanofluid, In: Komar

Epstein, M. and G.M. Hauser, 1980, Subcooled Forced-Convection Film Boiling In The Forward Stagnation Region Of A Sphere or Cylinder, Int. J. of Heat Mass Transfer, Vol. 23, pp 187-189

Fodemski, T.R., 1992, Forced Convection Film Boiling In The Stagnation Region Of A Molten Drop And Its Applications To Vapour Explosions, Int. J. Heat Mass Transfer, Vol. 35, No. 8, pp2005-2016

Frederking, T.H.K., R.C. Chapman and S,Wang, 1965, Heat Transport And Fluid Motion During Cool Down Of Single Bodies To Low Temperature, Adv. Cryog. Eng., Vol. 4, pp. 387-392

Frederkning, T.H.K. and J.A.Clark, 1963, Natural Convection Film Boiling On A Sphere, Adv. Cryogenic Eng., Vol. 8, pp 501-506

Fujio Tachibana and Shintaro Enya, 1973,Heat Transfer Problems In Quenching, Bull. J.S.M.E., Vol. 16, pp 100-109

Grigoriev, V.V. Klimenko and A.G. Shelepen, 1982, Pool Film Boiling From Submerged Sphere, Proc. Of 7th Int. Heat Transfer Conf., Munich, Germany, Vol 4, pp 387-392

H. Masuda, A. Ebata, K. Teramea, N. Hishinuma, 1993, Alteration Of Thermal Conductivity and Viscosity Of Liquid By Dispersing Ultra-Fine Particles (Dispersion of $\gamma$-$Al_2O_3$, $SiO_2$, and $TiO_2$ Ultra-Fine Particles), Netsu Bussei (Japan) Vol. 4, pp 227-233

Hamill, T.D. and K.J. Baumeister, 1967, Effect of Subcooling and Radiation On Film Boiling Heat Transfer From A Flat Plate, NASA TND –3925

Hamilton, R.L., Crosser, O.K., 1962, Thermal Conductivity Of Heterogeneous Two Component Systems, I & EC Fundamentals, 1, No. 182-191

Hendricks, R.C. , Baumeister, K.J.,1969, NASA Report TN. D-5124, Lewis Research Center, Cleveland, OH.

Hendricks, R.C. and K.J. Baumeister, 1969, Film Boiling from Submerged Spheres, NASA TN-5124

Irving, M.E. and J.W. Westwater, 1986, Limitations For Obtaining Boiling Curves By The Quenching Method With Spheres, Proc. 8th Int. Heat Transfer Conf., Vol. 4, pp 2061-2066,

Ito T., k.Nishikawa and T. Shigechi, 1981, Forced Convection Film Boiling Heat Transfer From A Horizontal Cylinder To Liquid Cross Flow Up Ward (1st Report, Saturated liquid, Bulletin of The JSME, Vol. 24, No. 198, pp 2107-2114

Ito, T. and K. Hishikawa, 1960, Two Phase Boundary Layer Treatment Of Forced Convection Film Boiling, Int. J. of Heat and Mass Transfer, Vol. 9, pp 117-130

J.A. Eastman, U.S. Choi, S. Li, G. Soyez, L.J. Thompson, R.J. Di Melfi, 1999, Novel Thermal Properties Of Nano Structured Materials, Mater. Sci. Forum 312-314, 629-634

J.A.Eastman, U.S. Choi, S.Li, 2000, Development Of Energy Efficient Nanofluids For Heat Transfer Applications, Research Briefs Argonne national Laboratory

J.D. Bernardin and I. Mudwar, 1996, Experimental and Statistical Investigation of Changes In Surface Roughness Associated With Spray Quenching, Int. J. Heat Mass Transfer, Vol. 39, No. 10, pp 2023-2037

James W. Westwater, John J. Hwalek, and Mark E. Irving, 1986, Suggested Standard Method For Obtaining Boiling Curves By Quenching, Ind. Eng. Chem. Fundam., Vol. 25, No. 4, pp. 685-692

Kobayasi, K., 1965, Film Boiling Heat Transfer Around A Sphere In Forced Convection, J. Nuclear Science and Technology, Vol. 2, No. 2, pp 62-67

Leinhard J.H. , Dhir, 1973, J. Heat Transfer, Vol. 95, pp. 152-8

Lin, D.Y.T., Westwater J.W, 1982, In Proceedings of the 7$^{th}$ International Heat Transfer Conference, Munich, Germany, Hemisphere Publishing: Washington D.C., Vol. 4, pp 155-60

Marschal, E. and L.C. Ferrar, 1975, Film Boiling From A Partly Submerged Sphere, Int. J. Heat Mass Transfer, Vol. 18, pp 875-878

Merte, Jr., H. and J.A. Clark, 1964, Boiling Heat Transfer With Cryogenic Fluids At Standard Fractional And Near-Zero Gravity, J. Heat Transfer, Trans. Of ASME, pp 351-359

Michyoshi, I.,O. Takahashi, and Y. Kikuchi, 1988, Heat Transfer and The Low Limit Of Film Boiling, Proc. of the first World Conf. On Experimental Heat Transfer, Fluid Mechanics, and Thermodynamics, Dubrovnik, Yugoslavia, pp 1404-1415

Motte, E.I., L.A. Bromley, 1957, Film Boiling Of Flowing Subcooled Liquid, Industrial and Engineering Chemistry, Vol. 49, No.11,

N.I. Kolev, 1998, Film Boiling On Vertical Plates and Spheres, Experimental Thermal Fluid Science, Vol. 18, pp 97-115

Nishakawa, K., T. Ito and K. Matsumoto, 1976, Investigation of Variable Thermo physical Property Problem Concerning Pool film Boiling from Vertical Plate with prescribed Uniform Temperature, Int. J. Heat Mass Transfer, Vol.19, pp. 1173-1182

Orozco, J. and L.C. Witte, 1986, Flow Film Boiling From A Sphere To Subcooled Freon-11, J. Heat Transfer, Trans. of the ASME, Vol. 108

P.J. Berenson, 1960, Transition Boiling Heat Transfer From A Horizontal Surface, M.I.T. Heat Transfer Laboratory Report, Report NO. 17

P.J. Berenson, 1962, Experiments on Pool Boiling Heat Transfer, Int. J. Heat Mass Transfer, Vol. 5, and pp 985-999

P.Keblinski, S.r. Phillpot, S.U.S. Choi, J.A. Eastman, 2002, Mechanism Of Heat Flow In Suspensions Of Nano-Sized Particles (Nanofluids), Int. J. Heat Mass Transfer

Peter Vassallo, Ranganathan Kumar, Stephen, D'Amico, 2004, Pool Boiling heat Transfer Experiments In Silica-Water, Nanofluids, Int. J. Heat Mass Transfer, Vol. 47, pp 407-411

S.K.Roy Chowdury R.H.S Winterton, 1985, Int. J. Heat Mass Transfer, Vol. 28, No, 10, pp 1881-1889

S.K.W. Tou and C.P. Tso, 1997, Improvement On The Modelling of The Film Boling On Spheres, Int. Comm. Heat Mass Transfer, Vol. 24, No. 6, pp 879-888

S.Lee, S.U., S.Choi, S. Li, J.A. Eastman, 1999, Measuring Thermal Conductivity Of Fluids Containing Oxide Nano-Particles, J. of Heat Transfer, Vol. 121, pp 280-289

Sakurai, A.M. Shiotsu, and K. Hata, 1990, A General Correlation Of pool Film Boiling Heat Transfer From A Horizontal Cylinder To Subcooled Liquid: part I – A theoretical Pool Film Boiling Heat Transfer Model including Radiation Contributions and Its Analytical Solutions, J. of Heat Transfer, Transactions of the ASME, Vol. 112, pp 430-440

Sakurai, A.M. Shiotsu, and K.Hata, 1990b, A General Correlation Of Pool Film Boiling Heat Transfer From A Horizontal Cylinder to Subcooled Liquid: Part 2-Experimental Data for Various Liquids and Its Correlation, J. Heat Transfer, Trans. Of The ASME, Vol. 112, pp 441-450

Sarit K. Das, Nandy Putra, Wilfred Roetzel, 2003, Pool Boiling Characterstics Of Nano-Fluids, Int. J. of Heat Mass Transfer, Vol.46, 851-862

Schmidt, W.E. and L.C. Witte, 1972, Oscillation Effects Up On Film Boiling From A Sphere, J. Heat Transfer, Trans. Of The ASME, pp 491-493

Shigechi T., T. Ito, and K. Nishikawa, 1983, Forced Convection Film Boiling Heat Transfer from A Horizontal Cylinder to Liquid Cross-Flow Upward, 2nd Report, Subcooled Liquid, Bulletin of The JSME, Vol. 26, No. 214, pp 554-561

Shih, C. and M.M.El-Wakil, 1981, Film Boiling And Vapour Explosions From Small Spheres, Nuclear Science and Engineering, Vol. 77, pp 470-479

Siviour, J.B. and A.J.Ede, 1970, Heat Transfer In Subcooled Pool Film Boiling, Proc. 4th Int., Heat Transfer Conf. Vol. 5, B 3.12, Paris-Versailles

Sparrow, E.M., 1964, The Effect Of Radiation Film Boiling Heat Transfer, Int. J. Heat Mass Transfer, Vol. 7, pp 229-238

S. M. You, and J. H. Kim, 2003, Effect of nanoparticles on critical heat flux of water in pool boiling heat transfer, Applied Physics Letters, Vol.83, No. 16

Susan E. Bayley, 1993, Subcooled Pool Film Boiling of Aqueous Surfactant Solutions from Small Spheres, Master Thesis, University of Wisconsine - Madison

T.H.K. Frederking and J.A. Clark, 1963, Advanced Cryogenic Engineering, Vol. 8, No. 501

Toda, S. and M. Mori, 1982, Subcooled Film Boiling And The Behaviour Of Vapour Film On A Horizontal Wire And A Sphere, Proc. 7th Int. Conf., Munich, Germany, Vol. 4, pp173-178

W. Peyayopankul and J.W. Westwater, 1978, Evaluation Of The Unsteady State Quenching Method For Determining Boiling Curve, Int. J. Heat Mass Transfer, Vol. 21, pp. 1437-1445

Wilson, S.D.R. , 1979, Steady and Transient Film Boiling On A Sphere In Forced Convection, Int. J. Heat Mass Transfer, Vol. 22, pp 207-218

Witte, L.C. and J. Orozco, 1984, The Effect Of Vapour Velocity Profile Shape On Film Boiling From Submerged Bodies, J. Heat Transfer, Trans, Of the ASME, Vol. 106, pp 191-197

Witte, L.C., 1968, Film Boiling From A Sphere, I & EC Fundamentals pp517-518.

Y. Xuan, Q. Li, 2000, Heat Transfer Enhancement Of Nanofluids, Int. J. Heat Fluid Flow, Vol. 21 pp 58-64

Y.Xuan, W. Roetzel, 2000, Conception for Heat Transfer Correlations Of Nanofluids, Int. j. Heat Mass Transfer, Vol. 43, pp 3701-3707

# APPENDIXES

# I. List of Existing Correlations

Film Boiling on a Sphere in Subcooled Nanofluids

| Regime | Reference | Correlation | Remark |
|---|---|---|---|
| Saturated Pool | Bromley 1950) | $Nu = C[Ar/Sp']^{1/4}$  C=0,62..Br | 1/4$^{th}$ power law |
| | Frederking | C=0,586..Fre | Applicable to limited ranges of diameter |
| | Dhir | C=0,8...Dhir | |
| | Merte | $Nu = C[Ar/Sp']^{1/3}$  C=0,15 | Better to take temperature effect |
| | Grigoriew ( | $Nu=0,7\ Ar^{1/4}\ Prv^{1/3}\ f_1(k)$  for Ar< $3\times10^7$<br>$f_1(k)= 1,0$    $k\leq1,4$<br>$f_1(k)= 0,92k^{1/4}$    $k>1,4$<br>$Nu=0,165\ Ar^{1/3}\ Prv\ f_2(k)$  for Ar≥ $3\times10^7$<br>$f_2(k)= 1,0$    $k\leq1,6$<br>$f_2(k)= 0,85k^{1/3}$    $k>1,6$<br>$k=hfg/Cpv.DTsup$ | Diameter effect and turbulent effect counted.<br>Includes ¼ for laminar film when diameter. is small and turbulent film when diameter is large.<br>Fits well with data for 5 liquids |
| | Michiyoshi | $Nu = K[Ar/Sp']^{1/4}Mc^{1/4}$<br>$Mc=E^3/[1+E/(Sp'Prl)]/(R\ Prl\ Sp')^2$<br>E=...<br>K=0,696 sphere....K=0,61 horiz.<br>Cylinder | Verified against data<br>Suitable for characterising pool film boiling in various non metallic liquids, specially in water<br>Valid for various conditions |
| Sub cooled Pool | Sakurai | $Nu/(1+2/Nu) = k(d')[Ar/Sp']^{1/4}Mc^{1/4}$<br>$k(d')=0,44d'^{1/4}$    $d'< 0,14$<br>$k(d')=0,75/(1+0,28d')$    $0,14<d'< 1,25$<br>$k(d')=2,1d'/(1+3,0d')$    $1,25<d'< 6,6$<br>$k(d')=0,415d''^{1/4}$    $d'>6,6$<br>$d'= d/[\sigma/g/(\rho l-\rho v)]^{1/2}$ | Diameter effect counted<br>Valid for various liquids<br>Ratio law |
| | | $Nu=Nusat+Nunc(Sc/Sp)($<br>$Nusat= 0,67[Ar/Sp']^{1/4}$,<br>$Nunc=1,45[Gr.Prl]^{1/4}$ | Addition law, Valid at atmospheric pressure.<br>For Tsup>500C, gives good correlation, else over predicts |
| | C,Lui & Theofanos | Same as Sakuri, except a factor of 1,4 is applied for the diameter effect | Good agreement with their data.<br>Can be used as complete correlation for pool |

*Film Boiling on a Sphere in Subcooled Nanofluids*

| Regime | Reference | Correlation | Remark |
|---|---|---|---|
| Saturated Forced | Kobayasi | $Nu=C.Rel^{1/2}(\mu_l/\mu_v)(kR^{1/4}/Sp)$ | C=0,393 (Kob.) |
| | Epstein | $K=\rho_l/\rho_v$ | C=0,553 (Eps.) |
| | Ito | $R=[(\mu\rho)_v/(\mu\rho)_l]^{1/2}$ | C=0,46(Ito) |
| | Lui, Shiotsu | $Nu/(1+2/Nu) = H(Fr,d')k(d')[Ar/Sp'\ Mc]^{1/4}$ | Verified for various liquids |
| | Sakurai | $H(Fr,d')=(1+0,68\ Fr^{2,5/4})^{1/2,5}+0,45\tanh\{0,04(d'-1,3)Fr\}$ $Mc.$ and $k(d')$ same | |
| | Shigechi, Ito | $Nu=1,15Rel^{1/2}\ Prl^{1/2}\ (\mu_l/\mu_v)(Sc/Sp)$ $Fr>1,5\quad Sc>0,05$ | Integral method was applied to both liquid boundary layer and vapor film layer |
| Sub cooled Forced | Epstein | $Nu=0,977Rel^{1/2}\ Prl^{1/2}\ (\mu_l/\mu_v)(Sc/Sp)$..highly sub cooled $Nu=(Nu_{sat}^4+Nu_{sub}^4)^{1/4}\qquad$ All sub cooling | Suggested a factor of 2,04 to the theoretical eqn |
| | Dhir | $Nu=Nup,s +0,8Rel^{1/2}\{1+(\mu_l/\mu_v)(Sc/Sp)\}$ $0,046<Fr^{1/2}<1,03\qquad 6330<Rel<19000$ $Nup,s=0,8(Ar/Sp')^{1/4}\quad$ saturated | For low speed lower than 0,5m/s |
| | C.Lui, Theofanos | $Nu=Nus+0,072Rel^{0,77}\ Prl^{1/2}(Sc/Sp')$ $Nus=0,5Rel^{1/2}(\mu_l/\mu_v)(R^4k/Sp')^{1/4}$ | Verified experimentally |

## II. Experiment Matrix

| Expt. | Type of Fluid | Temp. of Fluid,(°C) | Diam. of Sphere,(mm) | Ball released Temp. (°C) | (Remark) | File name of Data |
|---|---|---|---|---|---|---|
| Expt. Description: Quenching of the ball in highly subcooled fluid | | | | | | |
| 1 | D.water | 24 | 10 (friction) | 928 | Film collapses fast | S01 |
| 2 | " | 25 | " | 940 | Stable film was observed but no video recorded | S02 |
| 3 | " | 24 | " | 935 | Film collapses fast | S03 |
| 4 | " | 26 | " | 931 | Long sustained film | S04 |
| 5 | " | 27 | " | 922 | Film collapses fast, crack is observed on the ball | S05 |
| 6 | " | 28 | " | 937 | The oxide layer and the crack grow. | S06 |
| 7 | AlOOH | 23 | " | 1030 | Large oxide debris shell is removed from the ball | S07 |
| 8 | " | 24 | " | 940 | Film collapses fast, cracked ball | S08 |
| 9 | " | 25 | " | 888 | | S09 |
| 10 | " | 25,5 | " | 750 | | S10 |
| 11 | " | 27 | " | 1030 | The balled failed | S11 |
| 12 | " | 30 | 20 (welded) | 937 | Fast collapse of the film | S12 |
| 13 | " | 26 | " | 1110 | Stable film | S13 |
| 14 | " | 30 | " | 950 | Stable film, | S14 |
| 15 | " | 32 | " | 955 | Long sustained film | S15 |
| 16 | " | 36 | " | 900 | Stable film | S16 |
| 17 | " | 27 | " | 900 | Film collapses fast | S17 |
| 18 | " | 29 | " | 800 | No stable film | S18 |
| 19 | " | 33 | " | 1045 | Long sustained stable film | S19 |
| 20 | " | 38 | " | 680 | No film | S20 |
| 21 | D.water | 24 | " | 718 | Film collapses fast | S21 |
| 22 | " | 27 | " | 800 | " | S22 |
| 23 | " | 30 | " | 920 | Stable film | S23 |
| 24 | " | 28 | " | 1020 | Big oxide shell, no stable film | S24 |
| 25 | " | 31 | " | 1020 | " | S25 |
| 26 | " | Ball dropped just to remove the oxide, no expt. | | | | S26 |
| 27 | " | 30 | " | 1200 | The ball failed | S27 |
| | The DAS used is not reliable, a very noisy signal (S30-S35) | | | | | |
| 28 | D.water | 22 | 20 | 780 | No film | S30 |
| 29 | " | 25 | " | 1040 | Film collapses fast | S31 |

| | | | | | | |
|---|---|---|---|---|---|---|
| 30 | 5% 300nm, | 23 | " | 950 | Short film | S32 |
| 31 | " | 24 | " | 1050 | Better film than the above | S33 |
| 32 | " | 26 | " | 750 | No film, ball gets crack | S34 |
| 33 | " | 30 | " | 950 | Fast collapse,ball cracked | S35 |
| DAS and the ball changed, with different fluids, highly subcooled | | | | | | |
| 34 | D. Water | 20 | 10 | 960 | Film collapses fast | S100 |
| 35 | " | 24 | " | " | " | S101 |
| 36 | D. Water | 26 | 10 | 930 | " | S103 |
| | Expt. Description: degree of subcooling made small. | | | | | |
| 37 | D. Water | 91 | 10 | 955 | Very stable, thick long sustained film | S104 |
| 38 | " | 76 | " | 940 | Stable film | S105 |
| 39 | " | 68 | " | 935 | " | S106 |
| | Expt. Description: type of fluid changed, and highly subcooled | | | | | |
| 40 | 5% 300nm, Surfactant | 24 | " | 960 | Stable film, even at highly subcooled | S107 |
| 41 | " | 25 | " | 960 | " | S108 |
| 42 | " | 27 | " | 950 | " | S109 |
| 43 | " | 28 | | 1030 | Fast collapse compared to above | S110 |
| 44 | " | 26 | " | 900 | Thick stable film | S111 |
| | Expt. Description: The ball changed, a shiny smooth ball with long, thin stem is used. | | | | | |
| 45 | 5%,(no, sur) 27-50nm, | 23 | " | 990 | Stable film, | S112 |
| 46 | " | 23 | " | 950 | Film collapses fast | S113 |
| 47 | " | 23 | " | 910 | " | S114 |
| 48 | " | 24 | " | 830 | " | S115 |
| 49 | " | 24 | " | 1060 | Long sustained, thick film | S116 |
| 50 | D. Water | 20 | " | 960 | No film | S117 |
| 51 | " | 20 | " | 1060 | Thick, long sustained, stable film | S118 |
| 52 | " | 21 | " | 925 | Film collapses fast | S119 |
| | The ball washed, if the nfluid has stacked with the ball | | | | | |
| 53 | " | 19 | " | 1070 | Long sustained, stable film | S121 |
| 54 | " | 19 | " | 955 | No film | S122 |
| 55 | " | 19,5 | " | 1075 | Stable film | S123 |
| | Experiments with Nfluid, near saturation | | | | | |
| 56 | 5%,(no, | 80 | " | 965 | Stable film, thick | S124 |

| | sur) 27-50nm, | | | | | |
|---|---|---|---|---|---|---|
| 57 | " | 69 | " | 1065 | " | S125 |
| 58 | " | 69 | " | 865 | " | S126 |
| 59 | " | 68 | " | 915 | " | S127 |
| | Large Ball changed, friction joint | | | | | |
| 60 | " | 33 | 20 | 1070 | Stable film | S130 |
| 61 | " | 38 | " | 1060 | " | S131 |
| 62 | " | 44 | " | 940 | " | S132 |
| 63 | " | 48 | " | 850 | " | S133 |
| 64 | " | 79 | " | 910 | " | S134 |
| 65 | " | 77 | " | 855 | " | S135 |
| 66 | " | 78 | " | 1045 | | S136 |
| | Changing fluid for the same ball | | | | | |
| 67 | D. Water | 80 | | 860 | " | S140 |
| 68 | " | 80 | | 960 | " | S141 |
| | For small ball subcooled and near saturation for video recording | | | | | |
| 69 | D. Water | 48 | 10 | | film | S154 |
| 70 | " | 91 | " | | | S155 |
| 71 | D. Water | 30 | 10 | 1055 | Stable film | S160 |
| 72 | 10%(no, sur.) 27-50nm | " | " | " | " | S161 |
| 73 | " | | " | | No | S162 |
| 74 | " | | " | | " | S163 |
| 75 | " | | " | | " | S164 |
| 76 | " | | " | | " | S165 |
| 77 | 20%(no, sur.) 27-50nm | " | " | " | Stable film | S166 |
| 78 | " | | " | | No | S167 |
| 79 | " | | " | | " | S168 |
| 80 | " | | " | | " | S169 |
| 81 | D. Water | " | " | | Water before washing, no film | S170 |